Developing Penetration Rate Prediction Models to Enhance the Productivity Prediction of Microtunneling Construction Projects

by

Saeid Moharrami

A thesis submitted in partial fulfillment of the requirements for the degree of

Doctor of philosophy

in

Civil (Cross-disciplinary)

Department of Civil and Environmental Engineering

University of Alberta

Abstract

Predicting the productivity of microtunnelling construction projects is challenging due to the inherent complexities of this trenchless excavation method. One of these complexities has to do with estimating the micro-tunnel boring machine penetration rate, given that it is subject to a number of factors, including variations in ground conditions during microtunneling, uncertainty regarding underground conditions along the tunnel path, and the complexity of the mechanism underlying micro-tunnel boring machine excavation. A review of literature on predicting the penetration rate reveals a number of gaps with respect to the prediction of micro-tunnel boring machine penetration rate, including (1) the lack of a robust method for the use of machine-generated data for dynamically updating the project progress, (2) limited research on small-diameter microtunneling excavation through soft ground conditions, (3) the lack of mechanistic investigation of the mechanism governing micro-tunnel boring machine penetration into the soil, as well as the lack of a theoretical mechanistic relationship by which to quantify the influence of primary factors such as soil type, operational loads, and cutterhead characteristics, (4) the lack of integrated models by which to reduce uncertainty of micro-tunnel boring machine penetration rate in simulation-based microtunneling productivity studies, and (5) the lack of penetration rate prediction models suited for dynamic utilization during construction to update the penetration rate predictions and modify the project plan accordingly.

The research presented in this thesis to enhance the prediction of micro-tunnel boring machine penetration rate and productivity in microtunneling construction, proceeding in three phases. In Phase 1, a dynamic penetration rate prediction model that uses a machine-learning approach is developed. Phase 2 involves the development of a mechanistic approach for modelling micro-

tunnel boring machine penetration into soft ground. In this regard, a novel mechanistic approach (based on the contact mechanics theory) by which to model the interaction between the micro-tunnel boring machine and the ground is introduced. The developed mechanistic model is further improved by modelling in greater detail the micro-tunnel boring machine's engagement with the ground, taking into consideration in particular the engagement between cutting blade and soil, and quantifying the influence of this engagement on the micro-tunnel boring machine's penetration rate. In Phase 3, to enhance the production rate estimation in microtunneling construction projects, the micro-tunnel boring machine penetration rate prediction models developed in Phases 1 and 2 are integrated with simulation models. Two approaches are followed for integrating the mechanistic model for prediction of micro-tunnel boring machine penetration rate (developed in Phase 2) with operation simulation. The first approach is to use the exact mechanistic formula and incorporate it into the simulation model, while the second approach is to enhance the prediction made by the mechanistic model by leveraging observations (excavation times) made during construction and updating the initial predicted distribution of penetration rate accordingly. To integrate the dynamic machine-learning model for prediction of micro-tunnel boring machine penetration rate (developed in Phase 1) with an operation simulation model, a database of results is integrated with a simulation model. Whenever the micro-tunnel boring machine reaches specific locations along the tunnel in the simulation, it calls up the predicted penetration rate to be used for modelling excavation, and in this manner the entire microtunneling operation is simulated.

The feasibility and functionality of the developed models for predicting micro-tunnel boring machine penetration rate (as well as the prediction models integrated with simulation) are validated using both actual case studies and a synthetic dataset of fifty microtunneling projects generated using the Monte Carlo approach. Ultimately this research provides practitioners and researchers

with a systematic procedure for using machine-generated data and available geotechnical information during tunnelling to achieve more accurate prediction of micro-tunnel boring machine performance in dynamic geological conditions, and to update the project progress dynamically based on what is actually occurring on site. Furthermore, this research proposes a novel approach for mechanistic analysis of the interaction between the micro-tunnel boring machine and the ground, and develops a mechanistic model for micro-tunnel boring machine penetration rate that characterizes in a quantitative manner the relationship between penetration rate and the combined influence of three primary factors—soil properties, operational loads, and cutterhead characteristics.

Preface

This thesis is an original work by Saeid Moharrami. This thesis is organized in a paper-based format.

A version of Chapter 2 has been published as Mechanistic Approach. *Journal of Construction Engineering* and Management, 148(11), 04022128 and has been reprinted with permission from MDPI. Dr. AbouRizk and Dr. Bayat were supervisory authorities and were involved in supervisory authority and were involved in conceptualization, funding acquisition, project administration, manuscript review, and editing.

A version of Chapter 3 was submitted for publication as Moharrami S, Bayat A, and AbouRizk S. Mechanistic modeling of cutterhead-ground engagement influence on micro-tunnel boring machine penetration rate. *Journal of Construction Engineering and Management* on July 19, 2022. Dr. AbouRizk and Dr. Bayat were supervisory authorities and were involved in supervisory authority and were involved in conceptualization, funding acquisition, project administration, manuscript review, and editing.

A version of Chapter 4 will be submitted for publication as Moharrami S, Bayat A, and AbouRizk S. Dynamic Data-Driven approach for Penetration Rate Prediction in Microtunneling Construction. *Journal of Construction Engineering* and Management. Dr. AbouRizk and Dr. Bayat were supervisory authorities and were involved in supervisory authority and were involved in conceptualization, funding acquisition, project administration, manuscript review, and editing.

A version of Chapter 5 will be submitted for publication as Moharrami S, Bayat A, and AbouRizk S. Integrating MTBM penetration rate prediction models and operation simulation model to

enhance microtunneling productivity prediction in Microtunneling Construction. *Journal of Construction Engineering and Management*. Dr. AbouRizk and Dr. Bayat were supervisory authorities and were involved in supervisory authority and were involved in conceptualization, funding acquisition, project administration, manuscript review, and editing.

Dedication

This thesis is dedicated with love, admiration, and respect

to my kind mother, my dear father, and my young brother;

to my lovely wife;

to my beautiful daughter;

and particularly to my most intimate and dearest friend, Imam Mahdi.

Acknowledgements

I would like to express my deepest gratitude to my supervisors, Professor Simaan AbouRizk and Dr. Ali Bayat for their generous support and encouragement. I have been truly lucky to have both of them as my mentors. Dr. AbouRizk guided me with his keen advice, critical insight, and confidence throughout the whole dissertation process. Dr. Ali Bayat also inspired me with his wisdom, and his patience. I thank both of you for your assistance in carrying out this research.

I would like to acknowledge Dr. Yasser Mohamed for serving as my advisor and providing his invaluable feedback. I am also grateful to my examining committee, Dr. Samuel Ariaratnam, Dr. Derek Apel, Dr. Gaang Lee and Dr. Leila Heshemian for their valuable insights.

I would like to express my warm thanks to Dr. Catherine Pretzlaw, Maria Al-Hossein, Brenda Penner, Steve Hague, and all the friends that I made during my PhD. I am really grateful for having you in my journey. It was a pleasure to know you all.

Finally, I would like to express my deepest gratitude to my beloved family who taught me how to live. My sincere thanks to my lovely parents (Hamid and Fatemeh) for their never ending support. I am but a product of your dreams and sacrifices. Although I have been away from you, your prayers have always paved my road to success. I also express my deep appreciation to my kind brother, Masoud, and my dear parent-in-law, Naser and Nahid. I am also grateful to my other in-laws for their continual support and help, especially Hosein. My special heartfelt acknowledgement must go to my loving wife Maedeh, whose warm companionship and kind support can never be appreciated enough. Thank you for your continuous love, inspiration, and patience during this journey. Words cannot express my gratitude and everlasting love toward you.

Contents

Abstract……ii

Preface……..v

Dedication vii

Acknowledgements viii

Contents ……..ix

List of Tables xiv

List of Figures xv

List of Abbreviations xxi

Chapter 1: Introduction 1

1.1. Background and Problem statement 1

1.2. Research Objectives 5

1.3. Scope of Research 6

1.4. Research Methodology 6

1.5. Thesis Organization 9

Chapter 2: Modeling Micro-tunnel Boring Machine Penetration Rate Using a Mechanistic Approach* 12

2.1. Introduction 12

2.2. Research Background 14

2.3. Research Gaps on Modeling MTBM Penetration Rate into Soft Ground 18

2.4. Proposed Methodology 19

2.4.1. Introduction to Mechanistic Modeling of MTBM Penetration Rate 19

2.4.2. Mechanistic Approach for Analysis of MTBM-Ground Interaction 20
2.4.3. Mechanistic Model Development 21
2.5. Model Evaluation 27
2.5.1. Extreme Condition Test 27
2.5.2. Case Study 1 29
2.5.3. Case study 2 32
2.6. Discussion 34
2.7. Conclusion 35
2.8. Data Availability 37
2.9. Acknowledgment 37
Chapter 3: Mechanistic Modeling of Cutterhead-Ground Engagement Influence on Micro-tunnel Boring Machine Penetration Rate 38
3.1. Introduction 38
3.2. Research Background 40
3.3. Methodology 41
3.3.1. Mechanistic Approach for Analysis of Cutterhead-Ground Engagement 41
3.3.2. Cutterhead-Ground Engagement Model Development 43
3.4. Model Evaluation 48
3.4.1. Case Study 1 48
3.4.2. Case study 2 53
3.5. Conclusion 54
3.6. Data Availability 55
3.7. Acknowledgment 56

Chapter 4: Dynamic Data-Driven Approach for Penetration Rate Prediction in Microtunneling Construction 57
4.1. Introduction 57
4.2. Research Background 59
4.3. Methodology 61
4.3.1. Data source creation 63
4.3.2. Data preparation 63
4.3.3. Data analysis 63
4.3.4. Model development 64
4.3.5. Decision support 65
4.3.6. Data source updates 65
4.3.7. Dynamic aspect of machine learning model 65
4.4. Case Study 1 66
4.4.1. Data source preparation 66
4.4.2. Model development 68
4.4.3. Results and discussion 69
4.5. Case Study 2 71
4.6. Conclusion 73
Chapter 5: Integrating MTBM Penetration Rate Prediction Models and Operation Simulation Model to Enhance Microtunneling Productivity Prediction 74
5.1. Introduction 74
5.2. Research Background 76
5.3. Integrating mechanistic model for MTBM PR with operation simulation 77

5.3.1. Incorporation of exact mathematical expression of MTBM PR into simulation 78
5.3.2. Use of Bayesian updating approach for incorporating the mechanistic model for MTBM PR into the simulation 82
5.4. Integrating Machine-learning model for MTBM PR with Simulation 89
5.5. Case study analysis 90
5.5.1. Case study 1 91
5.5.2. Case study 2 94
5.6. Validation of integrated simulation and MTBM PR prediction models using Monte Carlo project generation approach 96
5.6.1. Introduction 96
5.6.2. Methodology 97
5.6.3. Results of project generation 111
5.6.4. Randomness test on generated projects 114
5.6.5. Randomness test results 115
5.6.6. Analysis of integrated Simulation + MTBM PR prediction models using generated projects 116
5.7. Summary and Conclusion 119
Chapter 6: Conclusions, Limitations, and Future Directions 122
6.1. Research Conclusions 122
6.2. Academic Contributions 125
6.3. Industrial Contributions 126
6.4. Research Limitations 127
6.5. Future Directions 128

References 130

List of Tables

Table 2. 1. Excavation conditions with corresponding model parameters and penetration rates. 28

Table 2. 2. Specifications of MTBM. 31

Table 2. 3. Geotechnical data collected from borehole sampling along tunnel length. 31

Table 4. 1. Initial borehole data obtained from geotechnical baseline report…….67

Table 4. 2. Initial borehole data obtained from geotechnical baseline report…….72

Table 4. 3. Summary of PR prediction accuracy for Sections A and B. 73

Table 5. 1. Consistency table defining SPT-N value for cohesive soils states……...104

Table 5. 2. Relative density table defining SPT-N value for cohesion-less soils states. 104

List of Figures

Figure 1. 1.Research phases defined and models developed to meet the corresponding research objectives 8

Figure 2. 1. Parameters used for experimental analysis of rock cutting by disc cutters for the CSM model..... 15

Figure 2. 2. Schematic representation of fundamental factors influencing the penetration of an object into a medium under subjected loads. 20

Figure 2. 3. Schematic illustrations viewing the ground and MTBM as (A) separate systems or (B) a united system. 21

Figure 2. 4. Proposed mechanistic model for penetration rate modeling based on contact mechanics theory for (A) two contacting bodies and the stresses between them due to applied loads and (B) MTBM penetration into the ground. 22

Figure 2. 5. Decoupled ground-MTBM interactions of thrust force and torque..... 23

Figure 2. 6. Normal thrust force of the MTBM at the MTBM-ground interface. 23

Figure 2. 7. Tangential torque force of the MTBM at the MTBM-ground interface. 24

Figure 2. 8. Mechanistic model input parameters for MTBMs. 27

Figure 2. 9. Borehole locations along sewer line of sanitary trunk project under study. Black and gray lines show the availability or unavailability of MTBM data respectively. 30

Figure 2. 10. Schematic representation of interpolated geological conditions along sewer line of sanitary trunk project for the selected sections under study between BH 4 to BH 6 based on geotechnical investigation report. 30

Figure 2. 11. Comparison of actual and model predicted penetration rates along the (A) BH 4 to BH 14 and (B) BH 5 and BH 6 portion of the project under study. 32
Figure 2. 12. Microtunneling alignment for the examined microtunneling project..... 33
Figure 2. 13. Comparison of actual and model predicted penetration rates along the (A) section A and (B) section B of tunnel. 34
Figure 3. 1. Proposed mechanistic model for penetration rate modeling based on contact mechanics theory for (A) two contacting bodies and the stresses between them due to applied loads; and (B) MTBM penetration into the ground (Moharrami et al., 2022). 42
Figure 3. 2. Schematic simulation of the actual engagement area at the cutterhead-ground interface (A) Cutter arrangement (B) Excavation traces (C) Actual engagement area (D) Simulated engagement area..... 43
Figure 3. 3. Schematic representation of MTBM penetration (δ) under thrust force (F) and torque (T) and the radius of engagement area (c) and radius of cutterhead (a). 44
Figure 3. 4. Relationship between normalized engagement radius (c/a) and engagement factor Alfa (α). 46
Figure 3. 5. Schematic representation of upper and lower penetration rate boundaries based on cutterhead engagement area with soil. 48
Figure 3. 6. Sewer line alignment and borehole locations of sanitary trunk project. Black and gray lines show the availability or unavailability of MTBM data respectively. The schematic representation of soil types at the boreholes for the selected sections of tunnel under study is also shown in the Figure..... 49
Figure 3. 7. MTBM data obtained from data acquisition system: Torque (% of max torque capacity) and RPM during excavation portion of tunnel between BH4 and BH14. 50

Figure 3. 8. Actual and predicted penetration rates boundaries along the (A) BH4 to BH14 and (B) BH5 and BH6 portion of the project under study. 51

Figure 3. 9. Actual penetration rate (PR) for tunnel section between BH4 to BH14 and corresponding cutterhead engagement factor Alfa (α) along the tunnel length. 52

Figure 3. 10. Actual and predicted penetration rates boundaries along the (A) section A and (B) section B of the microtunneling project. 54

Figure 4. 1. Conceptual framework of the proposed MTBM PR prediction approach……..62

Figure 4. 2. Dynamic aspect of the data-driven framework. 66

Figure 4. 3. Borehole locations along the sewer line alignment. 68

Figure 4. 4. Soil type interpolation along the tunnel path. 68

Figure 4. 5. Schematic representation of the dynamic prediction procedure for different tunnel segments. 69

Figure 4. 6. Penetration rate prediction accuracy based on different reference data and for different tunnel segments. 70

Figure 5. 1. Schematic example of considering inter-correlation among friction and torque when sampling the values from their distribution to input into the mechanistic model for MTBM PR. 79

Figure 5. 2. Element of the simulation model, referred to as “MechanisticPR”, in which the exact mathematical formula of the mechanistic model is coded. 81

Figure 5. 3. Parameters of mechanistic model defined as task elements in the simulation model. 81

Figure 5. 4. “TBM-excavation” task element in the simulation model. 82

Figure 5. 5. Simphony simulation model developed to obtain the prior predictive distribution of excavation time based on mechanistic model. 85

Figure 5. 6. Distribution of excavation time based on mechanistic model. 86
Figure 5. 7. Example of experiment records for determining distributions for the parameters of "Beta distribution of excavation time". 87
Figure 5. 8. Example of updating the prior predictive distribution using observations and obtaining posterior predictive distribution of excavation time. 88
Figure 5. 9. Example of MTBM PR predicted spectrum between boreholes in St. Albert microtunneling project. 89
Figure 5. 10. Simulation environment that includes "Database" element for calling the predicted PR using machine-learning approach and "Load Data" element to load the data into simulation model..... 90
Figure 5. 11. Obtaining the initial information required for both the mechanistic model and the machine-learning model for MTBM PR. 92
Figure 5. 12. Results of updating the project duration at (A) 37% project completion and (B) 60% project completion using the "integrated simulation and Bayesian updating mechanistic model for MTBM PR prediction" and comparison with predictions generated by practitioners and by the CPM method. 93
Figure 5. 13. Results of updating the project duration at (A) 37% project completion and (B) 60% project completion using an " integrated simulation and machine-learning model for MTBM PR prediction" and comparison with predictions generated by practitioners and by the CPM method. 94
Figure 5. 14. Results of updating the project duration at 22% project completion using (A) Simulation + Bayesian updating mechanistic model for MTBM PR and (B) Simulation + Machine-learning model for MTBM PR. 95

Figure 5. 15. Schematic representation of inter-dependencies among primary components of MTBM excavation. 97
Figure 5. 16. Main algorithm for the generation of microtunneling projects. 99
Figure 5. 17. Algorithm for generation of microtunneling project specifications (Algorithm A). 100
Figure 5. 18. Database of 27 microtunneling types and their specifications. 101
Figure 5. 19. Algorithm for generation of soil parameters at each borehole (Algorithm B). 102
Figure 5. 20. Schematic representation of Markov chain for transition between cohesive and cohesion-less soil zones. 102
Figure 5. 21. Algorithm for determining the SPT-N value for each borehole based on soil category. 104
Figure 5. 22. Algorithm for generation of the other geotechnical parameters corresponding to the generated SPT-N values based on soil properties correlation matrix. 107
Figure 5. 23. Algorithm for generating MTBM data based on correlation matrix between MTBM parameters and soil properties (Algorithm C). 109
Figure 5. 24. Schematic representation of four tunnel sections divided at 10, 20, and 30% project completion..... 109
Figure 5. 25. Schematic representation of external factors considered in the generated projects. 110
Figure 5. 26. Algorithm for considering the influence of external factors on generated projects. 111
Figure 5. 27. Results of generated projects..... 112
Figure 5. 28. Distribution of project characteristics over the generated projects. 113

Figure 5. 29. Runs randomness test results for project characteristics and for a data point produced in sample project #11. 116
Figure 5. 30. Results of integrated Simulation + Bayesian updating mechanistic model and Simulation + Machine-learning model for updating the project #43 duration at 10%, 20%, and 30% of project completion. 117
Figure 5. 31. Percentage of correctly predicted projects at 10%, 20%, and 30% project completion (by consideration of external factors). 118
Figure 5. 32. Percentage reduction on number of correctly predicted projects at 10%, 20%, and 30% project completions by including external factors for both the “integrated simulation + Bayesian updating mechanistic model for MTBM PR prediction” and the “integrated simulation + machine-learning model for MTBM PR prediction”. 119

List of Abbreviations

MTBM	Micro Tunnel Boring Machine
TBM	Tunnel Boring Machine
PR	Penetration Rate
ANN	Artificial Neural Network
BH	Borehole
CSM	Colorado School of Mines
LCM	Linear Cutting Machine
UCS	Unconfined Compressive Strength
NTNU	Norwegian University of Science and Technology in Trondheim
DRI	Drilling Rate Index
CLI	Cutter Life Index
BWI	Bit Wear Index
BI	Boreability Index
RPM	Revolution Per Minute

P	Depth of Penetration
D	Cutter Diameter
W	Tip Width
θ	Cutter Edge Angle
S	Cutter Spacing
RMC	Rock Mass Characteristic
k	Correction Factor
T	Torque
δ	Penetration Per Revolution
MPa	Mega Pascal
G	Shear Modulus
v	Poison's Ration
μ	Opening Ratio
f	Friction Coefficient
E	Young's Elastic Modulus

Chapter 1: Introduction

1.1. Background and Problem statement

Microtunneling is a trenchless technique for pipeline installation that has four main features: (1) the operation is controlled remotely (2) the tunnelling machine uses laser guidance for navigation, (3) pipe sections are jacked while the tunnel face is excavated and excavated material is removed, and (4) the tunnel face is continuously supported (ASCE, 2001). A look at the history of this trenchless technique reveals it has becoming increasingly popular in recent years, due in large part to its ability to minimize surface disruptions (especially in congested urban areas), its high accuracy in both line and grade pipeline installation (Chung et al., 2004), its minimal impact on traffic, and the low social cost compared with other methods (Hegab and Salem, 2010). Notwithstanding these benefits—not to mention the recent advancements in the technical features of microtunnel boring machines (MTBMs)—the microtunneling industry is still looking for solutions to enhance performance in terms of planning, control, and monitoring. Accurate prediction of productivity plays a key role in assisting owners in evaluating the contractor's performance and in aiding contractors in controlling the project, including adjusting the production rate as needed to meet the expected milestones. In microtunneling projects, productivity of construction is highly dependent on MTBM penetration rate (PR) (Hegab et al., 2006), which is defined as "instantaneous excavation distance per time while the MTBM is operating, typically

measured in inches per minute or millimeters per minute" (ASCE, 2015). There are a number of factors that make forecasting MTBM PR particularly challenging:

1. Variations in ground conditions during microtunneling: Since an MTBM operates in various ground conditions, its behaviour changes and is not constant during the excavation.
2. Uncertainty in underground condition along the tunnel path: This uncertainty includes, but is not limited to, the soil types encountered during tunneling, the presence of boulders, and unforeseen conditions that may affect the microtunnelling excavation operation.
3. Complexity of the MTBM excavation mechanism: Due to the complex nature of the MTBM excavation mechanism, practitioners lack an in depth understanding of the physics governing the PR or of the relationship between PR and primary mechanistic factors such as operational loads, soil properties, and cutterhead characteristics.

A review of the literature shows that prediction of TBM/MTBM PR has been the focus of several studies (Ozdemir et al., 1978; Sanio, 1985; Sato et al., 1991; Rostami and Ozdemir, 1993; Rostami, 1997, 2008; Alvarez et al., 2000; Sapigni et al., 2002; Ribacchi and Fazio 2005; Hegab et al., 2006; Yagiz, 2008; Eftekhari et al., 2010; Yagiz and Karahan, 2011; Hassanpour et al., 2009a, 2009b, 2011; Farrokh et al., 2012; Salimi and Esmaeili, 2013; Jamshidi, 2018; Elwakil and Hegab, 2018). Meanwhile, others have developed empirical equations by collecting rock mass characteristics and tunnel boring machine (TBM) performance data from multiple tunneling projects using machine-learning models (Alvarez et al., 2000; Eftekhari et al., 2010; Salimi and Esmaeili, 2013; Yagiz and Karahan, 2011; Sapigni et al., 2002; Hassanpour et al., 2009a, 2009b, 2011; Farrokh et al., 2012; Jamshidi, 2018), and some have used full-scale field tests to correlate field parameters with boring machine performance in order to deliver more accurate predictions (Rostami and Ozdemir, 1993; Rostami, 1997, 2008; Sato et al., 1991; Sanio, 1985; Ozdemir et al., 1978). Although the above-

mentioned studies provide valuable insights on prediction of PR, existing models (developed using databases compiled from several projects) have low accuracy when used in different geological conditions, are limited in application domain to rocky conditions and large-sized TBMs, and require specialized equipment and laboratory facilities in order to generate the required data. Moreover, the models that have been developed based on case study analysis of hard rock tunneling projects or experimental tests have been limited to specific TBM cutter configurations and are not applicable to soft geological conditions.

Another fact that is important to note is that, during tunneling/microtunneling excavation, the TBM/MTBM data generated represents the behaviour of the machine interacting with the ground. Although this data has been used for evaluation and prediction of operational loads such as torque and thrust (Shi et al., 2011; Han et al., 2017), it has not yet been widely applied for dynamically predicting the PR and updating the project productivity accordingly. Without a system that analyzes this data and transforms it into a format in which it can be used easily interpreted, decision makers will continue to rely mainly on practitioners' subjective decisions.

Leveraging the MTBM data generated during construction, practitioners can evaluate the MTBM performance and forecast the project progress using operation simulation modelling. Operation simulation modelling has been used to (i) model a variety of tunnel construction projects, such as shaft construction and tunneling (Al-Bataineh et al., 2013), and (ii) forecast the impact of various environmental factors, such as weather conditions (Shahin et al., 2014) and geological conditions (Zhang et al., 2017) on tunneling project performance. However, since existing tunneling simulation models are unable to incorporate new data (collected mainly from equipment-generated sources) in real time, they cannot be transformed into a reliable and comprehensive decision support system. Indeed, most of the simulation approaches described in the literature have been

designed to use only static historical data as an input for modelling uncertain activities. As a result, they are not able to capture the dynamic changes as the project progresses, and this limits their ability to represent the entire system. A review of the relevant literature reveals that there have been a number of studies aimed at recalibrating simulation parameters by incorporating newly generated information into the simulation parameters using a variety of approaches, such as the Markov chain Monte Carlo approach (Ji and AbouRizk, 2017) and the Baum-Welch approach (Werner et al., 2018). However, these models are not capable of updating the parameters involved in the microtunnelling construction domain (e.g., MTBM–ground interactions, MTBM PR).

In summary, an analysis of the literature reveals five main gaps that need to be addressed:

1) There is inadequate feedback with respect to the use of machine-generated data for dynamically updating the project progress.
2) Most of the available studies on predicting PR in tunneling projects are applicable only to large-diameter tunneling excavation through hard rock formations and are not applicable to small-diameter microtunneling through soft ground.
3) The mechanism of MTBM penetration into the soil has not been mechanistically investigated, and a theoretical mechanistic relationship that quantifies the influence of primary factors such as soil types, operational loads and cutterhead characteristics on MTBM PR has not yet been identified.
4) Models to reduce uncertainty of MTBM PR in simulation-based microtunneling productivity prediction have yet to be developed.
5) Existing PR prediction models are static and are not suited dynamic utilization during construction to update the PR predictions and modify the project plan accordingly.

Corresponding to these gaps in research and practice within this domain, the following research questions can be formulated:

1) How can MTBM data generated during excavation be used for (i) improving PR prediction dynamically as the project progresses, and (ii) enhancing the productivity predictions and updating the project plan?
2) How can the mechanistic behaviour of an MTBM operating in soft ground conditions be modelled, and how can the influence on PR due to primary factors such as operational loads, soil properties, and cutterhead characteristics be analyzed and evaluated in a quantitative manner?
3) How can mechanistic understanding of MTBM behaviour be used to enhance dynamic PR prediction during excavation and update the project productivity accordingly?

1.2. Research Objectives

The overall goal underlying this research is to develop models to enhance MTBM PR prediction and, consequently, improve the productivity forecasting conducted during the construction phase of microtunneling projects. In this regard and to address the above-mentioned research questions, the following research objectives are defined:

Objective 1: Improvement of MTBM PR prediction dynamically during microtunneling construction.

Objective 2: Mechanistic investigation of MTBM penetration into soft ground.

Objective 3: Enhancement of production rate estimation during microtunneling construction.

1.3. Scope of Research

In this research, it should be noted, the study of MTBM PR is limited to soft ground conditions (i.e., soil), whereas hard rock excavations are outside the scope of this research. Moreover, the tunnel face condition is assumed to be steadily stable while the MTBM is excavating.

1.4. Research Methodology

A distinct research phase is undertaken corresponding to each of the research objectives defined, as shown in Figure 1.1. In Phase 1, a dynamic PR prediction model that uses a machine-learning approach is developed. To construct this dynamic machine-learning model, a procedure is established to create the database required for its development. In this procedure, MTBM data generated during excavation is used as a dynamic data source that is updated as the project progresses, while geotechnical data obtained from geotechnical reports is used as a static data source that is constant during excavation. Based on this procedure, after cleaning the data, a geoscience approach is used to interpolate the geotechnical parameters along the tunnel path, and the MTBM PR is calculated accordingly. Based on the MTBM PR at the locations where the geotechnical parameters are interpolated, the database to be used for establishing the machine-learning model is created. Based on a comparison of the various machine-learning approaches, artificial neural network (ANN) is selected as the most suitable machine-learning approach for predicting the PR of the unexcavated portion of a tunnel based on geotechnical parameters. The dynamic aspect of this technique is that, as the project progresses and more information becomes available, the database is updated and a new ANN model is constructed for use in predicting the next tunnel section.

Phase 2 is divided into two sub-phases. In Phase 2.1, a mechanistic approach for modelling MTBM penetration into soft ground is developed. In this regard, a novel mechanistic approach based on

the contact mechanics theory is introduced to model the interaction between MTBM and ground. Simulating the MTBM–ground interaction based on this fundamental mechanistic theory results in a mechanistic mathematical model capable of characterizing the relationship between PR and the combined influence of three primary groups of factors (soil properties, operational loads, and cutterhead characteristics). In Phase 2.2, the developed mechanistic model is improved by modelling in greater detail the MTBM engagement with the ground, taking into consideration in particular the engagement between cutting blade and soil, and quantifying the influence of this engagement on MTBM PR. In this regard, using the contact mechanics theory mentioned above, this engagement phenomenon is modelled and the influence of this behaviour on MTBM PR is quantified.

In Phase 3, to enhance the production rate estimation in microtunneling construction projects, the MTBM PR prediction models developed in Phases 1 and 2 are integrated with simulation model. In this regard, in Phase 3.1, the mechanistic model for MTBM PR prediction is integrated with operation simulation. Two approaches are followed for this purpose. The first approach is to use the exact mechanistic formula and incorporate it into simulation model, while the second approach is to enhance the prediction made by the mechanistic model by leveraging observations (excavation times) made during construction and updating the initial predicted distribution of PR accordingly. In this regard, based on Bayes' law and applying Bayesian updating technique on a mechanistic model for MTBM PR, a Bayesian updating mechanistic model is developed and integrated with simulation. In Phase 3.2, the dynamic machine-learning model for MTBM PR prediction (developed in Phase 1) is integrated with an operation simulation model. In this regard, a database of results (including the predicted PRs and the locations where they are predicted) is connected with the simulation model. Whenever the MTBM reaches to the specific location along

the tunnel in the simulation, it calls the predicted PR to be used for modelling excavation, and then the entire microtunneling operation is simulated.

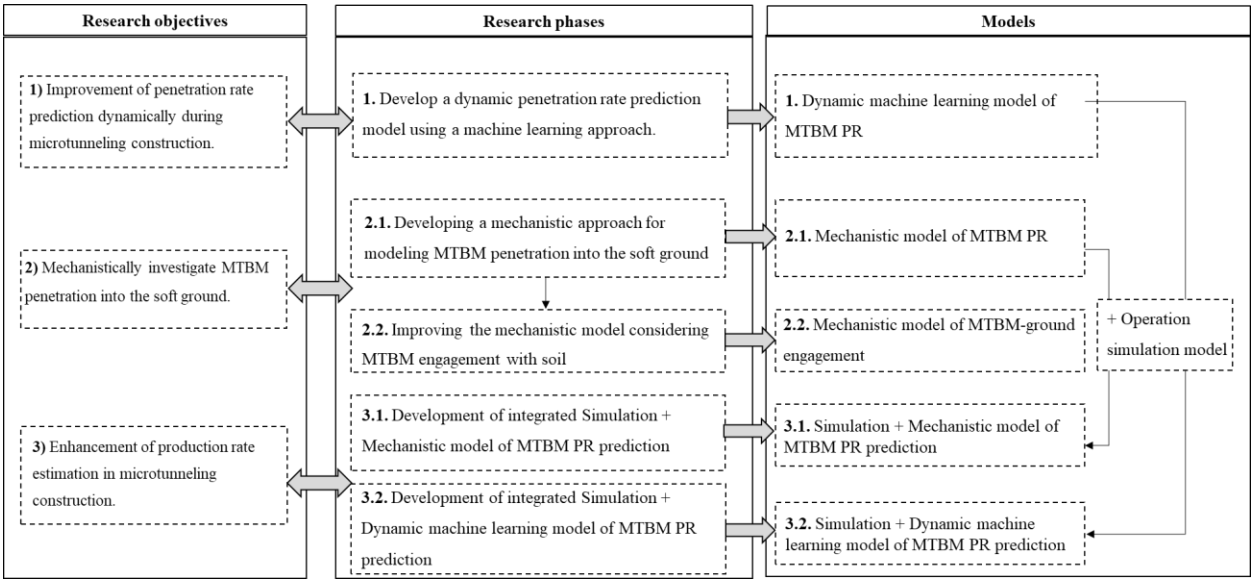

Figure 1. 1.Research phases defined and models developed to meet the corresponding research objectives

This research provides practitioners and researchers with a systematic procedure for using machine-generated data and available geotechnical information during tunneling to achieve more accurate prediction of MTBMs performance in dynamic geological conditions, to prevent schedule delays by considering appropriate measures to counter possible slow excavation progress based on forecast PRs, and to update the project progress dynamically in conjunction with what is actually occurring on site. Furthermore, this research proposes a novel approach for mechanistic analysis of MTBM–ground interaction and develops a mechanistic model for MTBM PR that characterizes in a quantitative manner the relationship between PR and the combined influence of three primary groups of factors (soil properties, operational loads, and cutterhead characteristics). By modelling the MTBM engagement at the interface of the cutting blade and the ground, its influence on MTBM PR can be analyzed and quantified. Finally, to improve the productivity of microtunneling construction, the developed MTBM PR prediction models are integrated with simulation. The

feasibility and functionality of the developed MTBM PR prediction models and the MTBM PR prediction models integrated with simulation are validated using both actual case studies and a synthetic dataset of fifty microtunneling projects generated using the Monte Carlo approach.

1.5. Thesis Organization

This thesis is organized following a paper-based format corresponding to the research objectives shown in Figure 1.1. The chapters in this thesis are organized as follows:

Chapter 2 investigates the physics governing MTBM excavation and mechanistic analysis of MTBM–ground interaction. By introducing a novel approach based on contact mechanics theory, a new state-of-the-art mechanistic model is developed. The developed mechanistic model not only identifies the primary factors governing MTBM PR (i.e., soil properties, operational loads, and cutterhead characteristics), but also sheds light on the complex relationships among PR and these factors. Moreover, the developed mechanistic model for MTBM PR provides insights on the mechanistic behaviour of MTBM during excavation that can aid practitioners in quantifying the influence on MTBM PR of various mechanistic factors, such as opening ratio and cutter head torque and diameter, and in evaluating MTBM performance under various geological conditions.

Chapter 3 describes how the mechanistic model for MTBM PR can be improved by considering in greater detail the MTBM–ground interaction and modelling the MTBM–ground engagement that occurs when the cutting blades are engaged with the ground during excavation. Modelling of the MTBM–ground engagement is a novel tool by which for practitioners to (1) improve MTBM design in consideration of the key factors/mechanisms in high MTBM–ground engagement (and, therefore, high PR), (2) evaluate the performance of various MTBMs in order to select the most appropriate one (particularly in terms of high engagement) for a specific project, and (3) calculate

the upper and lower PR boundaries for a specific MTBM as the project progresses based on consideration of the extreme cases of high and low engagement at the tunnel face. These boundaries in particular can assist engineers and project managers in anticipating the likely range of excavation speeds under various geological conditions during the project and adjusting the MTBM performance accordingly to improve the project productivity.

Chapter 4 describes the development of a novel model by which to dynamically predict MTBM PR as the project progresses. A dynamic procedure is developed that allows practitioners to use available geotechnical information and MTBM data generated during excavation to predict the MTBM PR using a machine-learning model. The dynamic aspect of the procedure assists engineers in continuously learning about the MTBM behaviour under various underground conditions for the purpose of improving prediction accuracy. The forecasts of PR along the tunnel, meanwhile, can be used to identify areas of low, moderate, and high productivity and therefore aids decision makers in planning effectively for future microtunneling excavations accordingly.

Chapter 5 describes the development of (1) approaches to integrate MTBM PR prediction models with operation simulation in order to enhance the prediction of productivity as the project progresses, and (2) a novel procedure for evaluating the integrated simulation-based productivity models by applying them to several synthetic microtunneling projects generated using a Monte Carlo approach. The first part of the chapter provides a detailed explanation of how to integrate both machine-learning models of PR prediction and mechanistic models of PR prediction with simulation. This information can aid practitioners in leveraging the developed PR prediction models to enhance their productivity prediction. The integration of the mechanistic model with operation simulation in particular provides a novel tool by which to assess the influence of various mechanistic factors (e.g., cutterhead design and characteristics) on the productivity of the overall

project. The second part of the chapter describes how to generate synthetic microtunnelling projects. The use of synthetic projects allows researchers and practitioners to evaluate and compare different productivity prediction models with respect to a wide variety of project specifications and tunnel conditions. This, in turn, leads to a deeper understanding of the performance of the prediction models and aids in the identification of bottlenecks for further enhancement of the productivity prediction models.

Chapter 6 summarizes the conclusions, research contributions, and limitations of the research presented in this thesis, and outlines possible avenues of future work.

Chapter 2: Modeling Micro-tunnel Boring Machine Penetration Rate Using a Mechanistic Approach*

2.1. Introduction

Demands for installation of utility service lines using microtunneling excavation as a non-disruptive method have been increasing due to the growing population of cities and communities. Microtunneling is a trenchless technique for pipeline installation in non-person entry tunnel diameters. The microtunneling process is controlled remotely by providing support to the excavation face, and the micro-tunnel boring machine (MTBM) advances using a laser-guided approach. In this process, hydraulic jacks simultaneously push the pipes and the MTBM forward while the excavated material is removed from the tunnel face (ASCE 2015).

The adoption of microtunneling following its introduction to the US was slow, as the MTBMs manufactured were not robust enough to handle ground conditions containing cobbles. MTBMs were later capable of excavating under various ground conditions, which consequently resulted in increased MTBM utilization. Additional microtunneling advantages, such as the ability to excavate in congested urban areas with minimal disruptions, the efficiency and cost-effectiveness in the context of utility installations, low risk of injury, fewer settlement issues, and the ability to accommodate social and environmental concerns, have led to increased MTBM usage in recent years (Luo and Najafi 2007).

---

*This chapter is adapted from published work as "Modeling Microtunnel Boring Machine Penetration Rate Using a Mechanistic Approach" in Journal of *Construction Engineering and Management* 148(11), 04022128. https://doi.org/10.1061/(ASCE)CO.1943-7862.0002402 (2022) and has been reprinted with permission from ASCE.

Despite these advancements, the ability to accurately predict productivity for the purposes of planning, controlling, and monitoring MBTM-based excavation remains an enduring issue. Without the ability to accurately predict penetration rates, owners are unable to effectively evaluate, control, and improve contractor performance. Problems of predicting productivity arise because of a wide variety of factors, such as the complexity of the underground operational process, and, more importantly, the penetration rate estimation of the MTBM. According to the Standard Design and Construction Guidelines for Microtunneling (2015), the penetration rate is defined as the "instantaneous excavation distance per time while the MTBM is operating, typically measured in inches per minute or millimeters per minute" (ASCE 2015). MTBM penetration rate prediction is a challenging, difficult, and unresolved problem due to the dynamic and complex interactions of the MTBM with uncertain and variable geotechnical conditions at the tunnel face that affect machine performance. Inaccurate prediction of machine penetration rates may lead to various types of issues including delays, cost overruns, and subsequent project failures (Wang et al. 2020).

To address these issues, several studies investigated the penetration rate of tunnel boring machines (TBMs) (Sapigni et al. 2002, Yagiz and Karahan 2011, Jamshidi 2018); however, the majority of the studies were applicable in the context of large diameter tunneling excavations through hard rock formations. Due to the inherent difference between the failure mechanisms of—and the parameters describing the penetration phenomenon into—rocks and soils, these previous studies are not applicable for penetration rate prediction of MTBMs into soft ground conditions. Moreover, the approaches employed in previous studies to mechanically analyze the penetration phenomenon were experimental in nature and required equipped laboratory setups or the collection of data from several field tests from a wide variety of tunneling projects (Yagiz and Karahan 2011).

Addressing these gaps opens a new avenue for researchers and industry practitioners to quantifiably understand the mechanistic behavior of MTBMs and provides new opportunities to evaluate its influential factors. Such understanding is crucial for improving MTBM penetration rate prediction.

This study proposes a novel theoretical mechanistic approach based on the fundamental theory of contact mechanics to model the penetration rate of MTBMs into soft ground conditions when access to experimental facilities and sufficient field data from multiple microtunneling projects is limited. The primary goal of this study is to improve the prediction of MTBM penetration rate in soft ground conditions using theoretical mechanistic approach by developing an analytical mechanistic model of penetration rate prediction. Here, a review of the literature is presented, followed by the research methodology and an illustration of mechanistic model development. Then, testing and validation of the model is described, followed by a discussion and the research conclusions.

2.2. Research Background

Penetration rate prediction of tunnel boring machines (TBMs) or MTBMs under different operational loads and various ground conditions has been one of the main challenges of tunneling/microtunneling projects. Research on developing a model for penetration rate prediction dates back to 1975, when Tarkoy (1975) worked on examining various geotechnical measurements and offered total hardness measurements for predicting penetration rates in hard rock formations. Since then, various models have been developed to predict penetration rates in hard rock formations. For mechanical analysis of penetration rate phenomenon, several scholars have used experimental approaches and developed empirical equations predicting TBM performance for tunneling through hard rock formations. Early studies investigated the TBM performance based on the forces acting on

disc cutters at the interface with different rock types and characteristics using laboratory tests or field tests data (Roxborough and Phillips 1975, Graham 1976, Ozdemir et al. 1978, Farmer and Glossop 1980, Snowdon et al. 1982, Bamford 1984, Lislerud 1988, Innaurato et al. 1991). Continuing experimenting disc cutter performance, one of the well-known mechanical models for TBM performance prediction in hard rock formations was established by Rostami and Ozdemir (1993), who developed the Colorado School of Mines (CSM) model based on linear cutting machine (LCM) tests. Taking advantage of extensive full-size tests under controlled field conditions on intact rock properties, including unconfined compressive rock strength (UCS) and tensile strength; cutting geometry, including cutter spacing (S) and depth of penetration (P); and cutter geometry, including cutter diameter (D), tip width (W), and cutter edge angle (θ), a penetration rate prediction model was developed based on forces acting on disc cutters. A summary of the parameters used in their experimental analysis is illustrated in Figure 2.1.

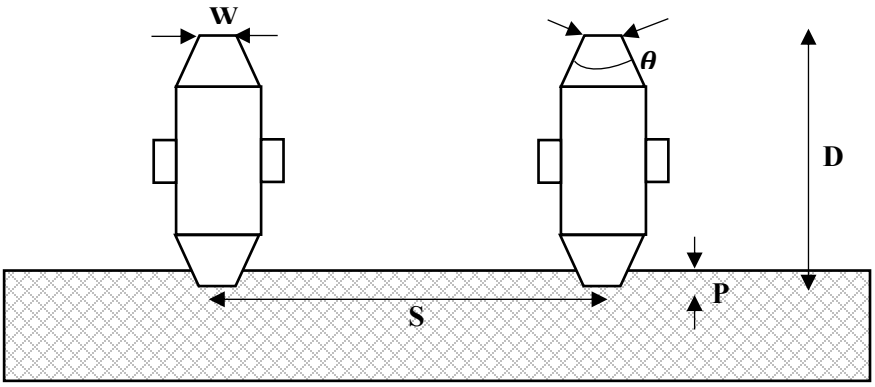

Figure 2. 1. Parameters used for experimental analysis of rock cutting by disc cutters for the CSM model

Another well-known study for predicting tunneling performance in hard rocks was performed at the Norwegian University of Science and Technology in Trondheim (NTNU) (Bruland 1998). In contrast to the CSM model that studied the forces on individual disc cutters, the NTNU model is based on the achieved performance of the machine in the field as a whole system. To construct the

NTNU model, several Norwegian drillability tests were performed to estimate TBM tunneling time. The basic input of the NTNU model requires values obtained from brittleness, Sievers J index, and abrasion tests. Based on these values, other indices, including drilling rate index (DRI), cutter life index (CLI), bit wear index (BWI), and correction factor (k) for joint class can be determined. These indices, along with cutter load capacity, average spacing of the cutters on the cutterhead, cutter diameter, and TBM parameters (e.g., diameter), were used to predict the base penetration rate (mm/rev), which can be converted to the instantaneous penetration rate (Bruland 1998). Although these studies provided well-defined models to estimate TBM performance, use of them on different projects, however, has revealed that they are applicable only to a specific range of geological conditions and require some adjustments or correction factors to be used on certain geological conditions (Hassanpour et al. 2010). This fact led to the study of TBM performance in the context of specific rock types and characteristic, such as the model developed by Hassanpour et al. (2009b) to predict TBM performance in carbonate-argillaceous rocks. In recent years, research on TBM performance has been directed towards examining various rock parameters and indices and developing new models based on them (Gong, and Zhao 2009, Hamidi et al. 2010, Jamshidi 2018 and Gong et al. 2022), or enhancing the previously well-known models by making them more generic by compiling comprehensive databases or reducing the limitations and number of input parameters required (Farrokh et al. 2012, Gong et al. 2022, Oreste and Spagnoli, 2022). For example, Hamidi et al. (2010) used a rock mass rating (RMR) system to develop an empirical performance prediction model of hard rock TBMs. Jamshidi (2018) used rock brittleness indices to establish statistical models for predicting the TBM penetration rate in rock by employing regression analysis to determine the correlation between TBM penetration rate and rock brittleness indices. Gong et al. (2022) used rock mass characteristic (RMC) model for

prediction of TBM penetration rate. In the RMC model, the basic concept is to find the correlation between the rock mass boreability index (BI) and TBM penetration rate using a power function. In their approach, they created a comprehensive database from laboratory cutting tests and actual job sites to model the interaction between rock mass and cutters. Oreste and Spagnoli (2022) developed a new probabilistic procedure based on the NTNU model to predict the advancement of TBM per revolution of TBM head. Their main goal was to facilitate the use of the NTNU model considering numerous parameters without the relative orientation of discontinuities of the rock with respect to the excavation face. Although, TBM performance through rock formations is studied extensively, research on the MTBM performance during microtunneling through soils is limited. Hegab (2005) studied the productivity of microtunneling projects by collecting data from 35 microtunneling projects done by four different contractors using six different MTBMs. Based on the collected data, Hegab et al. (2006) performed statistical regression analysis to correlate the MTBM penetration time to jacking force, diameter, jacking length and cutterhead shear force. By using that database, Elwakil and Hegab (2018) developed a probabilistic model of MTBM penetration rate for different classes of soil types. Although these models provided good insights for contractors to estimate the penetration time during microtunneling construction, the application of these models was, however, limited to specific ranges of drive length, diameter, and jacking and shearing forces, and more importantly did not mechanistically analyze the mechanism of MTBM behavior during excavation through soils. Thus, the aforementioned models cannot be used to examine the influence of various mechanistic factors, such as cutterhead characteristics, on the overall performance of MTBMs.

2.3. Research Gaps on Modeling MTBM Penetration Rate into Soft Ground

A review of literature on TBM performance modeling reveals that there are two main gaps for predicting MTBM performance through soft ground conditions. First, most of the research on TBM/MTBM performance were limited to hard rock formations, which have entirely different failure mechanisms than soils. Not only are the characterization parameters for rocks and soils different, but a greater number of factors are required to describe rock formations due to the variety of indices developed based on experimental tests. Therefore, existing models are not applicable for penetration rate analysis of MTBM into soft ground conditions (i.e., soils). Second, the approaches taken for developing TBM/MTBM performance models are primarily based on collecting data from multiple projects and/or laboratory tests and modeling the TBM/MTBM performance based upon different rock/soil characteristic and indices, which are limited to some extent to the specific ranges of rock/soil types and TBM/MTBM characteristics. One new approach to study the behavior of a system, other than performing experimental or data analytical analysis, is to use the fundamental laws of natural science to model the behavior of a system. Once a theoretical mechanistic model is constructed, it provides the opportunity to perform various analyses of mechanistic parameters and to evaluate their impact on the behavior of the system. Accordingly, to study TBM behavior, a theoretical mechanistic approach can be used to perform mechanistic analysis for predicting TBM penetration rate based on the force balance acting on the TBM during excavation. For instance, Wang et al. (2020) used a theoretical mechanistic approach for predicting the TBM penetration rate into rocks, and determined the rock breakage depth of a single cutter based on balancing forces on disc cutters. Once they found the rock breakage depth for a single disc cutter, they numerically summed the rock breakage depth over all the disc cutter areas and determined the total volume of rock breakage per revolution of the cutterhead. Knowing that the penetration

rate is a simple multiplication of excavation volume per revolution per surface area and the cutterhead revolution per minute (RPM), they developed a numerical model for predicting the penetration rate.

To fill the above-mentioned gaps, the present research aims to develop a theoretical mechanistic model of MTBM performance for microtunneling projects that describes the relationship between the penetration rate and a combined influence of factors, such as soil properties, MTBM specifications, and operational loads. This research will improve current MTBM performance modeling practice by (1) alleviating the need to collect field data from multiple projects and/or laboratory tests, thereby reducing the cost and time required for data collection, (2) eliminating the limitations of being site or machine specific, and (3) providing an opportunity to analyze the influence of various mechanistic parameters on the behavior of MTBMs during excavations.

2.4. Proposed Methodology

First, a new approach to mechanistically model the MTBM penetration rate is presented, and fundamental factors that must be included in a mechanistic model to predict the penetration rate are identified. Then, the procedure for MTBM penetration rate modeling is detailed, and a closed-form mechanistic model of the MTBM penetration rate is obtained.

2.4.1. Introduction to Mechanistic Modeling of MTBM Penetration Rate

The components of the mechanistic model required to estimate the penetration rate were investigated. Generally, for an object that penetrates into a medium, the following factors influence the penetration depth: (1) the properties of the medium that the object is penetrating into; (2) the loads that are transferred from the object to the medium to allow the object to penetrate into the medium; and (3) the shape and configuration of the object (Figure 2.2).

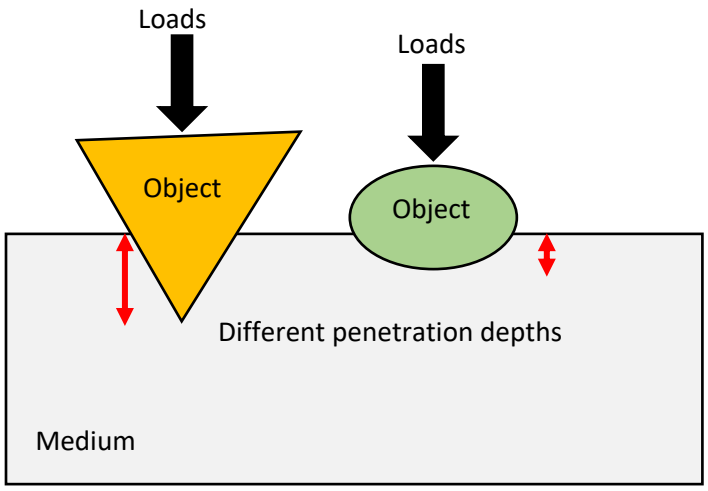

Figure 2. 2. Schematic representation of fundamental factors influencing the penetration of an object into a medium under subjected loads.

Therefore, the mechanistic model for penetration rate will be a function of the loads, properties of the medium, and characteristics of the object, as shown in Eq.2.1.

$$\text{Penetration Rate} = \text{f(loads, medium properties, object charactersitcs)} \quad (2.1)$$

2.4.2. Mechanistic Approach for Analysis of MTBM-Ground Interaction

The objective is to determine the mechanistic model, f, capable of estimating the MTBM penetration rates. One approach for examining the microtunneling process is to analyze the MTBM and ground separately (Figure 2.3A), which determines the influence of (1) MTBM operations on the ground, such as settlement, or (2) ground loads on the MTBM, such as estimating the jacking loads required to push the pipes and MTBM forward. Another approach is to analyze the MTBM and ground as a united ground-MTBM system (Figure 2.3B), which allows users to determine the dynamic, interactive influence between the MTBM and the ground, thereby allowing the relationship between operational loads and MTBM penetration rates to be determined. As such, the proposed approach views the ground and MTBM as a united ground-MTBM system, as

illustrated in Figure 2B. In this approach, the coupling interaction between the ground and MTBM must be considered to determine the load-displacement (i.e., deformation) relationship.

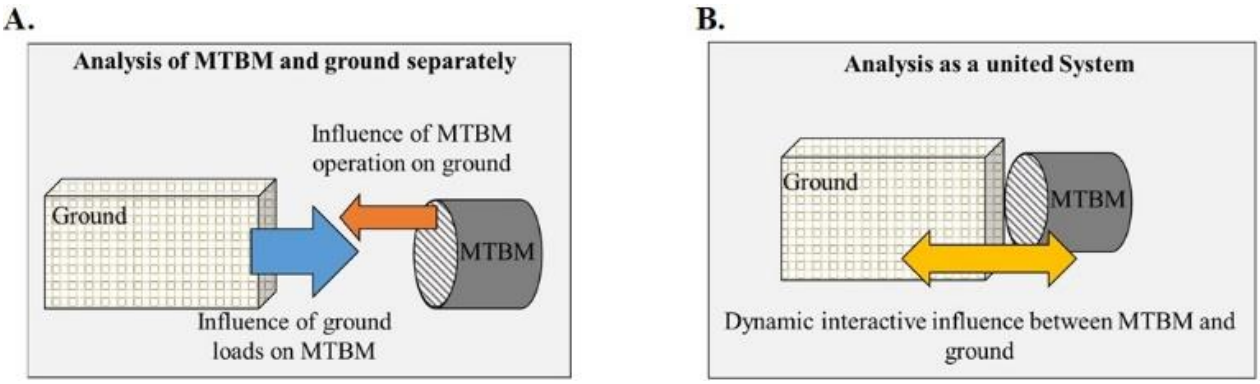

Figure 2. 3. Schematic illustrations viewing the ground and MTBM as (A) separate systems or (B) a united system.

The ground-TBM system was then mechanically examined to determine the load-displacement relationship. A new mechanistic model based on contact mechanics theory (Johnson 1985) was developed, allowing the relationship between the loads and the deformations (i.e., stresses and displacements) between two contacting bodies to be described. In the proposed modeling approach, the MTBM is assumed to be a rigid body during penetration, as the stiffness of the MTBM is much greater than the ground. By modeling the interaction between the MTBM and ground, based on defining the contact problems and solving them using the differential equations of equilibrium under the boundary conditions, the relationship between the penetration rate and the applied operational loads, soil properties, and cutterhead characteristics can be obtained.

2.4.3. Mechanistic Model Development

Contact mechanics theory is used to study the interaction between the MTBM and the ground. In this theory, the interaction between two bodies results in development of stresses at the contact point between them that consequently leads to the relative deformation of the two bodies with respect to each other, as shown in Figure 2.4A, where the MTBM is rigid (i.e., Body 1) and is

penetrating into the ground (i.e., Body 2). This interaction between the cutterhead and the ground during microtunneling is schematically shown in Figure 2.4B. During MTBM excavation, the thrust force drives the cutterhead forward, and the torque drives the rotation of the cutterhead to cut the ground. The coupling influence of the thrust and torque at the tunnel face leads to the penetration of the MTBM into the ground. This coupling phenomenon was studied, and a mechanical model capable of determining the mechanical relationship between the penetration rate and the operational loads to estimate MTBM penetration rates was developed.

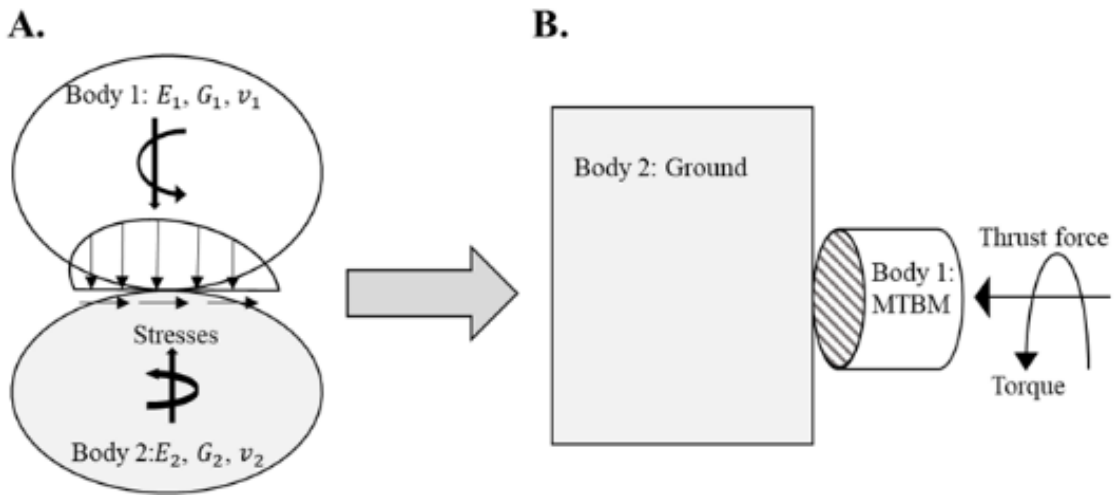

Figure 2. 4. Proposed mechanistic model for penetration rate modeling based on contact mechanics theory for (A) two contacting bodies and the stresses between them due to applied loads and (B) MTBM penetration into the ground.

Based on the theory of contact mechanics, analysis of this coupling interaction is performed by decoupling the influence of thrust force and torque on the ground. Here, the contact between the MTBM and the ground (Figure 2.5) is decomposed into two separate problems: (1) normal penetration due to the MTBM thrust force and (2) tangential rotation due to the MTBM torque.

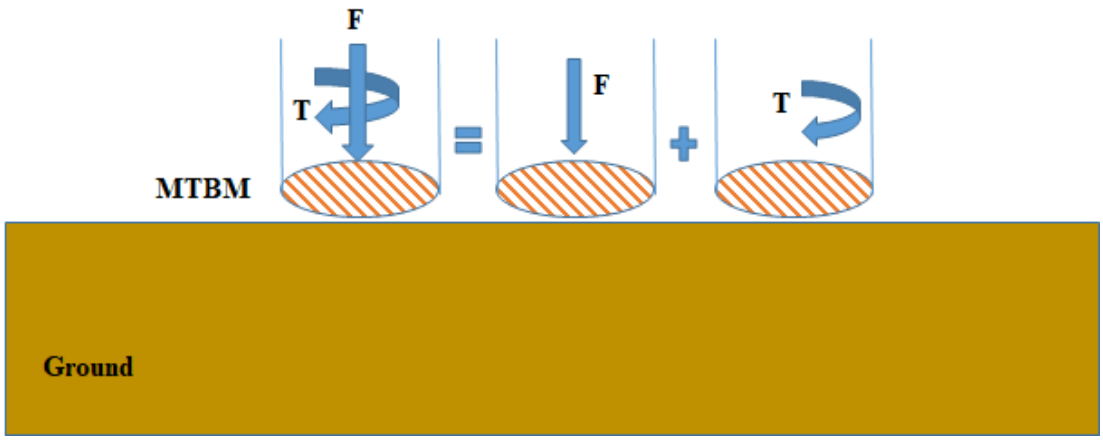

Figure 2. 5. Decoupled ground-MTBM interactions of thrust force and torque.

To obtain a mechanistic relationship between the thrust force and penetration (Figure 2.6), the differential equation of equilibrium for normal force under the boundary conditions is solved.

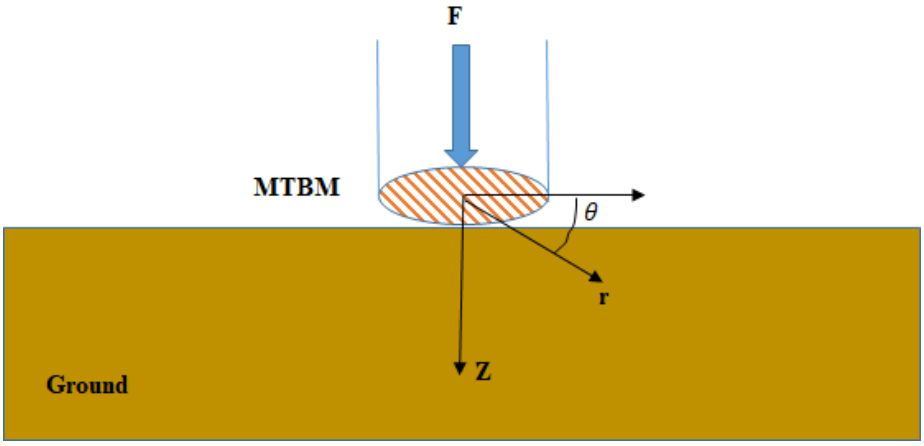

Figure 2. 6. Normal thrust force of the MTBM at the MTBM-ground interface.

Differential equations of equilibrium in cylindrical coordinates and boundary conditions for normal contact problem due to thrust force for normal contact problem are as presented as Eq.2.2 and Eq. 2.3, respectively.

$$\begin{cases} \frac{1}{1-2v}\frac{\partial}{\partial r}\left(\frac{\partial U_r}{\partial r}+\frac{U_r}{r}+\frac{\partial U_z}{\partial z}\right)+\nabla^2 U_r-\frac{U_r}{r^2}=0 \\ \frac{1}{1-2v}\frac{\partial}{\partial z}\left(\frac{\partial U_r}{\partial r}+\frac{U_r}{r}+\frac{\partial U_z}{\partial z}\right)+\nabla^2 U_z=0 \end{cases} \quad (2.2)$$

$$\begin{cases} U_z(r,0) = \delta & 0 \le r \le a \\ \sigma_{rz}(r,0) = 0 & 0 \le r \le a \\ \sigma_{zz}(r,0) = 0 & r > a \end{cases} \tag{2.3}$$

where $(U_r,\ U_z)$ are displacements in the directions of (r, z), respectively, v is Poisson's ratio of the soil , δ is penetration depth, a is the MTBM radius, and σ_{zz} and σ_{rz} are the normal and tangential stress respectively

By solving the differential equations of equilibrium under the above boundary conditions, the normal stress distribution σ_{zz} under the MTBM is obtained as Eq.2.4.

$$\sigma_{zz}(r,0) = \frac{E\delta}{\pi(1-v^2)\sqrt{a^2-r^2}} \qquad 0 \le r < a \tag{2.4}$$

where E is Young's elastic modulus. Similarly, for the tangential rotation problem due to the MTBM torque (Figure 2.7), the differential equation of equilibrium is solved under the corresponding boundary conditions.

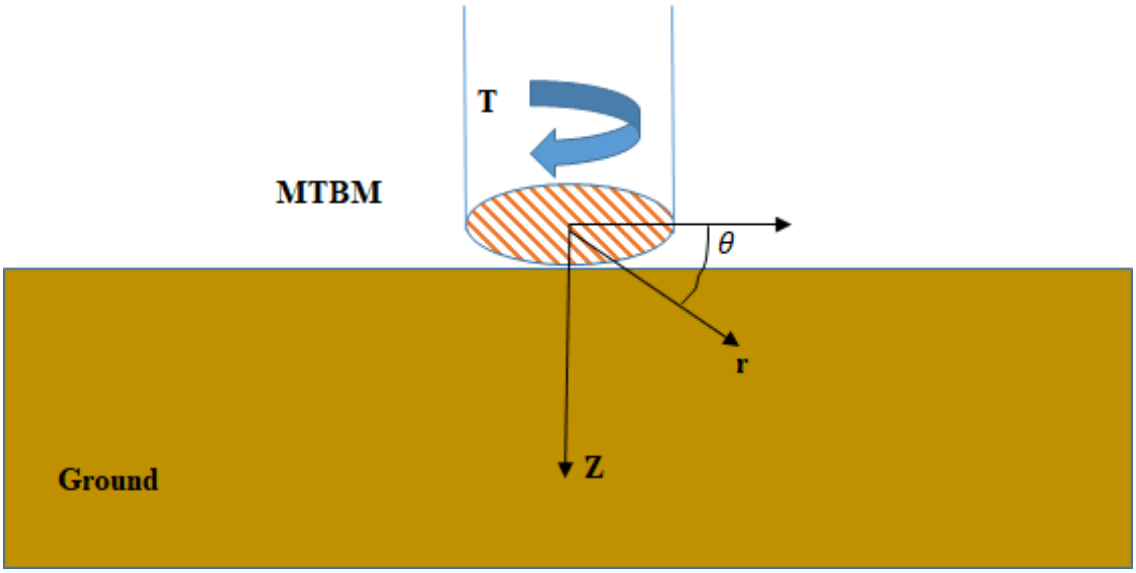

Figure 2. 7. Tangential torque force of the MTBM at the MTBM-ground interface.

The differential equations of equilibrium in cylindrical coordinates for torsional contact problem is described by Eq. 2.5.

$$G\left(\frac{\partial^2 U_\theta}{\partial r^2}+\frac{\partial U_\theta}{r\partial r}-\frac{U_\theta}{r^2}+\frac{\partial^2 U_\theta}{\partial z^2}\right)=0 \tag{2.5}$$

where (U_θ) is displacements in the directions of (θ). The boundary condition of the MTBM problem in terms of the tangential rotation of the cutterhead and considering the coefficient of friction, f, and Coulomb's friction law is shown in Eq.2.6.

$$\begin{cases}\tau_{z\theta}(r,0)=f\sigma_{zz}(r,0), & 0\le r\le a\\ \tau_{z\theta}(r,0)=0 & r\ge a\end{cases} \tag{2.6}$$

The tangential rotation problem, under the boundary conditions described in Eq. 2.6, can be solved using a normal stress distribution, σ_{zz}, that is determined using Eq. 2.4. Considering the ground as an isotropic space ($G=\frac{E}{2(1+v)}$), the shear stress distribution $(\tau_{z\theta})$ under the MTBM is obtained as Eq. 2.7.

$$\tau_{z\theta}(r,0)=\frac{2Gf\delta}{\pi(1-v)\sqrt{a^2-r^2}} \tag{2.7}$$

Once the shear stress distribution under the MTBM cutterhead is obtained, the total operational torque force can be calculated by taking the integral of the shear stress over the effective contact area between the MTBM cutterhead and the ground. The effective cutterhead area, A_e, is calculated by subtracting the opening area from the total area, A_t, as shown by Eq. 2.8.

$$A_e=(1-\mu)A_t=\int_0^a\int_0^{2\pi}(1-\mu)rd\theta dr \tag{2.8}$$

where μ is the opening ratio defined as the ratio of opening area to the total cutterhead area.

By taking the integral of the shear stress distribution over the effective contact area, the relationship between torque (T) and penetration per revolution (δ) is obtained as Eq. 2.9.

$$T = \int_0^a \int_0^{2\pi} (\tau_{z\theta}\, r)(1-\mu) r d\theta dr$$

$$= \int_0^a \int_0^{2\pi} \left(\frac{2Gf\delta}{\pi(1-v)\sqrt{a^2-r^2}} r \right)(1-\mu) r d\theta dr$$

$$= \int_0^a \left(\frac{4Gf(1-\mu)\delta}{(1-v)\sqrt{a^2-r^2}} r \right) r dr$$

$$T = \frac{\pi G f \delta a^2 (1-\mu)}{(1-v)} \tag{2.9}$$

As $\mathrm{PR}(\frac{\mathrm{mm}}{\mathrm{min}}) = \mathrm{RPM}(\frac{\mathrm{rev}}{\mathrm{min}}) \times \delta(\frac{\mathrm{mm}}{\mathrm{rev}})$, and rearranging Eq. 9, the mechanistic penetration rate (PR) model is developed as Eq. 2.10.

$$PR = \frac{RPM\, T}{\pi} \times \frac{(1-v)}{G} \times \frac{1}{f a^2 (1-\mu)} \tag{2.10}$$

The developed model enables engineers to determine MTBM behavior by (1) considering soil behavior parameters (i.e., shear modulus and Poisson's ratio) that are influential in terms of the response of the soil under cutterhead loads; (2) incorporating the influence of cutterhead characteristics, namely diameter and opening ratio, which influence MTBM performance considerably; and (3) incorporating operational load factors, such as torque and RPM.

As such, the developed model establishes a state-of-the-art relationship between MTBM penetration rates and the integrated influence of soil properties, operational loads, and cutterhead characteristics, as shown in Figure 2.8.

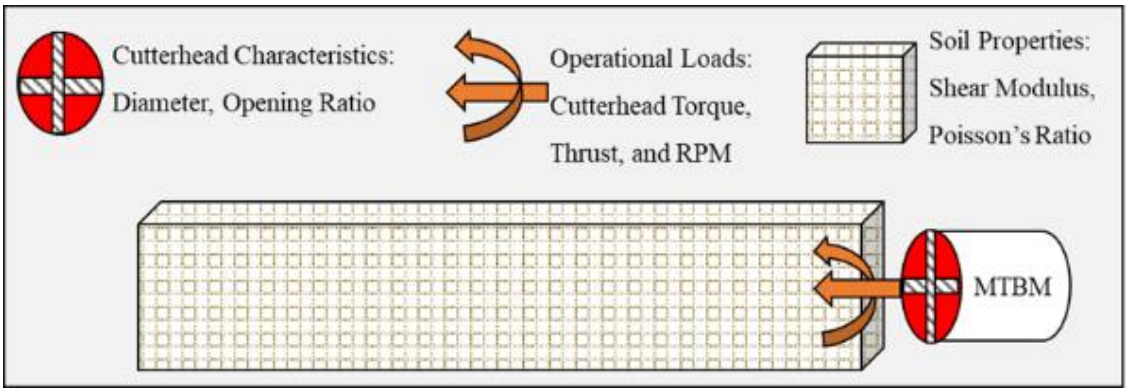

Figure 2. 8. Mechanistic model input parameters for MTBMs.

2.5. Model Evaluation

Two approaches were used to test the proposed mechanistic model. First, the model was tested under extreme conditions to evaluate model performance over a wide range of soil/MTBM conditions. Then, the predictive capability of the model was evaluated following its application in a microtunneling project case study. Results are detailed as follows.

2.5.1. Extreme Condition Test

To test model performance under extreme conditions in terms of soil and MTBM characteristics, and to compare the results with typical conditions, a set of different microtunneling excavation conditions was considered and the corresponding penetration rate for each condition was calculated, as shown in Table. 2.1.

Table 2. 1. Excavation conditions with corresponding model parameters and penetration rates.

Excavation Conditions (Soil/MTBM)	G (MPa)	$\boldsymbol{\nu}$	$\boldsymbol{a}$ (m)	$\boldsymbol{\mu}$ (%)	f	RPM (rev/min)	T (%)	PR (mm/min)
Hard soil/ Large diameter	80	0.1	1.4	45	0.4	1.2	88	4.82
Very soft soil/ Small diameter	10	0.4	0.4	10	0.1	2	6	87.54
Medium stiff soil/ Moderate diameter	20	0.25	0.75	30	0.25	1.6	20	21.34
Hard soil/ Moderate diameter	80	0.1	0.75	45	0.4	1.2	88	16.81
Very soft soil/ Moderate diameter	10	0.4	0.75	10	0.1	2	6	24.90

The extreme conditions were considered based on the degree of soil stiffness and on the MTBM diameter, which generally falls in the small diameter tunneling category (i.e., less than 3 m) (Ueki et al. 1999). Penetration rates predicted for the extreme conditions of very soft soil/small diameter and hard soil/large diameter microtunneling construction (87.54 mm/min. (5.25 m/h) and 4.82 mm/min. (0.29 m/h), respectively; Table 2.1), were consistent with expectations that smaller diameter tunnels with soft soils would yield a greater penetration rate than larger diameter tunnels with hard soils.

Under the more typical conditions of medium stiff soil/moderate diameter tunnels, the model predicted a penetration rate of 21.34 mm/min. (1.28 m/h), which is consistent with penetration rates under similar conditions observed in microtunneling practice (Elwakil and Hegab, 2018). Together, these results demonstrate that the model is responsive to changes in input conditions and is able to generate results that are expected and observed in microtunneling practice.

2.5.2. Case Study 1

To validate the application of the developed mechanistic model for penetration rate prediction, the penetration rates predicted by the proposed methodology were compared to actual values obtained from microtunneling data collected during the construction of a sanitary trunk in Alberta, Canada.

The project used a number of drilling methods, including open cut from Borehole 1 to Borehole 11, horizontal directional drilling from Borehole 11 to Borehole 12, and microtunneling from Borehole 12 to Borehole 16 (Figure 2.9). The diameter and length of the tunnel were 1.5 m and 2.6 km, respectively, and tunnel depth ranged from 6 m to 15 m. The tunnel was composed of silty clay to clayey silt soil types, and, at some locations, traces of silty sand were identified. The soil types found at each borehole along the microtunneling sections under study are illustrated in Figure 2.10. Since MTBM data were only available for two microtunneling sections, BH 4 to BH 14, and BH 5 to BH 6, in the present study these two sections were examined in developing the model. Moreover, since the MTBM is passing through different soil types in these two tunnel sections, the model will be tested on different ground conditions to show its practicality in the context of varied soil types.

Operational load parameters (i.e., torque and RPM) were obtained from the MTBM data acquisition system; cutterhead characteristics (i.e., cutterhead radius and opening ratio) were obtained from project specification documents; and soil properties were obtained from geotechnical field investigation reports.

Geotechnical information obtained from borehole sampling data were used to interpolate geotechnical conditions for the entire length of the tunnel. A summary of geotechnical data at each borehole along the microtunneling potion of the tunnel is provided as Table 2.3. The Poisson's ratio for the entire tunnel length was assumed to be 0.25, and the shear modulus (G) was calculated

based on Young's elastic modulus (E) assuming that the soil material is isotropic. The main MTBM specifications used for this project are detailed in Table 2.2.

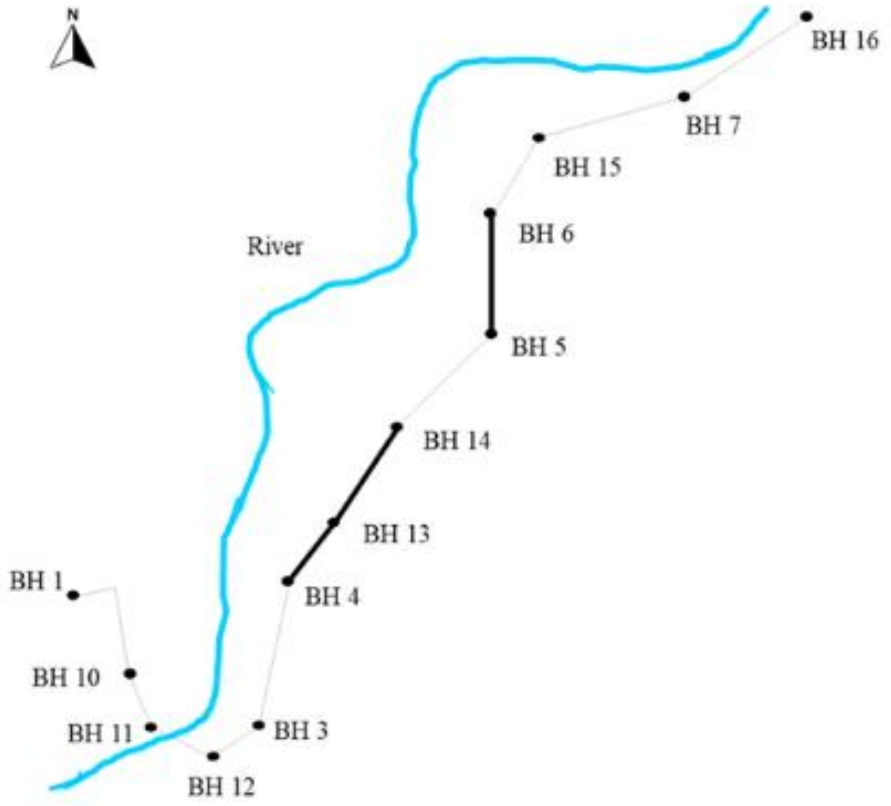

Figure 2. 9. Borehole locations along sewer line of sanitary trunk project under study. Black and gray lines show the availability or unavailability of MTBM data respectively.

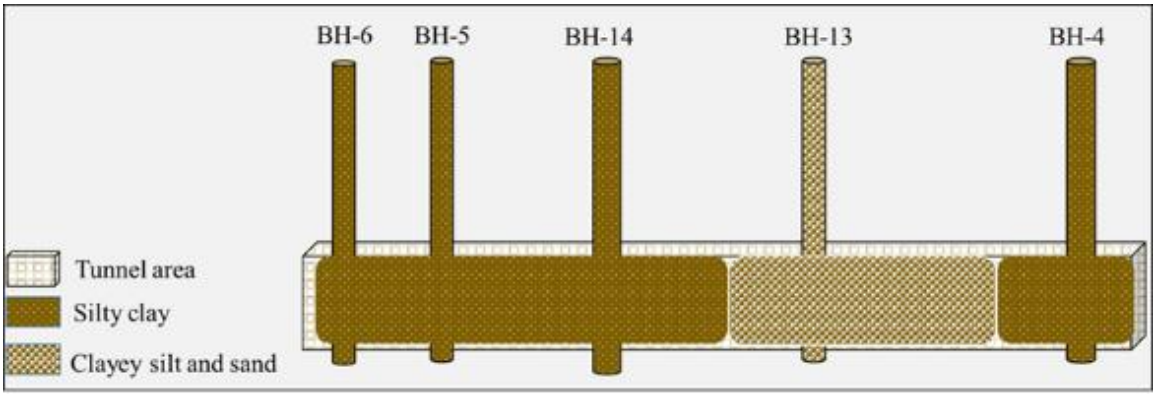

Figure 2. 10. Schematic representation of interpolated geological conditions along sewer line of sanitary trunk project for the selected sections under study between BH 4 to BH 6 based on geotechnical investigation report.

Table 2. 2. Specifications of MTBM.

Cutterhead Parameter	Value
Opening ratio (μ; %)	30
Diameter (R; mm)	1500
Speed (RPM)	0-3
Torque (nominal; kN·m)	550
Maximum operating thrust (ton)	630

Table 2. 3. Geotechnical data collected from borehole sampling along tunnel length.

Closest Station	Borehole	Soil Type	UCS (MPa)	Strain at Failure (%)	E (MPa)
11+100	BH 4	Silty Clay	30	3	10
11+300	BH 13	Clayey Silt + Sand	75	3.1	24.19
11+600	BH 14	Clayey Silt	47	2.2	21.36
11+900	BH 5	Silty Clay	68	9.7	7.01
12+200	BH 6	Silty Clay	54	4.4	12.27
12+500	BH 15	Silty Sand	74	5.2	14.23
12+700	BH 7	Clayey Silt	60	10.4	5.76
13+100	BH 16	Silty Clay	43	9.1	4.72

A comparison of the actual and predicted penetration rates for two different tunnel sections (BH 4 to BH 14 and BH 5 to BH 6) is presented in Figure 2.11. Since the frequency of fluctuations in penetration rate is very high along tunnel length, it is not possible to graphically show the results clearly for the entire tunnel sections, therefore only short portions of tunnel sections are presented in Figure 2.11. Model accuracy was calculated using the mean absolute percentage error formula (De Myttenaere et al. 2016), and was determined to be 83% overall for two tunnel sections, indicating that the developed model is able to provide a reasonable estimate of MTBM penetration rates when compared to rates obtained from similar microtunneling productivity studies (Hegab 2005, Hegab et al. 2006).

Moreover, the covariance between the two datasets was 84%, demonstrating that the proposed mechanistic model was capable of predicting the trends and fluctuations in penetration rates along the microtunneling portion of the project. This is important feature of the developed model, as it indicates that the behavior of MTBM with soft ground conditions, in terms of direction of changes on MTBM penetration rate due to facing different soil types under various operational loads is properly modeled.

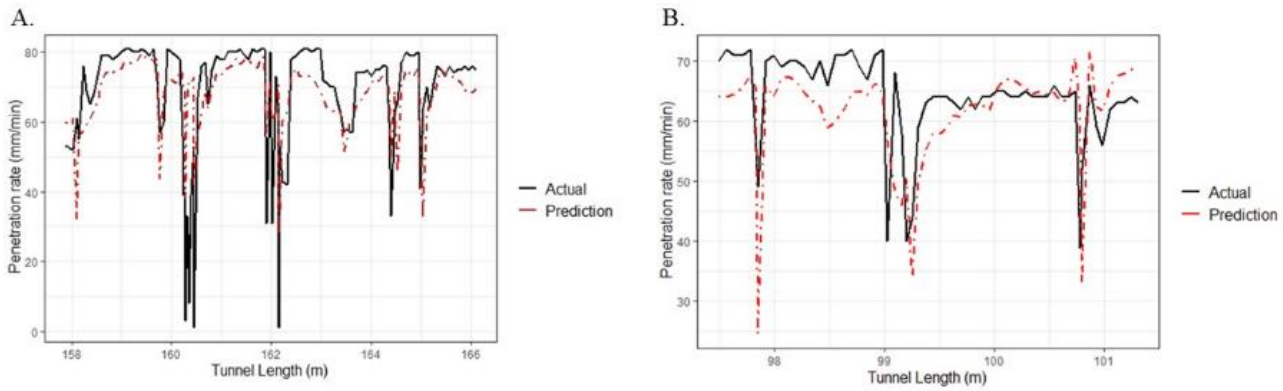

Figure 2. 11. Comparison of actual and model predicted penetration rates along the (A) BH 4 to BH 14 and (B) BH 5 and BH 6 portion of the project under study.

2.5.3. Case study 2

The developed framework was applied to microtunneling construction in Edmonton, Canada. This project consists of two microtunneling sections between BH 18 to BH 15 (section A) and between BH 4 to BH 10 (section B) (Figure 2.12). To excavate the ground a hydraulic pressure cutter with a maximum torque capacity of 22 MPa pressure is used. Based on project document specifications each 1 MPa pressure is equal to 1.2 T.m torque. During the MTBM excavation the opening ratio varies between minimum 30% and 50% with a mode of 40% and the RPM varies between 1.2 to 1.92 with a mode of 1.51. The diameter of tunnel was 1.69. According to the geotechnical investigation report a shear modulus along the tunnel varies between 5 to 25 MPa and Poisson' ratio is between 0.2 to 0.25. The friction coefficient between cutterhead and ground is determined

by expert to be between 0.15 to 0.35 with an average of 0.25. The developed model is examined for both section A and B. The results of the comparison of the actual and predicted penetration rates along these two tunnel sections are shown in Figure 2.13. Model accuracy was 76 % for overall two tunnel sections, indicating that the developed model is able to provide a reasonable prediction of MTBM penetration rates along the various tunnel sections.

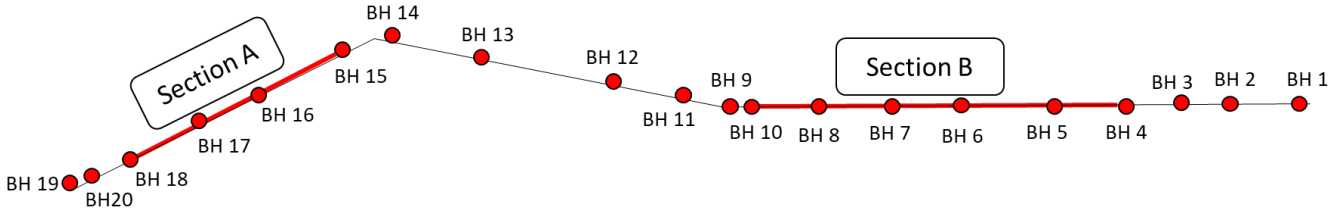

Figure 2. 12. Microtunneling alignment for the examined microtunneling project.

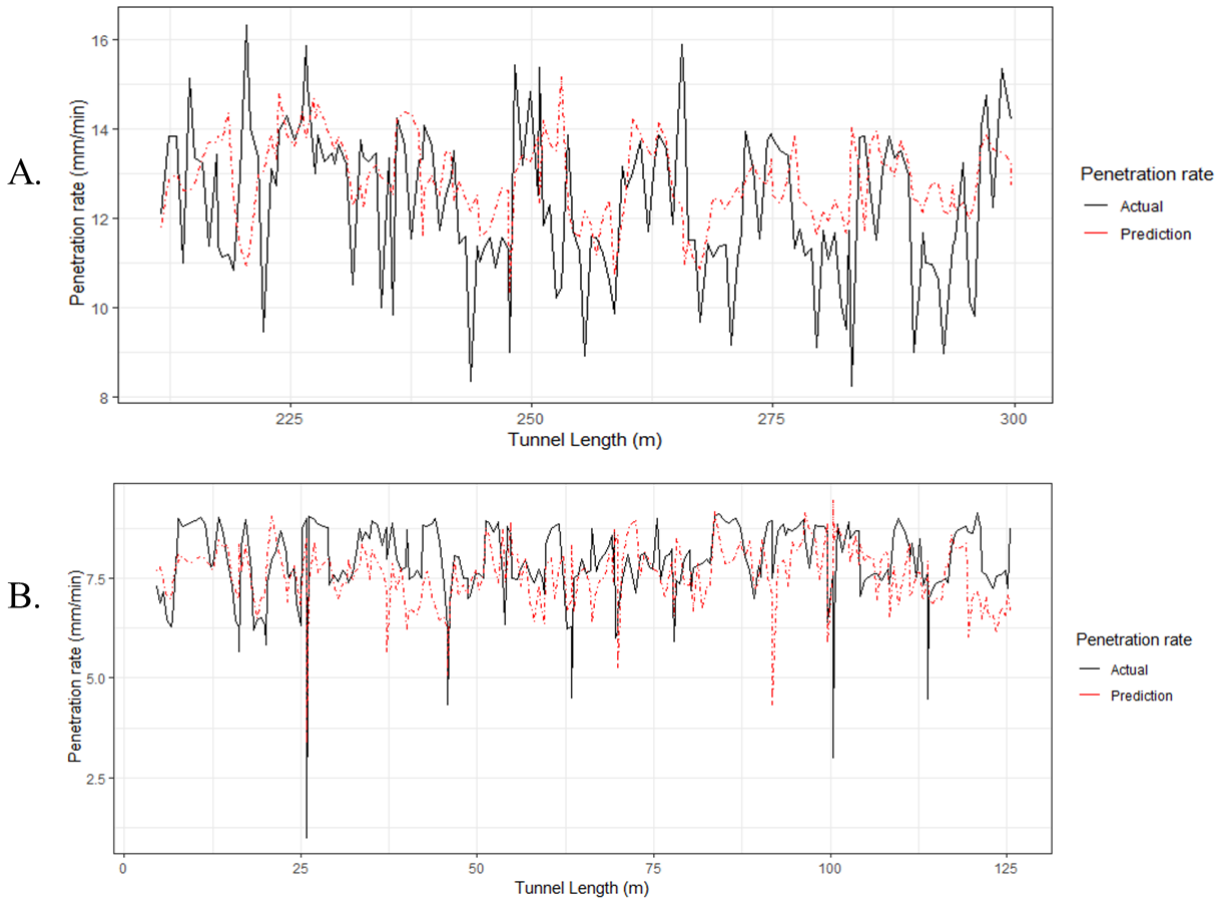

Figure 2. 13. Comparison of actual and model predicted penetration rates along the (A) section A and (B) section B of tunnel.

2.6. Discussion

This study proposes a novel, contact mechanics theory-based mechanistic model for MTBM penetration rate modeling in microtunneling excavation projects. To construct the mechanistic model, fundamental factors affecting the MTBM penetration rate were studied and the primary components of a mechanistic model for MTBM penetration rate modeling were identified. Then, the mechanistic approach for analysis of MTBM-ground interaction is illustrated and two fundamental mechanistic approaches for analysis of MTBM-ground interaction are presented. One is to look at the MTBM and ground as separate systems interacting with each other, and the other is to analyze their interaction as a united system. It is shown that in order to be able to determine

the dynamic, interactive influence between the MTBM and the ground, the later approach should be used. Accordingly, to analyze the MTBM and ground as a united system, a contact mechanics theory is employed and a mechanistic model of MTBM penetration rate is constructed. The developed model incorporates the primary components that are expected to be in the mechanistic model including soil properties, cutterhead characteristics, and operational loads.

Accuracy, functionality, and reasonableness of the proposed mechanistic model were evaluated using both an extreme conditions test and an event validity test using a real case study (Sargent 2013). Two tunnel sections with different soil types and characteristics were selected to show the applicability of the model on various soil types. The proposed mechanistic model was found to be responsive to changes in soil and MTBM characteristics, was capable of generating reasonable results with high accuracy, and was able to mimic the fluctuations in penetration rates observed in a real project. The ability of the developed model to correctly predict the variations in MTBM penetration rate due to varied soil types indicates that the MTBM behavior was successfully modeled. This enables engineers to forecast sudden drops or jumps in penetration rate, thereby avoiding problems, such as failure of MTBM operation, because the necessary steps can be taken in advance to prepare for successful operation of MTBMs.

2.7. Conclusion

MTBM penetration rate prediction is one of the key elements of successful planning and controlling in microtunneling projects. The present research identified two main research gaps in the context of modeling the MTBM penetration rates through soft ground conditions (i.e. soils). The first is the geology: Most research studies examined rock formations, which have entirely different characteristics than soils. The second is that other studies used different approaches to model the penetration rate phenomenon. A common approach for modeling the TBM/MTBM

penetration rates was limited to either the use of data collected from multiple projects or performing laboratory tests to analyze the behavior of TBM/MTBMs under various soil/rock mass properties and indices. Although this approach provided well-established models, it does, however, still suffer from the challenge of needing a comprehensive list of various projects with a wide variety of machine specifications and soil/rock properties. Therefore, the approach is limited to specific ranges of available machine types and soil/rock properties. In this regard, the present study aims to address these gaps by developing a mechanistic model of MTBM penetration rate through soils using the fundamental theoretical contact mechanics approach. The developed model identified the relationships between the penetration rate and three primary influential factors, specifically operational loads, soil properties, and cutterhead characteristics, thereby providing an analytical tool that facilitates the analysis and prediction of MTBM penetration rates and their variability under the influence of these factors. This provides a great opportunity for practitioners to evaluate the impact of changes to each of model parameters on MTBM penetration rate without the need to undertake time-consuming and expensive field tests, especially in the early stages of a project.

The proposed mechanistic model is expected to enhance the planning of microtunneling projects by providing practitioners with an objective and comparatively accurate method to predict penetration rates along a tunnel length for new projects. More accurate penetration rate predictions are expected to improve the planning of microtunneling projects by reducing deviations from planned schedules resulting from inaccurate productivity estimates or by identifying high and low penetration rate zones enabling mitigation strategies (i.e., those that would prevent cutterhead clogging) to be more effectively implemented.

The present research should be considered in light of being limited to soft ground (i.e., soil) conditions with a stable tunnel face. It is not applicable for excavations through rock formations due to the difference in their characteristics. Future research may include considering wearing between cutterhead and the ground and modeling its influence on the MTBM penetration rate. Moreover, extensive theoretical mechanistic analysis of the impact of cutterhead characteristics on MTBM penetration rate would be insightful for selection of appropriate MTBMs for new projects.

2.8. Data Availability

All models generated or used during the study are available from the corresponding author upon reasonable request. Case study data used in this research were provided by a third party. Direct requests for these materials may be made to the provider indicated in the Acknowledgements.

2.9. Acknowledgment

This project was supported by a Collaborative Research and Development Grant (CRDPJ 532148) from the Natural Sciences and Engineering Council of Canada. The authors would like to thank the Shanghai Construction Group Canada Corp. for their continued support and for providing case study data.

Chapter 3: Mechanistic Modeling of Cutterhead-Ground Engagement Influence on Micro-tunnel Boring Machine Penetration Rate

3.1. Introduction

The microtunneling method has found widespread application in the context of pipeline installation in recent decades due to its non-disruptive and environmentally friendly characteristics. In this non-person entry construction method, a micro-tunnel boring machine (MTBM) is remotely controlled from the surface and the MTBM typically navigates using a laser-guided approach. While a hydraulic jack pushes the MTBM and pipe sections into the soil, the excavated materials are continuously removed from the tunnel face. The excavation process underground happens out of sight, which makes the planning of such construction operations a challenging task due to lack of visual monitoring of the excavation processes at the tunnel face. Therefore, prediction of MTBM performance and its behavior plays a key role in terms of planning and controlling microtunneling projects. One of the critical MTBM performance factors for accurate planning of micro tunneling construction is estimation of the MTBM penetration rate into the soil.

Research on developing a model for penetration rate prediction dates back to 1973, when Tarkoy (1975) worked on examining various geotechnical measurements and offered total hardness measurements for predicting penetration rates in hard rock formations. Since then, various models have been developed to predict penetration rates in hard rock formations. Several scholars have used experimental approaches and analyzed forces acting on disc cutter (Rostami and Ozdemir

1993, Bruland 1998) or performed statistical analysis of various rock indices and examined the influence of different rock parameters (Hassanpour et al. 2009b and 2010; Hamidi et al. 2010; Jamshidi, 2018; Oreste and Spagnoli, 2022) and developed empirical equations predicting tunnel boring machine (TBM) performance. Although the penetration rate of TBMs for hard rock tunneling projects has been extensively studied, there are few studies that aimed to study the penetration rate of MTBMs into soils. The existing models for penetration rate estimation of MTBM into the soft ground conditions are based on statistical and data analytical approaches (Hegab et al., 2006; Elwakil and Hegab, 2018). For instance, Hegab et al (2006) collected data from 35 microtunneling projects and developed a regression model for penetration rate estimation of MTBMs. Elwakil and Hegab (2018) used the same database as Hegab et al. (2006) and developed a penetration rate prediction model using statistical regression analysis for different soil types. Based on the collected data and soil type classification, they developed different regression equations to estimate the MTBM penetration time.

While these studies of MTBM penetration rate provide construction managers with good insights into the MTBM penetration time into soil, they do not illustrate mechanistically the mechanism of MTBM penetration rate for the purposes of assessment of MTBM performance and predictions of its behavior for the unexcavated tunnel length. In fact, a mechanistic approach for understanding the underlying physics of MTBM interaction with soil has not yet been extensively studied. In this regard, the aim is to mechanistically study the cutterhead-ground engagement mechanism and analyze its influence on the MTBM penetration rate. By employing a contact mechanics theory and analyzing the engagement area between the cutterhead and ground, a mechanistic model of MTBM penetration rate based on cutterhead engagement is developed. Further analysis of cutterhead engagement area, and consideration of two extreme cases of largest and smallest

engagement areas at tunnel face, lead to development of an upper boundary and a lower boundary for penetration rate estimation. These boundaries determine the range within which the actual penetration rate is and therefore can be used for reducing the planning uncertainties. Moreover, these two boundaries can be used to evaluate MTBM performance in the context of a variety of soil types and conditions based on the degree of cutterhead engagement with soil.

3.2. Research Background

Successful planning and execution of a tunneling/microtunneling project requires accurate determination of the TBM/MTBM penetration rates. Penetration rate is a function of cutterhead-ground interaction, therefore, an analysis of cutterhead behavior at the tunnel face interface is required to determine the penetration rate. In this regard, several studies have been done to analyze this phenomenon. Analysis of cutterhead behavior has been done for various purposes such as development of cutterhead thrust and torque estimation models (Shi et al. 2011, Han et al. 2017); analysis of stability of excavation face, soil discharging rate, and cutterhead torque and wear (Wu et al. 2013, Jin et al. 2021); modeling the effects of penetration depth and disc cutter linear velocity on the performance of disc cutter cutting process (Fang et al. 2021); and analysis of disc cutter failure modes and their causes during tunneling (Ling et al. 2022). Review of literature reveals that although cutterhead behavior has been studied thoroughly, there remains a gap in terms of analyzing the mutual interactive engagement between the cutterhead and the ground. In other words, review of literature shows that the studies on interaction between cutterhead and ground belong primarily to one of two major groups: either the studies analyzed (1) the response of ground under cutterhead loads, or (2) the response of cutterhead due to the ground. This perspective on cutterhead behavior analysis has led to the development of models that aimed to analyze the response of ground, such as face stability and tunnel face failure (Group 1), or models that aimed

to analyze the response of cutterhead, such as cutterhead torque and disc cutter failure and wear (Group 2). However, there is a third group of studies that investigated the mutual interactive engagement between cutterhead and ground. In this group of studies, analysis of the cutterhead-ground engagement for the purpose of understanding its influence on the MTBM penetration rate into the ground has not yet been studied from a mechanistic perspective. Moreover, the existing models on cutterhead-ground mutual interactions are complex, requiring several computational inputs, are limited to project specifications and are not user friendly enough to provide construction engineers with a clear picture of cutterhead-ground engagement influence on MTBM penetration rate. In this regard, the present research aims to address these gaps through mechanistic analysis of cutterhead-soil engagement and by developing analytical models based on fundamental theoretical laws that shed light on the influence of cutterhead-ground engagement on MTBM penetration rate. The analytical models developed in the present study may be easily employed by construction engineers and managers to improve productivity of microtunneling construction projects by incorporating it into modeling the entire microtunneling operation system.

3.3. Methodology

First, the mechanistic approach to modeling the cutterhead-ground engagement is illustrated. Then, the procedure for modeling is detailed, and a closed-form mechanistic model of the cutterhead-ground engagement is presented.

3.3.1. Mechanistic Approach for Analysis of Cutterhead-Ground Engagement

To study and model the interaction between the MTBM and the ground, the present research employs the fundamental theory of contact mechanics. Based on this theory, the interaction between two bodies contacting each other can be analyzed and their relative deformation due to the stresses at the contact between them can be determined as shown in Figure 3.1-A. By applying

this theory, the interaction between MTBM and ground is modeled by assuming MTBM as Body 1 and the ground as Body 2 as shown in Figure 3.1-B. At the contact between MTBM and ground, the MTBM penetrates into the ground due to the thrust force that propels the cutterhead forward and torque force that rotates the cutterhead to cut the ground at the tunnel face.

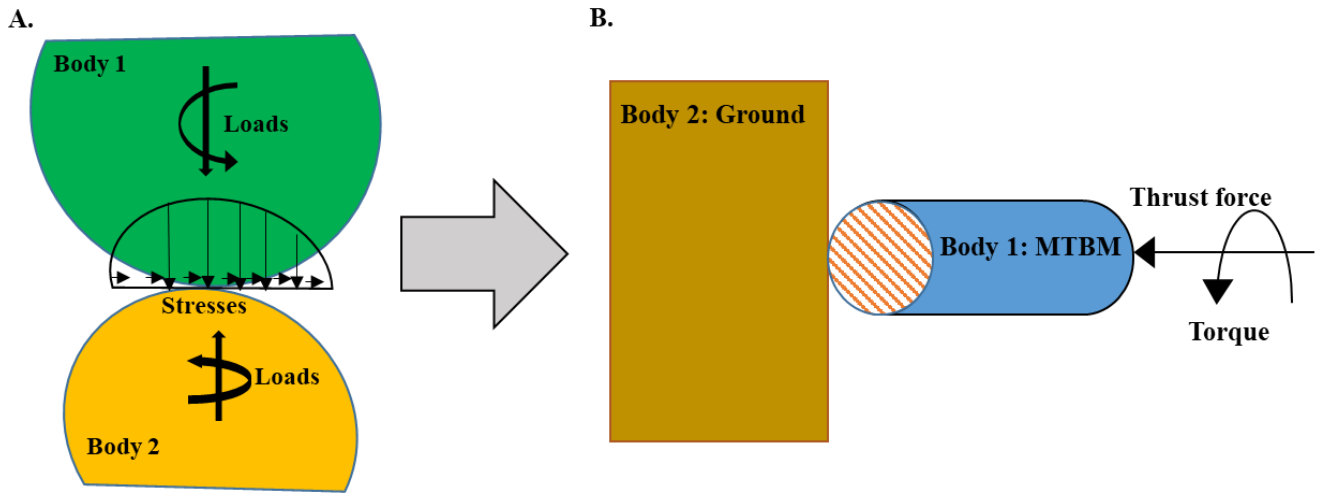

Figure 3. 1. Proposed mechanistic model for penetration rate modeling based on contact mechanics theory for (A) two contacting bodies and the stresses between them due to applied loads; and (B) MTBM penetration into the ground (Moharrami et al., 2022).

Mechanically, if two bodies are in contact by a normal force and consequently are subjected to a tangential force, then the interface contact area will be composed of an inner stick zone and an outer frictional zone (Johnson, 1985). Hence, the contact area between the MTBM and the ground due to normal thrust force and consequent tangential torque force can be decomposed into an inner engagement area and outer frictional area. Considering the disc cutter arrangement on the cutterhead (Figure 3.2-A), during excavation disc cutters produce the excavation trace by cutting the soil along the cutting direction (Figure 3.2-B), and while continuing the excavation disc cutters create an actual engagement area shown in Figure 3.2-C. In the present research, the actual engagement area is modeled by considering the equivalent circular engagement area in the center of the cutterhead (Figure 3.2-D). During excavation, the actual engagement area changes, which

results in variation of penetration rate. As the engagement of cutterhead increases, during each rotation of cutterhead the larger tunnel face area will be excavated, which leads to a higher penetration rate. In terms of simulating cutterhead excavation, the actual engagement area of the cutterhead can be obtained from experimental tests; however, by considering instead the two extreme cases of largest and smallest engagement area, an upper and lower boundary for penetration rate of the MTBM can be obtained.

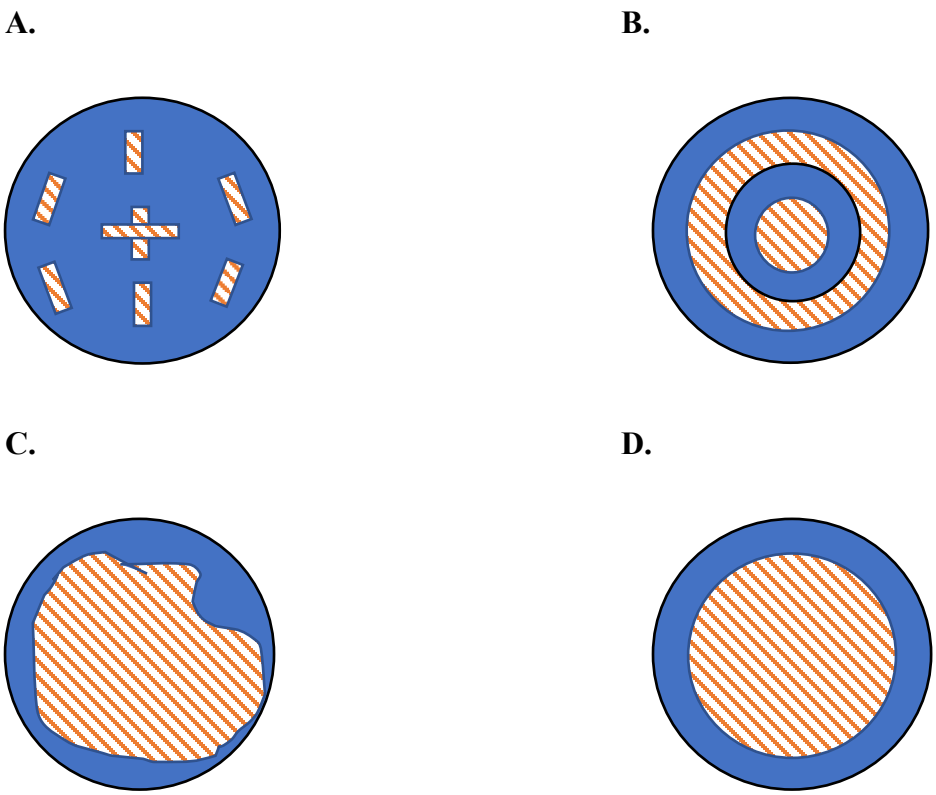

Figure 3. 2. Schematic simulation of the actual engagement area at the cutterhead-ground interface (A) Cutter arrangement (B) Excavation traces (C) Actual engagement area (D) Simulated engagement area.

3.3.2. Cutterhead-Ground Engagement Model Development

Based on the theory of contact mechanics, analysis of cutterhead–ground engagement is performed by establishing the boundary conditions for the normal stress σ_{zz}, and tangential stresses $\tau_{z\theta}$ and

normal displacement w and tangential displacement U_θ between MTBM and ground as shown in Eq. 3.1 and finding the normal and torsional stresses at the contact between cutterhead and ground.

$$\begin{cases} w\,(r) = \delta & 0 \le r \le a \\ U\,(r) = r\varphi & 0 \le r \le c \\ \tau_{z\theta}(r) = f\sigma_{zz}(r) & c < r \le a \\ \sigma_{zz}(r) = 0 & r > a \\ \tau_{z\theta}(r) = 0 & r > a \end{cases} \tag{3.1}$$

where δ is the penetration depth, φ is the torsion angle, f is friction coefficient, r is polar radius in the contact plane, and c and a are radius of cutterhead engagement and cutteread radius respectively (Figure 3.3). Referring to Moharrami et al., (2022), the solution for the normal contact problem between rigid MTBM and ground with elasticity of E and Poisson's ratio of v has been solved and the corresponding normal stresses are obtained as shown in Eq. 3.2.

$$\sigma_{zz}(r) = \frac{E\delta}{\pi(1-v^2)\sqrt{a^2-r^2}} \tag{3.2}$$

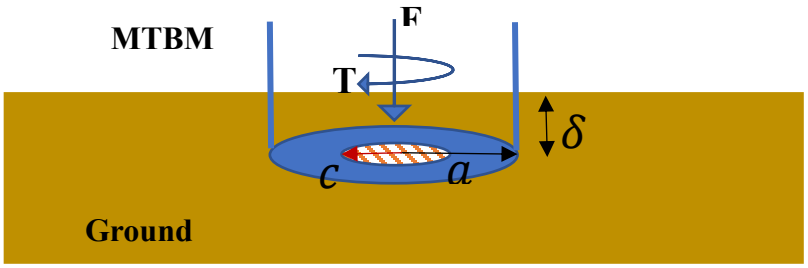

Figure 3. 3. Schematic representation of MTBM penetration (δ) under thrust force (F) and torque (T) and the radius of engagement area (c) and radius of cutterhead (a).

The solution for torsional contact is to find the function $\varphi(x, a)$ such that the boundary conditions in Eq. 3.1 are satisfied. The solution must satisfy Coulomb's law in the frictional area, and must describe a rigid body rotation in the area of engagement. In the frictional area the shear stress follows the Coulomb's friction law shown in Eq. 3.3.

$$\sigma_{\varphi z} = f\sigma_{zz} \qquad c < r \leq a \tag{3.3}$$

where f is friction coefficient and σ_{zz} is the normal stress. In the engagement area, the shear stress $\sigma_{\varphi z}$ can be obtained by Eq. 3.4 (Johnson, 1985) and its relationship with torque can be obtained by calculating the integral of the shear stress distribution over the contact area (s), as shown in Eq. 3.5.

$$\sigma_{\varphi z} = \int_c^a \frac{r q_0(s)}{\sqrt{a^2 - r^2}} ds \qquad 0 < r \leq c \tag{3.4}$$

$$T = 2\pi(1-\mu)\int_C^a \sigma_{\varphi z} s^2 ds \tag{3.5}$$

where $q_0(s)$ is the shear stress density and μ is the opening ratio of cutterhead. By analysis of shear stress at the transition boundary from engagement to the frictional area, the shear stress density $q_0(s)$ is obtained from Eq. 3.6.

$$q_0(s) = \frac{-2f}{\pi}\frac{d}{ds}\int_s^a \frac{\sigma_{zz}(a,x)}{\sqrt{x^2 - s^2}} dx \qquad c < r \leq a \tag{3.6}$$

Substituting $q_0(s)$ into the Eq. 3.4 and then substituting the result ($\sigma_{\varphi z}$) into Eq. 3.5, the function for $T(c,a)$ is obtained as shown in Eq. 3.7.

$$T = \frac{8fc^3(1-\mu)}{3}\int_c^a \frac{\sigma_{zz}(a,x)}{\sqrt{x^2 - a^2}} dx \tag{3.7}$$

Substituting normal stress distribution σ_{zz} from Eq. 2 into Eq. 3.7, the relationship between torque (T) and penetration (δ) is obtained as shown in Eq. 3.8.

$$T = \frac{fEH(1-\mu)}{\pi a(1-\nu^2)}\delta \tag{3.8}$$

where H is a parameter that is a function of engagement radius (c) and cutterhead radius (a) as presented in Eq. 3.9.

$$H = [\frac{8}{3}c^3K(\sqrt{1-\frac{c^2}{a^2}}) + 8\int_c^a x^2K(\sqrt{1-\frac{x^2}{a^2}})dx] \quad (3.9)$$

where $K()$ is the complete elliptical integral of the first kind.

Rearranging Eq. 3.8 and considering the fact that penetration rate (PR) is proportional to the δ by the rotational speed of cutterhead (in RPM) (Eq. 3.10) and assuming the ground as an isotropic space ($G = \frac{E}{2(1+\nu)}$), the result is an expression for the penetration rate that considers the influence of engagement radius (c) as shown in Eq. 3.11 and Eq. 3.12.

$$PR(mm/min) = RPM(rev/min) \times \delta(mm/rev) \quad (3.10)$$

$$PR = \alpha \times RPM \times T \times \frac{(1-\nu)}{G} \times \frac{1}{fa^2(1-\mu)} \quad (3.11)$$

$$\alpha = \frac{\pi a^3}{2H} \quad (3.12)$$

To analyze the developed penetration rate model and evaluate the influence of engagement area on penetration rate, the relationship between engagement factor Alfa (α) and normalized engagement radius (c/a) is plotted in Figure 3.4.

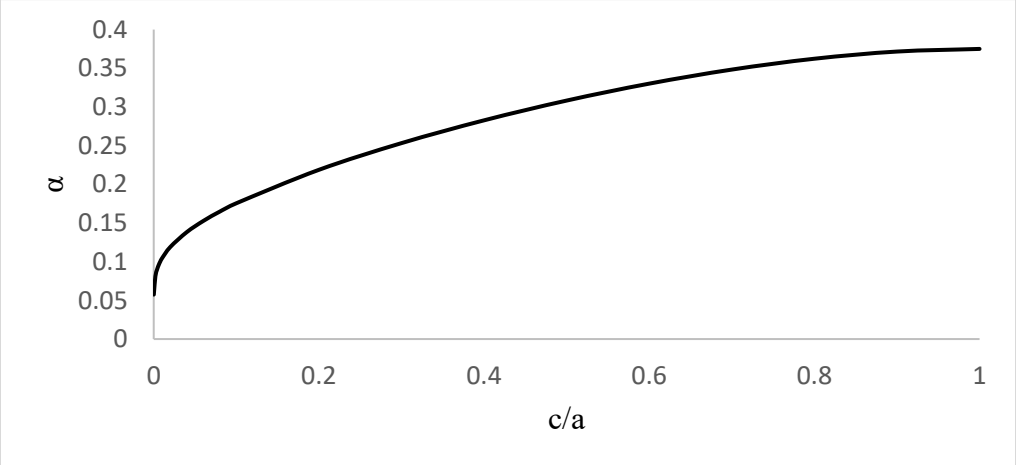

Figure 3. 4. Relationship between normalized engagement radius (c/a) and engagement factor Alfa (α).

An analysis of Figure 3.4 shows that as the engagement radius increases, the engagement factor Alfa (α) increases until it reaches a maximum value of 0.375. Therefore, the upper boundary for the MTBM penetration rate based on consideration of complete engagement (i.e., $c = a$) is obtained as shown in Eq. 3.13.

$$PR = 0.375 \times RPM\ T \times \frac{(1-v)}{G} \times \frac{1}{fa^2(1-\mu)} \tag{3.13}$$

On the other hand, when the engagement radius decreases, the engagement factor decreases as well until it asymptotes to an infinitesimal number for very small engagement radius. By assuming a minimum engagement radius to be 20% of cutterhead radius, a lower boundary for MTBM penetration rate is defined and shown in Eq. 3.14.

$$PR = \frac{3\pi}{16K(0.96)} \times RPM\ T \times \frac{(1-v)}{G} \times \frac{1}{fa^2(1-\mu)} \tag{3.14}$$

When the cutterhead engagement area with soil increases, it more effectively excavates the tunnel face and therefore the penetration rate increases. In ideal conditions, when the cutterhead is fully engaged, the penetration rate would be at the highest rate. On the other hand, when the cutterhead loses engagement with soil and slips on it, the penetration rate decreases. It follows that Eq. 3.13 and 3.14 are two mechanistic models of MTBM penetration rate that determine the boundaries of penetration rate where the actual MTBM penetration rate would be found between the two boundaries (Figure 3.5).

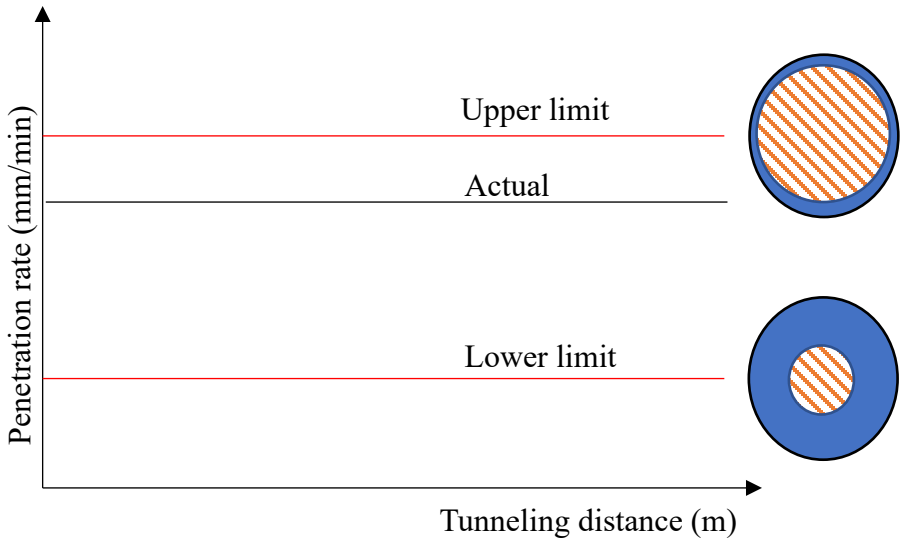

Figure 3. 5. Schematic representation of upper and lower penetration rate boundaries based on cutterhead engagement area with soil.

In order to find the actual area of MTBM engagement, experimental investigation is required to be performed which is beyond the scope of the present study. To examine the developed MTBM penetration rate boundaries, they are applied in a microtunneling project case study.

3.4. Model Evaluation

3.4.1. Case Study 1

The predictive capability of the model was evaluated following its application in a microtunneling project case study. Results are detailed as follows. To validate the application of the developed mechanistic model for penetration rate prediction, the penetration rates predicted by the proposed model were compared to actual values obtained from microtunneling data collected during the construction of a sanitary trunk in Alberta, Canada.

The project used a number of drilling methods, including open cut from Borehole 1 to Borehole 11, horizontal directional drilling from Borehole 11 to Borehole 12, and microtunneling from Borehole 12 to Borehole 16 (Figure 3.6). The section diameter and length of the tunnel were 1.5

m and 2.6 km, respectively, and tunnel depth ranged from 6 m to 15 m. The tunnel was composed of silty clay to clayey silt soil types, and, at some locations, traces of silty sand were identified. Based on geotechnical investigation report, soil types at the boreholes along the microtunneling sections under study are illustrated in Figure 3.6.

The underground geology was mainly silty clay to clayey silt soil types along with some traces of silty sand. The Young's elastic modulus (E) range was between 5 to 24 MPa, the Poisson's ratio was 0.25 and the shear modulus (G) is calculated based on Young's elastic modulus (E) assuming soil to be isotropic material. The cutterhead used in this project has the following characteristics: Cutterhead opening ratio (μ) was 30 % and the cutterhead diameter (a), speed (RPM), nominal torque capacity, and maximum operating thrust limit were 1500 mm , 0–3 rev/min, 550 kN.m and 630 ton, respectively.

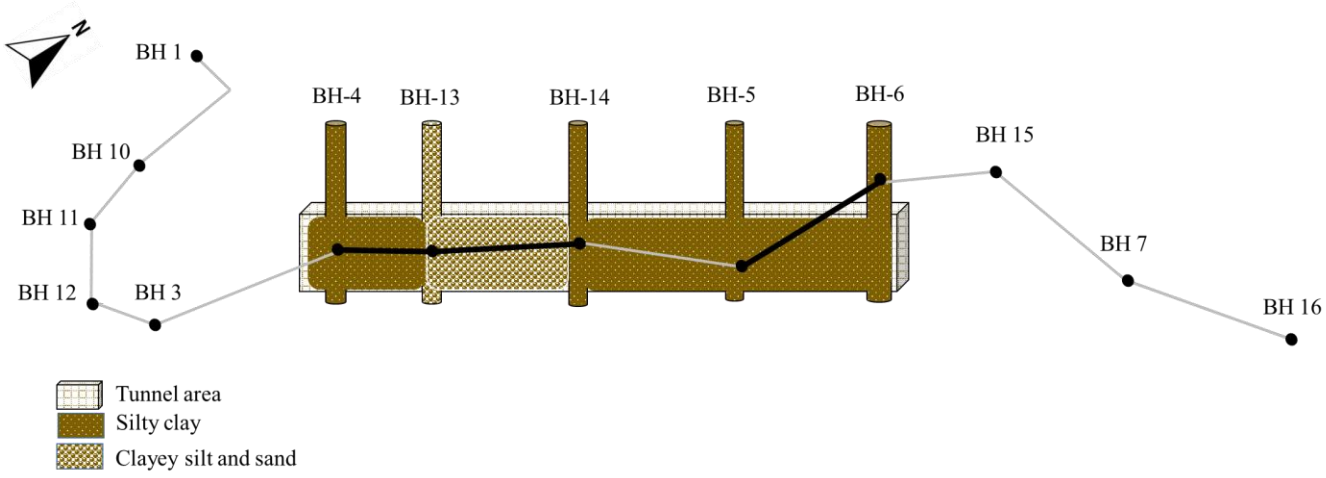

Figure 3. 6. Sewer line alignment and borehole locations of sanitary trunk project. Black and gray lines show the availability or unavailability of MTBM data respectively. The schematic representation of soil types at the boreholes for the selected sections of tunnel under study is also shown in the Figure.

The inputs of the mechanistic parameters including operational load parameters (i.e., torque and RPM) were obtained from the MTBM data acquisition system (Figure 3.7); cutterhead characteristics (i.e., cutterhead radius and opening ratio) were obtained from project specification

documents; and soil properties were obtained from geotechnical field investigation reports. Based on these above-mentioned parameters, upper and lower boundaries of MTBM penetration rate were determined using the proposed mechanistic models. Comparison of the actual penetration rate, and the developed boundaries for two different tunnel sections between BH4 to BH14 and BH5 to BH6 along the tunnel length are presented in Figure 3.8.

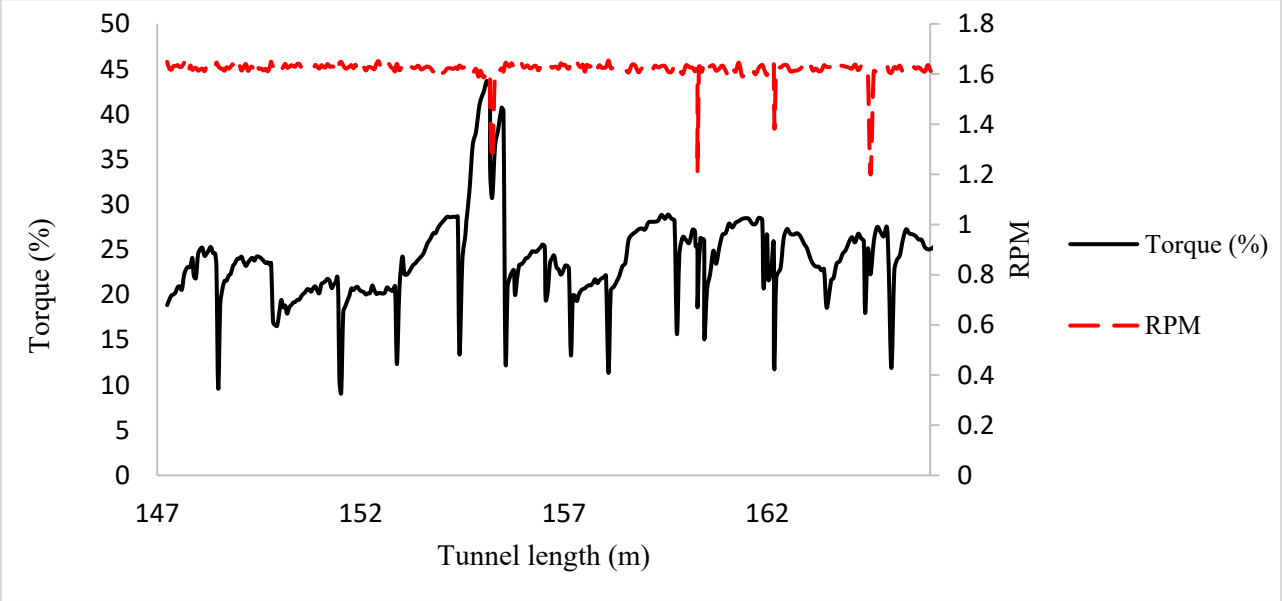

Figure 3. 7. MTBM data obtained from data acquisition system: Torque (% of max torque capacity) and RPM during excavation portion of tunnel between BH4 and BH14.

A.

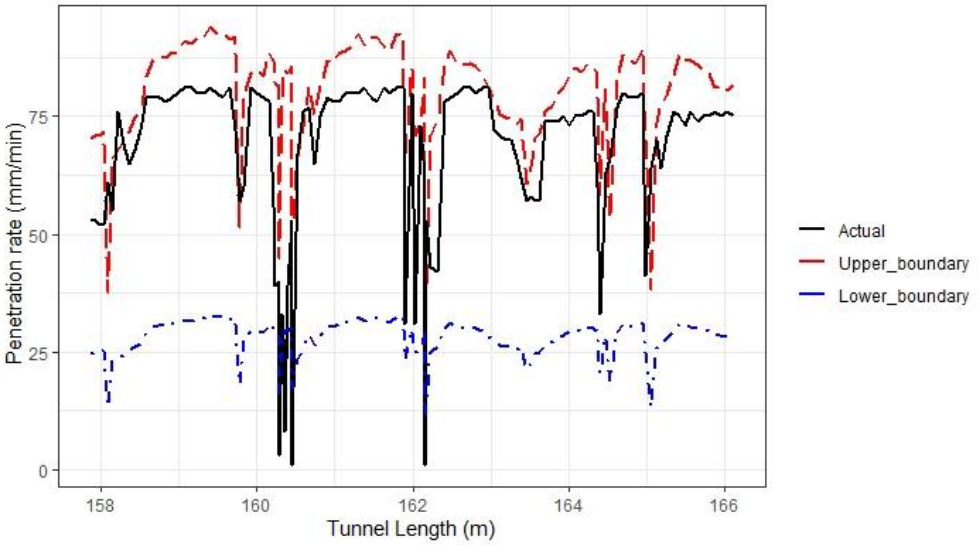

B.

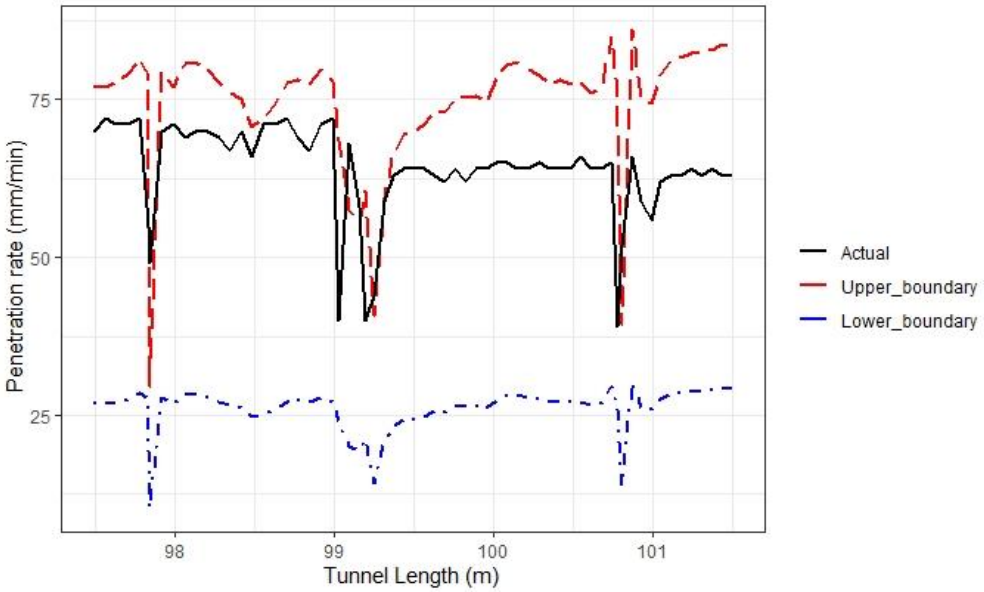

Figure 3. 8. Actual and predicted penetration rates boundaries along the (A) BH4 to BH14 and (B) BH5 and BH6 portion of the project under study.

As shown in Figure 3.8, the actual penetration rate lies between the upper and lower boundaries and is closer to the upper boundary for both tunnel sections, which indicates the relatively high

engagement of MTBM with ground, leading to the high penetration rate. To further anlyze the influence of engagement area on penetration rate, the actual penetration rate for the tunnel section between BH4 to BH14 along the tunnel length was analyzed and the corresponding engagement factor Alfa (α) at each point are plotted as shown in Figure 3.9. This analysis shows that a huge drop in penetration rate occurs at low engagement factor Alfa (α) that corresponds to the low engagement radius (c) of cutterhead with ground (Figure 3.9). Moreover, the analysis shows that during excavation of this tunnel section, the average value of enagement factor was 0.371, which, based on Figure 3.4, corresponds to a ratio of engagement radius (c) to cutterhead radius (a) of 90%, indicating high engagement area during the course of tunneling excavation.

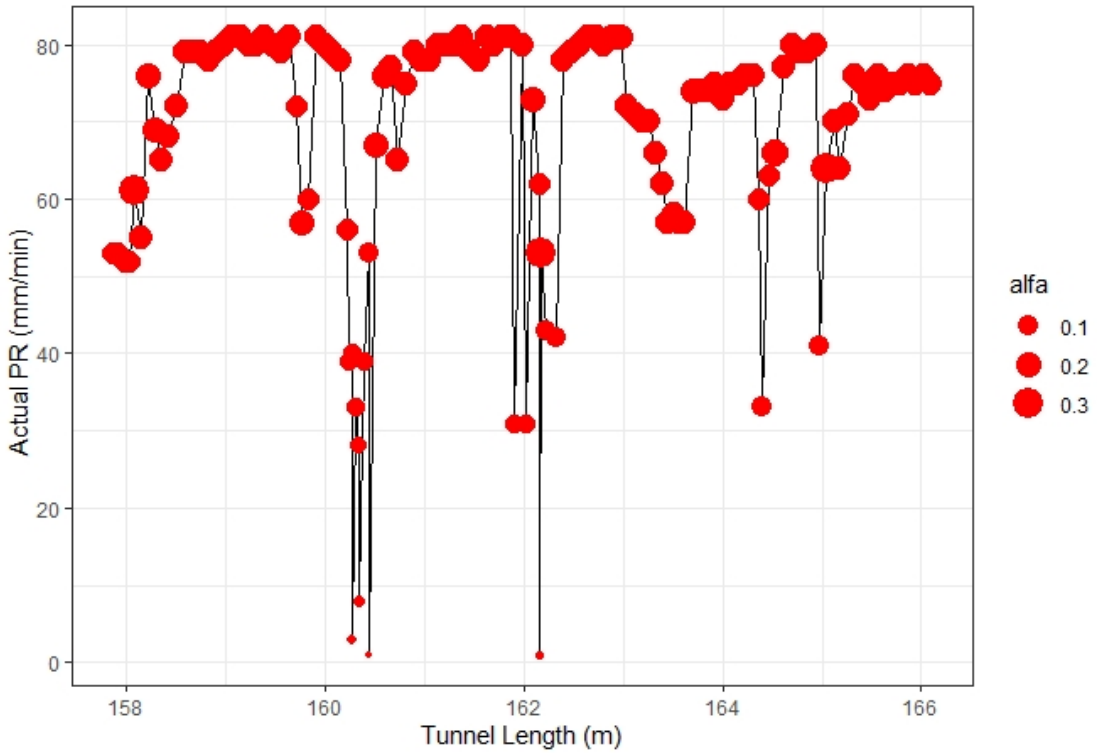

Figure 3. 9. Actual penetration rate (PR) for tunnel section between BH4 to BH14 and corresponding cutterhead engagement factor Alfa (α) along the tunnel length.

3.4.2. Case study 2

The developed framework was applied to microtunneling constrcution in Edmonton, Canada. This project consists of two microtunneling sections between BH 18 to BH 15 (section A) and between BH 4 to BH 10 (section B). The project description is provided in Chapter 2, Section 2.5.3. Section A of the microtunnelling was from BH4 to BH10, and Section B was from BH18 to BH15. Analysis of the engagement model shows that (Figure 3.10), the actual penetration rate occurs between the upper and lower boundaries and is closer to the upper boundary for both tunnel sections. This shows the relatively high engagement of MTBM with ground for both section A and B of the project. The penetration rate boundaries are not constant during the tunnel excavation and the influence of both soil properites and MTBM operational loads led to variation in MTBM engagament areas and therfore results in variation of upper and lower boundaries at different locations of tunnel path.

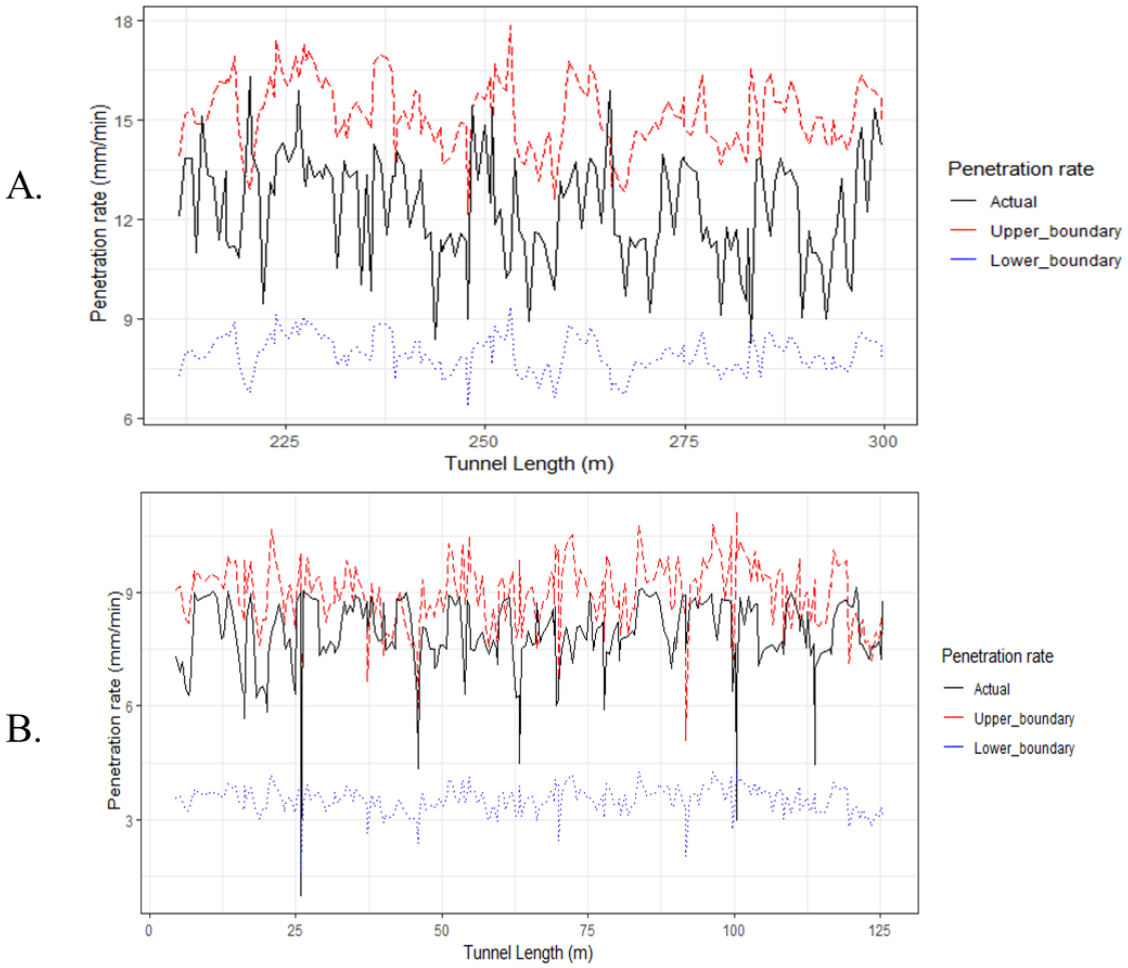

Figure 3. 10. Actual and predicted penetration rates boundaries along the (A) section A and (B**)** section B of the microtunneling project.

3.5. Conclusion

Complex interaction between the cutterhead and soft ground makes the prediction of MTBM penetration rate a challenging task which consequently affects the prediction of the overall productivity of microtunneling projects. This complexity arises from various interactions that occur between cutterhead and ground such as engagement phenomeon between cutterhead and the ground during an excavation process. Although this engagement phenomeon highly influences the MTBM penetration rate, this phenomenon has not yet been thoroughly investigated from a mechanistic perspective. Therefore, in the present research, the main goal was to fill this gap and

mechanistically investigate the engagement of cutterhead with ground and evaluate the influence of this phenomenon on the MTBM penetration rate. To achive this goal, by applying the theory of contact mechanics, the engagement of cutterhead with ground is modeled and the mathematical expression for calculation of the MTBM penetration rate based on the radius of cutterhead engagement with ground is developed. Considering two cases of largest and smallest engagement areas the upper and lower boundaries for MTBM penetration rate were determined. To examine the developed mechanistic MTBM penetration rate boundaries and also the cutterhead engagement influence on penetration rate, the data from two microtunneling projects was studied. Analysis of the results for two different tunnel projects showed that the actual MTBM penetration rate lies between the developed upper and lower boundaries and is closer to the upper penetration rate boundary. Moreover, it is found that a drop in penetration rate occurs at locations where the engagement area was smaller. Further analysis showed that during the course of tunneling excavation, the engagement radius on average was about 90% of the cutterhead radius which indicates high engagement of cutterhead with ground. Results also showed that the developed upper and lower boundaries provide a promising range within which the actual MTBM penetration rate is likely to occur. Obtaining this range helps to reduce the uncertainity of MTBM penetration rate prediction and to facilitate the planning of microtunneling projects by considering these boundaries for production rate analysis. The developed penetraton rate boundary models should be considered in light of being limited to soft ground (i.e, soil) with stable tunnel face conditions.

3.6. Data Availability

All models generated or used in the present study are available from the corresponding author upon reasonable request. Case study data used in this research were provided by a third party.

Direct requests for these materials may be made to the provider indicated in the Acknowledgements.

3.7. Acknowledgment

This project was supported by a Collaborative Research and Development Grant (CRDPJ 532148) from the Natural Sciences and Engineering Council of Canada. The authors would like to thank the Shanghai Construction Group Canada Corp. for their continued support and for providing case study data.

Chapter 4: Dynamic Data-Driven Approach for Penetration Rate Prediction in Microtunneling Construction

4.1. Introduction

Microtunneling was introduced in Japan in the early 1970s, and it later spread to Europe and the United States (Luo and Najafi, 2007). Its application in North America has undergone continuous growth since the 1980s (Chung et al., 2004). According to the American Society of Civil Engineers (ASCE), microtunneling is a trenchless construction method for pipeline installation that is remotely controlled and that uses laser guidance (ASCE, 2001). During microtunneling projects, pipe sections are jacked while the tunnel face is excavated and soil materials are removed, and the face of the tunnel is continuously supported (ASCE, 2001). Several factors have led to an increase in microtunneling applications, including its ability to minimize surface disruptions (especially in congested urban areas) and its high accuracy of both line and grade pipeline installation (Chung et al., 2004). Moreover, improvements in the technical features of microtunnel boring machines (MTBMs) have allowed for their use in various geological and geotechnical conditions.

Although these advancements have increased the application of microtunneling, a key challenge facing the industry is accurate prediction for planning, control, and monitoring purposes. For instance, productivity prediction provides insightful information for owners in their efforts to control and evaluate the contractor's performance and assess project progress. One of the key parameters in predicting the productivity of microtunneling projects is the penetration rate (PR) of the MTBM (Hegab et al., 2006). The Standard Design and Construction Guidelines for

Microtunneling (2015), define PR as "instantaneous excavation distance per time while the MTBM is operating, typically measured in inches per minute or millimeters per minute" (ASCE, 2015).

The complexity of MTBM interactions with various ground conditions, as well as changes in geological or geotechnical conditions at the tunnel face, make PR prediction a challenging task. Various models have been developed to predict PR, and scholars have developed empirical equations by collecting rock mass characteristics and tunnel boring machine (TBM) performance data from multiple tunneling projects using machine learning models such as Artificial Neural Networks (ANNs) (Alvarez et al., 2000; Eftekhari et al., 2010; Salimi and Esmaeili, 2013), particle swarm optimization (PSO) (Yagiz and Karahan, 2011), and single- or multi-variate regression analysis (Sapigni et al., 2002; Hassanpour et al., 2009a, 2009b, 2011; Farrokh et al., 2012; Jamshidi, 2018). Researchers have also used full-scale field tests to correlate field parameters with boring machine performance in order to deliver more accurate predictions (Rostami and Ozdemir, 1993; Rostami, 1997, 2008; Sato et al., 1991; Sanio, 1985; Ozdemir et al., 1978). A review of existing models for predicting PR shows that most of them have been developed for tunneling excavations through hard rock formations (Alvarez et al., 2000; Sapigni et al., 2002; Ribacchi and Fazio 2005; Yagiz, 2008; Hassanpour et al., 2009b and 2011, Farrokh et al., 2012; Jamshidi, 2018), whereas relatively few studies have targeted the prediction of PR for microtunneling excavations, particularly those involving soft underground conditions (Hegab et al., 2006; Elwakil and Hegab, 2018). Moreover, existing approaches for PR prediction require either extensive data collected from multiple projects representing a wide variety of geotechnical conditions or the use of specialized equipment and laboratory facilities. In addition, existing prediction approaches use static data (e.g., laboratory test results, database of historical project data)—rather than dynamic MTBM data generated during the tunneling process—to predict the PR.

This research aims to address these limitations by providing a new dynamic data-driven approach that integrates near-real-time machine-generated data (i.e., MTBM data) with geotechnical data to predict the PR of MTBMs. The key features of this approach is that it dynamically learns from the MTBM data and enhances the prediction accuracy as the excavation proceeds.

4.2. Research Background

As noted above, research on the use of TBM-generated data collected during microtunneling operations to improve productivity prediction is limited. The data generated by TBMs is typically stored and is seldom used for project management purposes. Although the generated TBM data is typically used for evaluating TBM responses such as the jacking force required to push the pipes (Khazaei et al., 2004; McCabe et al, 2012, Ji et al., 2019) or analyzing cutterhead torque (She et al., 2011, Lin et al, 2022), instantaneous TBM PR data has been used in a few studies for evaluating overall project productivity (Hegab et al., 2006; Elwakil and Hegab, 2018). However, the aim of these studies was to statically evaluate the project productivity, and they did not investigate the use of TBM data for continuously evaluating and updating the project plan and productivity. A review of the literature in this domain reveals that continuous project plan-updating has been done using a variety of methods and considering different factors of interest (Haas and Einstein, 2002; Einstein, 2004; Sousa and Einstein, 2012; Špačková et al., 2013; Mahmoodzadeh et al. 2021). For instance, continuous project plan-updating during tunnelling operations has been applied to reduce the negative impacts of geological and geotechnical uncertainties on project time and cost. In this regard, Haas and Einstein (2002) underscored the need for ongoing productivity projections during construction as a way of improving scheduling, resource allocation, financial planning, and so on. They proposed a procedure that not only replaces the original prediction with actual data from excavation, but that also includes a learning component that uses information from the actual

excavation to improve prediction for the length of tunnel yet to be excavated. They used Bayes' theorem to devise a method that learns from the actual excavation and considers observations made during construction. Sousa and Einstein (2012), meanwhile, presented a method to evaluate the risks associated with tunnel construction. They developed a framework that uses a geologic prediction model to predict geological conditions in the length of tunnel to be excavated, combining it with another model that enables users to select the construction strategy that poses the least risk based om the given conditions. Both the geological prediction model and the construction strategy decision models used to update project information were developed using the Bayesian network technique.

Špačková et al. (2013) developed a model for updating the construction time predictions based on observed geotechnical conditions. Using the dynamic Bayesian network (DBN), they developed a framework for probabilistic prediction of tunnel construction time and cost, considering in particular the stochastic dependencies involved in probabilistic estimates of tunneling construction time and cost. More recently, Mahmoodzadeh et al. (2021) used continuous space–discrete state Markov process for forecasting geological conditions in order to reduce the effects of geological and geotechnical uncertainties on tunnel construction time and cost.

The common aim of these studies was to predict the geological conditions ahead of tunneling operations and, taking into account observations made during excavation, develop a decision support tool for tunneling construction accordingly. However, in these studies, TBM performance was not considered a key factor in continuous updating of planning during tunneling excavation. As such, there is a gap with respect to the use of continuously generated TBM data for forecasting and updating the project schedule. This gap is particularly notable considering that continuously generated TBM data is capable of representing TBM–ground interactions, which can in turn be

used as the basis for dynamically predicting tunneling progress, as well as predicting TBM performance for the purpose of taking preventative measures against TBM failure when passing through similar ground conditions during excavation.

4.3. Methodology

To achieve more efficient project control, a novel decision-support framework for predicting MTBM PR during the microtunneling excavation phase is developed. Generally, the inputs to this framework can be categorized into two groups: MTBM data (i.e., PR) and geotechnical data (e.g., soil properties). Since the progress is based upon the availability of data, the approach underlying the developed framework is to dynamically use the MTBM data generated from excavation of different tunnel segments. The conceptual framework of the dynamic data-driven approach, illustrated in Figure 4.1, consists of seven components: studying of the system, data acquisition, data source creation, data cleaning and transformation, data analysis, model development, and decision support.

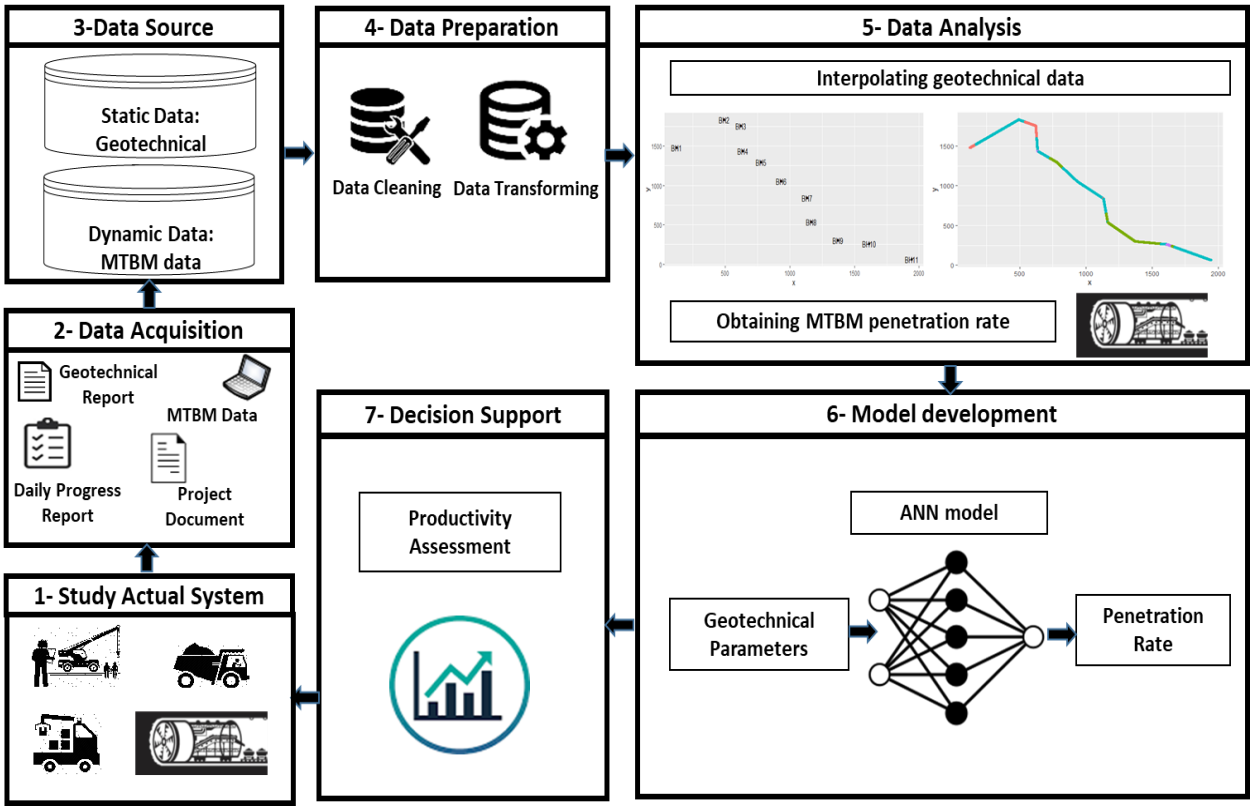

Figure 4. 1. Conceptual framework of the proposed MTBM PR prediction approach.

As illustrated in the figure, the first step is to study the actual microtunneling system to gain understanding of the factors influencing the MTBM PR. Then, in the data acquisition module, different data sources, such as geotechnical reports, MTBM data, project documents, and daily progress reports, are collected to form the initial data set. The data source module extracts the dynamic MTBM data and the static geological and geotechnical data, then stores them in a database for analysis. The data preparation module processes the raw data by performing data cleaning. The data analysis module then interpolates the geotechnical parameters between boreholes and calculates the MTBM PR from the MTBM data to establish the prediction model. In the model development module, an artificial neural network (ANN) model is developed to predict the PR for the unexcavated length of tunnel based on the interpolated geotechnical data. Finally, the decision-support module uses the predicted MTBM PR to support decision-making

and improve the overall productivity of microtunneling operations. It is important to note that the results of the decisions are reflected in the progress of the actual system. Each of these modules is described in greater detail below.

4.3.1. Data source creation

The initial data source is prepared by reviewing geotechnical baseline reports—such as soil type and Standard Penetration Test results (SPT-N value)—from different borehole locations. The initial geotechnical database having been created, the values between borehole locations need to be predicted, this task being performed by the data analysis module. The MTBM data, meanwhile, are collected once the MTBM starts excavation. After a section of a tunnel has been excavated, the MTBM data collected is stored into a data source module (as near-real-time data) to be used subsequently in the data preparation module.

4.3.2. Data preparation

In this module, the near-real-time MTBM data collected are cleaned, and the outliers for each factor are removed using the R programing language (R Core Team 2013). Since the MTBM data are generated in 1-second intervals, the resulting data set is large; thus, the data are grouped into 1-minute intervals (i.e., mm/minute) in preparation for the work of the data analysis module.

4.3.3. Data analysis

The purpose of this module is to interpolate the geotechnical parameters between boreholes and obtain the MTBM performance parameters. The geoscience interpolation technique known as the inverse distance weighted (IDW) method is used to interpolate between boreholes. This method uses distance to weight the influence of observations. The concept underlying this method is that locations that are in close proximity to one another are more alike than those that are further apart. The IWD is a deterministic method for interpolation between scattered set of points. The IWD is

used to predict the unknown value $\hat{y}(S_0)$ in the location S_0 given the observed y values at the sampled locations S_i based on the following equation (Lu and Wong 2008):

$$\hat{y}(S_0) = \sum_{i=1}^{n} \lambda_i y(S_i) \tag{4.1}$$

The predicted value in S_0 is a linear combination of the weights (λ_i) and observed values in S_i.

The weights (λ_i) are defined as following:

$$\lambda_i = {d_{0i}^{-\alpha}}\Big/{\sum_i^n d_{0i}^{-\alpha}} \tag{4.2}$$

With

$$\sum_{i=1}^{n} \lambda_i = 1 \tag{4.3}$$

In Eq. 4.2, the numerator is the inverse of distance (d_{0i}) between S_0 and S_i with the power α and the denominator is a the sum of the inverse distance weights for all locations i. The sum of all weights λ_i's for an unsampled point is unity as shown in Eq.4.3. To obtain the MTBM performance parameters, the MTBM data recorded during excavation of a section of tunnel are used. Once soil properties are interpolated and MTBM penetration rate is calculated, then a database for developing a machine learning model is created.

4.3.4. Model development

Various machine learning models are tested to determine which one provides the highest PR prediction accuracy. In comparing ANN, random forest, linear regression, and decision tree, the ANN model is found to provide the best results (results of comparison are explained in case study 1). This is also found in several penetration rate prediction studies (Alvarez Grima et al. 2000; Benardos and Kaliampakos 2004; Yavari and Mahdavi 2005; Yagiz et al., 2009; Eftekhari et al.,2010; Gholamnejad and Tayarani 2010; Ghulami et al., 2012; Salimi and Esmaeili, 2013;

Torabi et al., 2013). To predict the MTBM PR for unexcavated tunnel length, an ANN model is constructed. The inputs to the ANN model are the geotechnical parameters interpolated along the tunnel length, while the output is the predicted MTBM PR for unexcavated tunnel length.

4.3.5. Decision support

By predicting PR along the tunnel path, the areas of high or low PR can be identified, and this information, in turn, can aid decision makers in adjusting the tunneling process accordingly. More importantly, practitioners can estimate the project's progress and productivity and, as a result, modify the tunneling schedule accordingly.

4.3.6. Data source updates

The data source is updated anytime a new tunnel section is excavated and new MTBM data are generated. The newly obtained MTBM data are appended to the previous MTBM data (i.e., the MTBM data obtained during excavation of the previous tunnel section), and the MTBM data source is updated. Moreover, based on the observations from excavated soil materials, the interpolated geotechnical parameters, such as soil type, can be updated according to the actual site conditions, and the geotechnical data source updated accordingly.

4.3.7. Dynamic aspect of machine learning model

The developed framework is meant to be used dynamically during project execution. The neural network model constructed is not static, and will be reconstructed several times during excavation. In other words, the ANN model constructed based on excavation of a given tunnel section will be used to predict the next tunnel section; the next tunnel section having been excavated, based on the obtained MTBM data for the newly excavated section and corresponding geotechnical data for that section, the main database will be updated, and a new ANN model will be created for predicting the PR for the subsequent tunnel section. This process continues until excavation is

complete. Figure 4.2 shows the dynamic process of updating the main database and creating new ANN models.

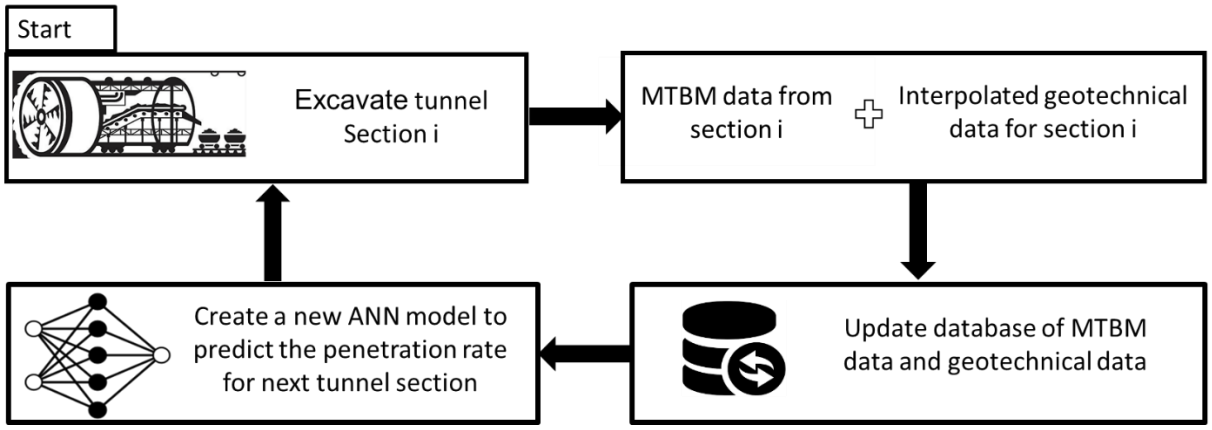

Figure 4. 2. Dynamic aspect of the data-driven framework.

4.4. Case Study 1

The proposed framework was applied to the construction of a sanitary trunk project in Alberta, Canada. This project consisted of 11 boreholes and three different tunneling methods: open-cut (from Borehole 1 (BH1) to BH2), horizontal directional drilling (from BH2 to BH4), and microtunneling (from BH4 to BH11). The microtunneling diameter and length were 1.5 m and 2.6 km, respectively, and the tunnel depth ranged from 6 m to 15 m.

4.4.1. Data source preparation

Based on information obtained from the boreholes logs and the geotechnical report, the initial database of geotechnical parameters was constructed. Table 4.1 shows the initial geotechnical data obtained, including soil type descriptions, standard penetration test results (SPT-N values), and water content. The stability number, which assesses the soil behaviour based on the undrained shear strength of the soil (Terzaghi, 1950; Heuer, 1974), was also determined, along with the stability number at collapse, which is a function of tunnel face pressure and the cover-to-depth

ratio (C/D), where C is the thickness of the cover of soil over the tunnel, and D is the cut diameter of the tunnel (Terzaghi, 1950; Heuer, 1974).

Table 4. 1. Initial borehole data obtained from geotechnical baseline report.

Borehole number	Soil type	SPT-N value	Water content (%)	Stability number	Stability number at collapse
BH1	clayey silt	26	20.5	3.5	8.2
BH2	silty clay	34	13.9	4.4	8.1
BH3	clayey silt	6	16.5	4.1	11.1
BH4	silty clay	20	18.6	5.7	11.7
BH5	clayey silt with sand	30	20.4	5.7	10.2
BH6	silty clay	19	29.7	4.9	9.6
BH7	silty clay	30	21.0	5.5	9.6
BH8	silty clay	11	4.8	4.4	9.3
BH9	clayey silt with sand	15	27.7	4.5	8.4
BH10	silty sand	12	13.7	4.4	8.7
BH11	silty clay	8	38.8	5.1	8.7

The raw MTBM data collected were cleaned and the outliers removed. Based on the geographical position of each borehole (Figure 4.3), the geotechnical data were interpolated, and the database of geotechnical parameters along the tunnel path was constructed. The results of the data interpolation of soil type along the tunnel path is shown in Figure 4.4 as an example.

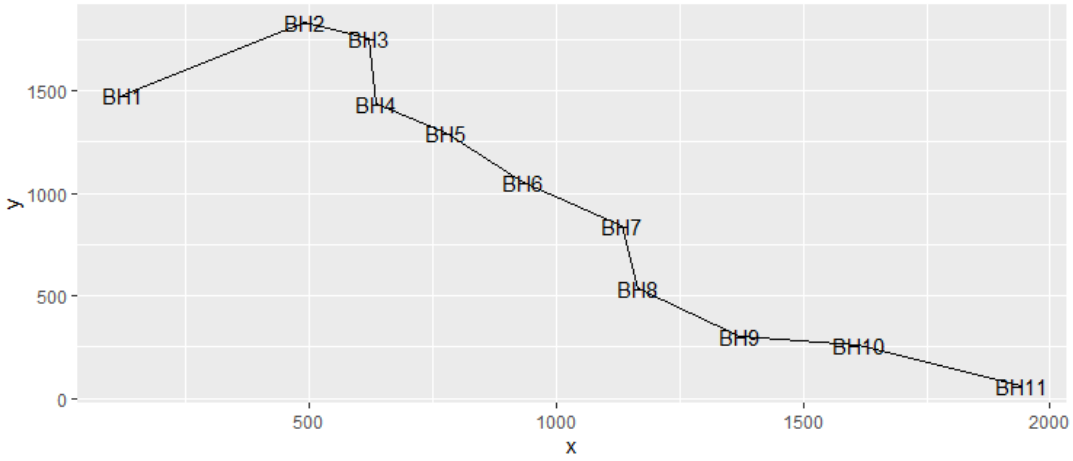

Figure 4. 3. Borehole locations along the sewer line alignment.

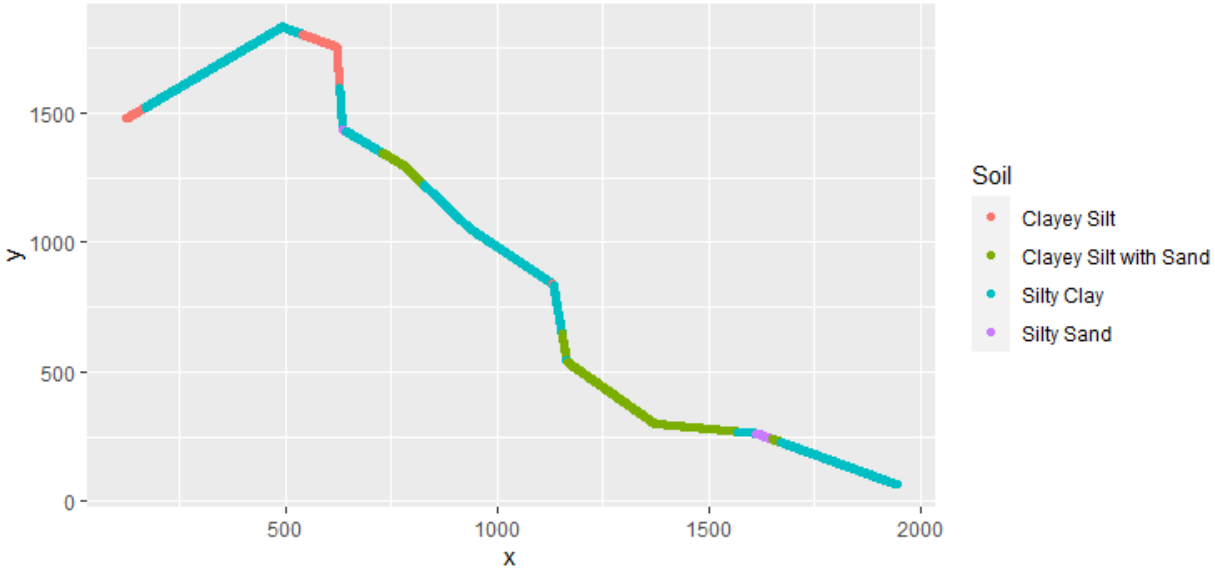

Figure 4. 4. Soil type interpolation along the tunnel path.

4.4.2. Model development

As noted above, the ANN model was selected based on a comparison of four machine-learning models, the other three being random forest, decision tree, and multiple linear regression. Based on the models trained using data from Segment 1, the PR was predicted for the subsequent tunnel segment. Analysis of the four models revealed that the ANN model provides the highest prediction accuracy—92%, compared with 81%, 86%, and 70% for random forest, decision tree, and multiple

linear regression, respectively. For the model development, the microtunneling procedure was divided into multiple excavation segments. The initial excavation segment (Segment 1) was from BH4 to BH6. For this segment, the MTBM data were collected, and the MTBM PR was calculated accordingly. Using the geotechnical and MTBM PR from the first excavation segment, an ANN model was constructed to predict MTBM PR for the remaining tunnel length based on the interpolated geotechnical data. After predicting the PR for the remaining unexcavated tunnel segments, the same procedure was continued on the second segment (from BH6 to BH7) and the third segment (from BH7 to BH8). The procedure ended with the prediction of the PR for the fourth tunnel segment (from BH10 to BH11). After excavation of each new tunnel segment, the database of MTBM performance parameters and the developed ANN for predicting PR were updated to increase the accuracy of the prediction.

4.4.3. Results and discussion

In the developed framework, reference data were defined to illustrate the dynamic prediction procedure. The MTBM data used for PR prediction of the next tunnel segment (Figure 4.5) served as the reference data. For example, in Figure 4.5, “reference data A” refers to the MTBM data generated during excavation of the first tunnel segment, while “reference data B” refers to the MTBM data generated during excavation of the first and second tunnel segments.

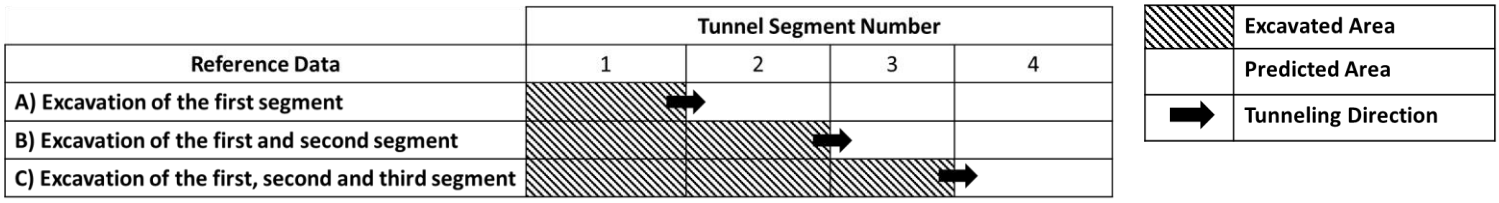

Figure 4. 5. Schematic representation of the dynamic prediction procedure for different tunnel segments.

The PR prediction accuracy values (calculated based on mean absolute percentage error) for different reference data and for different tunnel segments are shown in Figure 4.6. This figure shows that the prediction accuracy increased as more tunnel segments were excavated. For example, for Segment 4, the prediction accuracy based on excavation of the first segment was 81%, and it increased with the data from the second and third segments to 83% and 91%, respectively. This increase in prediction accuracy was the result of a growing set of MTBM data and the learning of MTBM behavior based on a widening range of ground conditions.

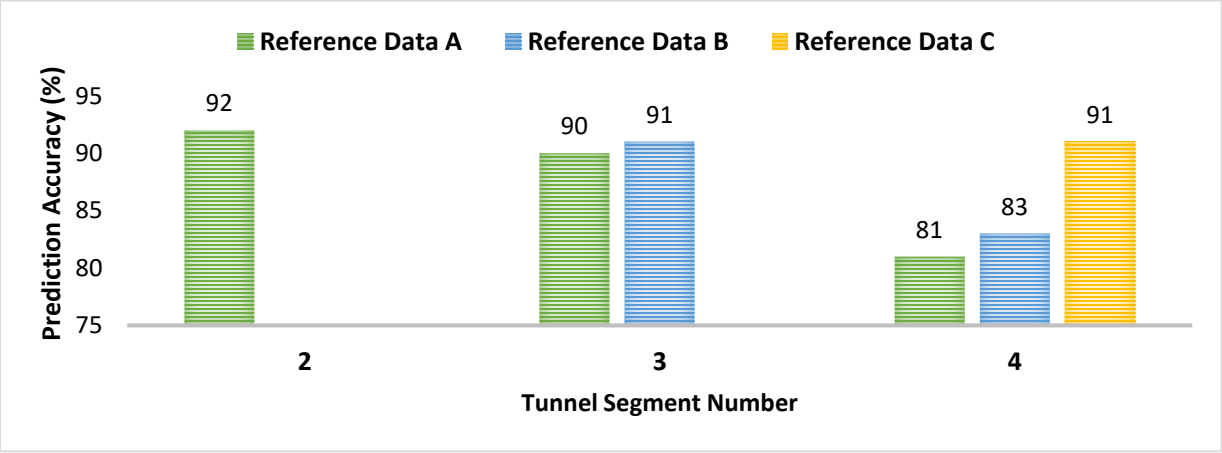

Figure 4. 6. Penetration rate prediction accuracy based on different reference data and for different tunnel segments.

On the other hand, the prediction accuracy for each set of reference data decreased as the distance between predicted segment and the reference data segment increased. This is also illustrated in Figure 4.6, where it can be seen that the prediction accuracy based on the excavation of the first segment (reference data A) for Segment 2 was 92%, whereas the prediction accuracy decreased for subsequent segments (i.e., Segments 3 and 4) to 90% and 81%, respectively. The reason for the reduction in accuracy is that the probability of facing new ground conditions increases as the distance between predicted segment and the excavated tunnel face increases. In reference data A (excavation of first segment), the MTBM passed through two soil types—i.e., “clayey silt with

sand" and "silty clay"—whereas it encountered "silty sand" in Segment 4 (between BH10 and BH11); thus, the prediction accuracy dropped to 81% for Segment 4.

4.5. Case Study 2

The developed framework was applied to microtunneling construction in Edmonton, Canada. The project description is provided in Chapter 2, Section 2.5.3. Section A of the microtunnelling was from BH4 to BH10, and Section B was from BH18 to BH15. Based on information obtained from the borehole logs and geotechnical report, the initial database of geotechnical parameters was constructed. Table 4.2 shows the initial geotechnical data obtained, including soil type descriptions, standard penetration test results (SPT-N values), and water content. The soil type code (STC) was used for transforming the soil type descriptions into numeric parameters to be used in the ANN model. In addition to the geotechnical information, the MTBM data required was also provided by the contractor. To validate the dynamic data-driven framework, the PR for the tunnel segment between BH17 and BH16 in Section A was predicted based on excavation data for the segment from BH18 to BH17, also in Section A. Excavating subsequent segments (BH17 to BH16), a new ANN model was constructed based on information from BH18 to BH16, and the prediction was made for the segment from BH16 to BH15. For Section B, similarly, based on excavating BH4 to BH5, the PR is predicted for the segment between BH5 and BH6. Then, by continuing excavation of the segment between BH5 and BH6, the PR for the tunnel segment between BH6 and BH7 can be predicted. Table 4.3 shows a summary of the accuracy of predictions for both Section A and Section B.

Using the concept of reference data introduced in the developed framework, the analysis of the results shows that, in Section A, when considering the data for the segment between BH18 and BH17 as the reference data for ANN model training, the prediction accuracy for the segment

between BH17 and BH16, which has a similar soil type (silty clay with sand), is 86%. By considering the segment between BH18 and BH16 as the reference data for ANN model training, the prediction accuracy for the segment between BH16 and BH15, which has a different soil type (silty clay) is 81%. These findings demonstrate that the data obtained from excavating further segments helps to enhance the prediction accuracy if the target prediction area has similar ground conditions. Further analysis of the results for Section B also shows that, if in continuing the excavation the reference data for ANN model training includes some component of the target prediction area, the prediction accuracy increases. For instance, the initial reference data for the portion of tunnel between BH4 and BH5 in Section B does not have similar ground conditions to the portion of tunnel between BH5 and BH6, and the prediction accuracy is 74%. In continuing the excavation between BH5 and BH6, the reference data for ANN model training contains similar ground conditions (silty clay) to the portion between BH6 and BH7, and the prediction accuracy increases to 81%.

Table 4. 2. Initial borehole data obtained from geotechnical baseline report.

Borehole number	Soil type	SPT-N value	Water content (%)
BH4	silty clay with sand	11	38.4
BH5	silty clay with sand	10	33.5
BH6	silty clay	9	35.2
BH7	silty clay	11	36.6
BH8	silty clay with sand	7	38.3
BH9	silty clay with sand	20	24.5
BH10	silty clay with sand	14	27.4
BH15	silty clay	10	31.1
BH16	silty clay with sand	17	16.3
BH17	silty clay with sand	15	20.8
BH18	silty clay with sand	12	20.5

Table 4. 3. Summary of PR prediction accuracy for Sections A and B.

Reference data	Predicted segment	Accuracy	Tunnel area
Excavation of BH18 to BH17	Between BH17 and BH16	86%	Section A
Excavation of BH18 to BH16	Between BH16 and BH15	81%	
Excavation of BH4 to BH5	Between BH5 and BH6	74%	Section B
Excavation of BH4 to BH6	Between BH6 and BH7	81%	

4.6. Conclusion

In this chapter, a new dynamic data-driven based approach for predicting PR in microtunneling construction was proposed. It uses near-real-time MTBM and geotechnical data to predict MTBM PR for unexcavated tunnel length. The key contribution of this approach is that it dynamically learns the MTBM performance in different ground conditions as the excavation proceeds in order to enhance the prediction accuracy for the next tunnel sections. In addition, since both the data sources and the ANN model used for prediction of PR are dynamically updated, the prediction accuracy can be continuously enhanced if the target prediction area has similar ground conditions to the data source used for training the ANN model. As tunnel excavation continues, the area that that is yet to be observed and learned by the machine-learning model decreases and the probability of enhancing the prediction accuracy increases. It should be noted that, since the proposed framework uses machine-generated data, it is limited to steady microtunneling excavation during construction. Occurrence of unusual events, such as encountering foreign materials or machinery problems, is not considered. Hence, the expert opinion could be used in conjunction with the machine-generated data to increase the prediction accuracy by taking into consideration additional factors that may affect microtunneling PR.

Chapter 5: Integrating MTBM Penetration Rate Prediction Models and Operation Simulation Model to Enhance Microtunneling Productivity Prediction

5.1. Introduction

Accurate productivity estimation in microtunneling construction can improve project planning and scheduling, as well as reduce the risk of project delays and cost overruns. One of the main approaches to predicting the productivity of microtunneling construction projects is to model the entire process using operational simulation modelling. The applicability and practical advantages of this approach have been verified in a number of studies (Al-Battaineh et al., 2006; Luo and Najafi, 2007; Trung, 2013; Werner and AbouRizk, 2015; Moharrami et al., 2022). For example, Luo and Najafi (2007) used simulation modelling to assess the parameters affecting the productivity of microtunneling construction. Having found productivity of microtunneling operation to be highly dependent on soil conditions, they analyzed the impact of soil conditions on productivity by conducting a field study at Louisiana Tech University. Werner and AbouRizk (2015) used simulation to analyze the influence of delays due to equipment breakdowns and unexpected conditions on the productivity of tunneling projects.

Although these studies have reported promising results of using simulation modelling to predict and/or evaluate the productivity of tunneling/microtunneling constructions, there are still challenges yet to be addressed with regard to modelling activity durations in simulation. One of the key activities in microtunneling is the process of excavation by micro tunnel boring machine

(MTBM), which involves penetration of the MTBM into the ground. In this respect, the instantaneous rate of MTBM penetration into the ground—defined as the MTBM penetration rate (PR)—is a crucial piece of knowledge for modelling the excavation process in simulation (Luo and Najafi, 2007; Chung, 2007; Moharrami et al., 2022). It is particularly critical when the intended purpose of the simulation is to enhance the productivity estimation of ongoing construction, where there may be a need to update the existing plan or redirect the excavation process to the original schedule. Considering that PR estimation is inherently challenging due to complexities of interactions of the MTBM with various ground conditions and changes in geological and geotechnical conditions at the tunnel face, PR typically is either estimated in an ad hoc, experienced-based manner by experts or is estimated based on historical data. As such, there is high degree of uncertainty associated with the MTBM PR inputs used in the simulation of microtunneling construction projects. This underscores the need to enhance simulation-based microtunneling productivity prediction models by improving the accuracy of MTBM PR inputs. To address this gap, this research proposes a novel approach that integrates MTBM PR prediction models with simulation modelling to enhance the prediction of microtunneling productivity.

In this regard, two approaches for forecasting the MTBM PR are used as the basis for the MTBM PR prediction models developed in the present research. The first approach is to mechanistically analyze the cutterhead-ground interactions in order to develop a mechanistic model based on the physics governing the MTBM PR and find the mathematical solution that predicts the MTBM PR. The second approach is to develop a dynamic data-driven framework that uses MTBM data generated during the course of construction in conjunction with geotechnical data at borehole locations to predict the MTBM PR for an unexcavated length of tunnel. By integrating the resulting MTBM PR prediction models with simulation modelling, two productivity models—an

"integrated simulation + Bayesian updating mechanistic model for MTBM PR prediction" and an "integrated simulation + machine-learning model for MTBM PR prediction"—are developed. These are successfully implemented in two case studies of actual projects to demonstrate their practicality and applicability for estimating the PR in microtunnelling operations. Moreover, to further evaluate the proposed simulation-based integrated approaches, using Monte Carlo approach, fifty pseudo-random microtunneling projects are generated, and the practicality of the proposed productivity prediction models is examined by applying them on the generated projects.

5.2. Research Background

Discrete-event simulation (DES) has been widely used by researchers to predict tunneling productivity and to evaluate TBM performance. Simulation inputs for modelling tunneling activities can be determined by using similar project data. For example, Frough et al. (2019) used DES simulation to predict TBM utilization factor and advance rate and to find the distributions for the various tunneling activities. They applied their work to the Karaj Water Tunnel project as a case study, constructing a simulation model based on data from this project. To improve the quality of the simulation input, it should be noted in this regard, a notable approach is to use the Bayesian updating technique, which is based on observations made during tunneling operations (Zouaoui and Wilson, 2003; Chung et al., 2006). For example, Chung et al. (2006) considered the PR of a TBM and showed how the original distribution determined based on expert opinion can be updated using actual PR observations. They also showed that updates early in tunneling operations can improve the accuracy of predictions of project productivity by eliminating the uncertainty of the original subjective distributions. Although these research studies show the advantages of using the Bayesian updating technique, in each case the prior distribution (original assumption for activity duration) has been obtained either by data fitting using similar projects or by using subjective

expert opinions (which pose inherent uncertainties as an input for simulation modelling). To address this issue concerning the use of the Bayesian updating technique, a separate model for predicting the prior distribution of TBM PR is needed. However, a review of the relevant literature reveals that an integrated system combining a simulation model and a separate MTBM PR prediction model for predicting the prior distribution of excavation time has yet to be developed.

Another approach for improving the quality of simulation inputs is to use data-driven models that utilize machine-learning tools to forecast the activity durations for the simulation. This approach requires a continuous stream of data both to serve as a dynamic input to the machine-learning tools and for predicting the activity durations (Akhavian and Behzadan, 2014, 2015). For example, Akhavian and Behzadan (2015) used built-in smartphone sensors to collect data for construction equipment activities and simulation input modelling. They used the case study of front-end loader operation to demonstrate the performance of their data-driven approach for action recognition and for recognizing the various states of construction equipment (e.g., engine off, idle, busy). They obtained satisfactory results with respect to classifying activities and obtaining activity durations.

Although there have been attempts to improve the quality of simulation inputs for various construction activities, an integrated system combining a simulation model and MTBM PR prediction models for microtunneling operations in construction has yet to be developed.

5.3. Integrating mechanistic model for MTBM PR with operation simulation

To integrate the mechanistic model for MTBM PR described in Chapter 3 with simulation, two approaches are developed. The first approach is to incorporate the exact mathematical expression of MTBM PR into simulation, while the second approach is to leverage Bayesian law to enhance

the predictions made by the mechanistic model using the observations of PR obtained during the excavation. In the following subsections, each of these approaches is presented.

5.3.1. Incorporation of exact mathematical expression of MTBM PR into simulation

To incorporate the exact mathematical formula underlying the mechanistic model into the simulation, two important considerations need to be taken into account: (1) the distributions of the parameters of the mechanistic model, and (2) the inter-correlations among the parameters of the mechanistic model.

5.3.1.1. Distributions of parameters of mechanistic model

The developed mechanistic model for MTBM PR can predict the PR to the exact value only if the user knows the exact values for the parameters of the model. Given that, in the absence of access to the MTBM data generated during excavation or laboratory analysis of the ground properties as the basis for obtaining exact values of ground properties, the exact values of the mechanistic model parameters are unknown, and bearing in mind that practitioners typically prefer to use simulation to predict productivity prior to or in the early stages of construction, a mechanistic model for MTBM PR can be used to produce distributions of PR based on distributions of model parameters.

To obtain an accurate prediction of MTBM PR distribution using the mechanistic model, it is important to find the proper distributions for each parameter of the model. Considering that the parameters of the mechanistic model fall into three categories (i.e., operational loads, ground properties, cutterhead characteristics), a distribution for each of the mechanistic model parameters can be obtained from the following sources of information. The distribution for operational load parameters (i.e., cutterhead torque, RPM) can be determined based on data from similar projects, data from recently excavated tunnel sections from the same project under construction, and

expert's judgements. The distribution of ground properties (e.g., Poisson's ratio, shear modulus), meanwhile, can be determined based on geotechnical reports and expert's judgements. The distribution of cutterhead characteristics (e.g., cutterhead opening ratio, diameter, and friction coefficient), finally, can be obtained from MTBM design specification documents.

5.3.1.2. Inter-correlations among parameters of mechanistic model

The range of each parameter of the model having been determined, a value must be sampled for each parameter. During the sampling process, it is important to consider the inter-correlations that exist among the parameters of mechanistic model; otherwise, the sample inputs to be used in the mechanistic model for predicting PR will not be reflective of the real relationships among the parameters, resulting in errors in the predicted PR values. For example, once the distributions of friction coefficient and torque have been properly defined, values for each of these parameters in simulation model need to be sampled before they can be reliably implemented in the mechanistic model for MTBM PR. Given that torque is strongly correlated with the friction coefficient, if any values is sampled from the lower tail of the friction coefficient distribution, correspondingly, the values sampled from the torque distribution should also be taken from the lower tail, as shown in Figure 5.1.

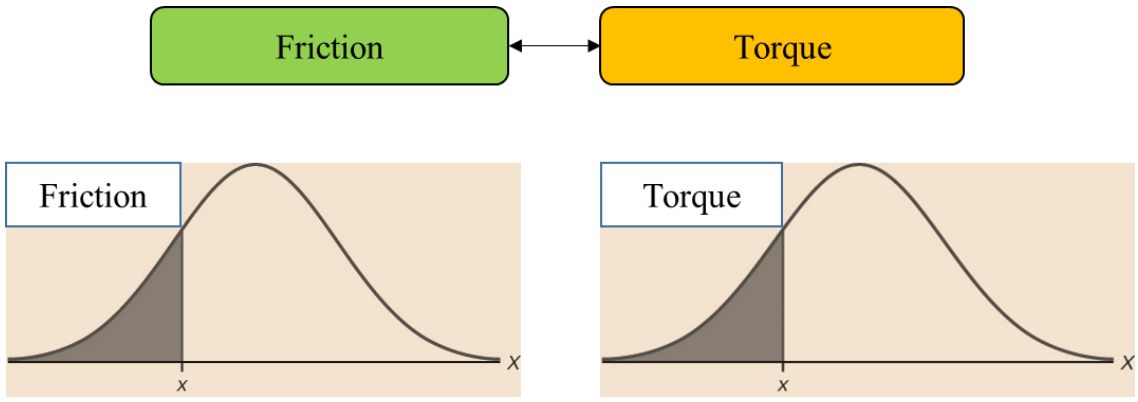

Figure 5. 1. Schematic example of considering inter-correlation among friction and torque when sampling the values from their distribution to input into the mechanistic model for MTBM PR.

To consider this inter-correlation between variables of mechanistic model, a joint correlated distribution is defined and implemented in the simulation model. For this purpose, the well-established Copula function is used. Copula, it should be noted, is a multivariate distribution that examines the associations or dependencies among many variables, allowing for multiple univariate distributions to be combined in a single multivariate distribution.

A joint multivariate distribution among all variables of mechanistic model parameters can be obtained by considering the correlation matrix (P) among them. Then, by assuming the normal marginal distribution for all variables of the mechanistic model, the Gaussian Copula function can be used to produce the joint multivariate distribution.

Gaussian Copula function

The Gaussian Copula is a distribution over the interval [0,1]. For a given correlation matrix P, the Gaussian copula can be expressed as follows:

$$C_P^{Gauss} = \varphi_P(\varphi^{-1}(u_1), \ldots., \varphi^{-1}(u_d)) \quad (5.1)$$

where φ^{-1} is the inverse cumulative distribution function of a standard normal distribution, and φ_P is the joint cumulative distribution function of a multivariate distribution with a mean vector of zero and a covariance matrix equal to the correlation matrix P.

5.3.1.3. Incorporation of MTBM PR model into simulation

Recalling the developed mechanistic model for MTBM PR, as shown in Eq. 3.10 in Chapter 3.

$$PR = \frac{RPM\,T}{\pi} \times \frac{(1-\nu)}{G} \times \frac{1}{fa^2(1-\mu)} \quad (3.10)$$

This exact mathematical formula of the mechanistic model is coded in the Simphony simulation model referred to as “MechanisticPR”, as shown in Figure 5.2. In this element of the simulation

model, the correlations among various attributes of the mechanistic model are then coded. Moreover, to make it easier for the user to define the distributions of each of the mechanistic parameters, they are all defined as task elements in the user interface of the Simphony simulation model, as shown in Figure 5.3. In this way, to define the distribution of a given mechanistic parameter, the user simply clicks on it and defines its distribution as a duration of the task element.

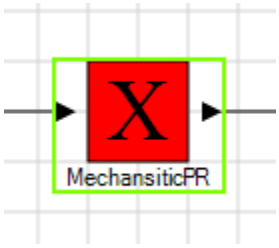

Figure 5. 2. Element of the simulation model, referred to as "MechanisticPR", in which the exact mathematical formula of the mechanistic model is coded.

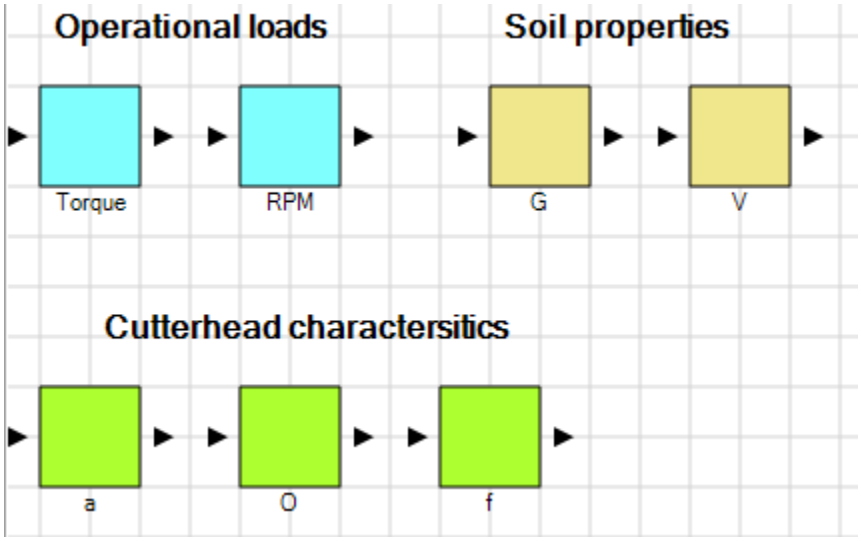

Figure 5. 3. Parameters of mechanistic model defined as task elements in the simulation model.

Once the user has defined the distribution for each of the mechanistic parameters, the "MechanisticPR" element of the simulation model calculates the PR based on the mechanistic model as a local variable Lx(10), and then calculates the duration of the MTBM excavation as a local variable Lx(11). This value serves as the duration input to the "TBM-Excavation" task element in the simulation model, as shown in Figure 5.4.

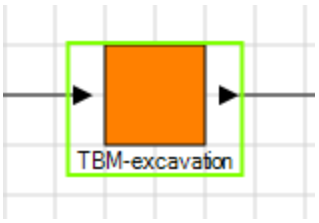

Figure 5. 4. "TBM-excavation" task element in the simulation model.

The other processes of microtunneling construction defined in the simulation model are then run and the entire project duration estimated accordingly.

5.3.2. Use of Bayesian updating approach for incorporating the mechanistic model for MTBM PR into the simulation

To leverage the PR observations made during microtunneling construction and improve the predicted distribution of PR based on the mechanistic model, the Bayesian updating technique is applied to the mechanistic model. In the following subsections, a brief overview of Bayesian updating technique is first provided, followed by a summary of the steps involved in applying this technique in conjunction with the mechanistic model for MTBM PR.

5.3.2.1. Overview of Bayesian updating techniques

Bayes' theorem is defined in the following equation:

$$P(\mathrm{A}|\mathrm{B}) = \frac{\mathrm{P}(\mathrm{B}|\mathrm{A})\mathrm{P}(\mathrm{A})}{\mathrm{P}(\mathrm{B})} \tag{5.2}$$

where P(A|B) is a conditional probability, i.e., the probability of event A occurring given that B is true, also referred to as the posterior probability of A given B; P(B|A) is the likelihood of A given B; and P(A) and P(B) are the probabilities of observing A and B, respectively, without any given conditions, the latter also being known as the prior probability. Based on this theorem, if the input distribution for an activity in the simulation model is continuous and has an underlying probability density function, this prior distribution can be updated using Bayes' theorem when actual observations become available. The updated distribution is referred to as the posterior distribution.

The posterior distribution is proportional to the prior distribution and the likelihood of observations, as expressed in the following equation:

$$Posterior\ distribution \propto Prior\ distribution \times Likelihood\ of\ observations \tag{5.3}$$

The derivation of the posterior distribution of a parameter can be simplified mathematically if the prior distribution of the parameter is selected in consideration of the underlying random variable. This means that, if a given prior distribution is a conjugate of the distribution of the underlying variable, a posterior distribution can be obtained using the same mathematical form as the prior (Ang and Tang, 1975). For example, if a prior distribution is a normal distribution with a mean of μ' and a standard deviation of σ', the posterior distribution parameters can be obtained from the following equation, where the mean and standard deviation of the observations are $\bar{x}$ and σ and the number of observations is n (Ang and Tang, 1975).

$$\mu'' = \frac{\bar{x}\,(\sigma')^2 + \mu'(\sigma^2/n)}{(\sigma')^2 + (\sigma^2/n)} \tag{5.4}$$

$$\sigma'' = \sqrt{\frac{(\sigma')^2(\sigma^2/n)}{(\sigma')^2 + (\sigma^2/n)}} \tag{5.5}$$

Based on the Bayesian updating technique described in this section, the distribution of PR obtained from the mechanistic model can be updated once observations of the PR / excavation time become available as the project progresses. In the following subsection, the procedure for using the Bayesian updating technique in combination with the mechanistic model for MTBM PR is presented.

5.3.2.2. Bayesian updating mechanistic model for MTBM PR

To use the Bayesian updating concept in conjunction with the mechanistic model for MTBM PR to develop a Bayesian updating mechanistic model for MTBM PR, three steps are followed as outlined below:

1- Find the prior predictive distribution of PR / excavation time based on mechanistic model

2- Obtain the PR / excavation time observations; and

3- Obtain the posterior predictive distributions of PR / excavation time.

5.3.2.2.1. Finding the prior predictive distribution of PR / excavation time based on the mechanistic model

A prior predictive distribution is a prior distribution in which the parameters of the distribution each have their own uncertainties. For example, a prior predictive distribution of MTBM PR based on the mechanistic model is the prior knowledge that the MTBM PR distribution obtained using the mechanistic model and the parameters of the PR distribution (assuming a beta distribution) has uncertainties (e.g., Alfa, which is one of the parameters describing beta distribution, has a triangular distribution). To find the prior predictive distribution of PR / excavation time, a prior distribution of PR / excavation time based on mechanistic model must first be determined, following which the uncertainties of the prior distribution's parameters are calculated.

To find the initial distribution of the MTBM excavation duration based on the mechanistic model, the type of distribution that the mechanistic model produces for the excavation duration must first be determined. In the Simphony simulation environment, a simple model is created that includes the mechanistic model for MTBM PR, which is coded in the "MechanisticPR" element shown in Figure 5.5. In turn, the MTBM excavation time is calculated. A user-friendly interface is developed to input the ranges of the mechanistic model parameters into simulation environment. Based on the analysis of the mechanistic model achieved by inputting the ranges of mechanistic model

parameters in the simulation environment (shown in Figure 5.5) and calculating the PR and excavation time, and fitting a distribution to the excavation time results obtained, it is determined that the mechanistic model produces a “Beta” distribution for the MTBM excavation duration, as shown in Figure 5.6.

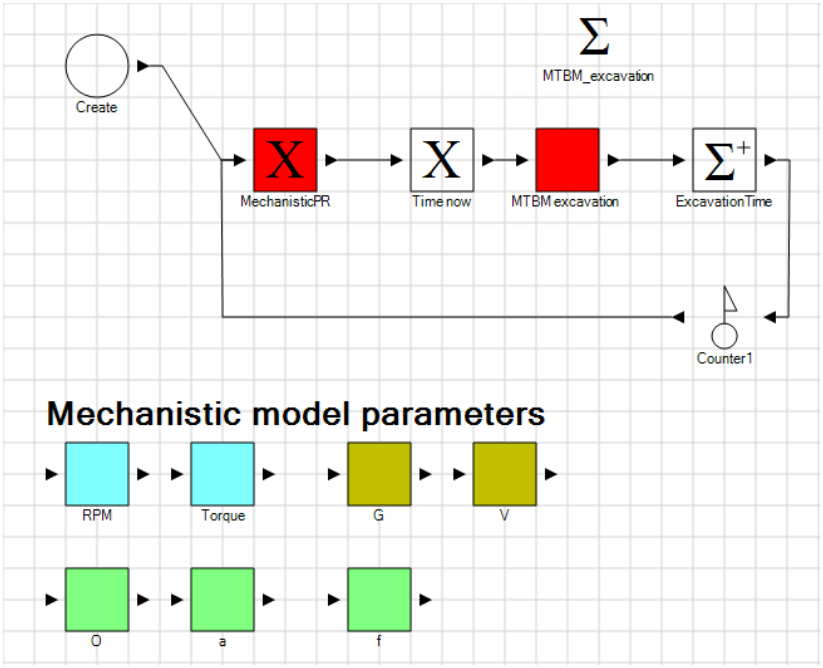

Figure 5. 5. Simphony simulation model developed to obtain the prior predictive distribution of excavation time based on mechanistic model.

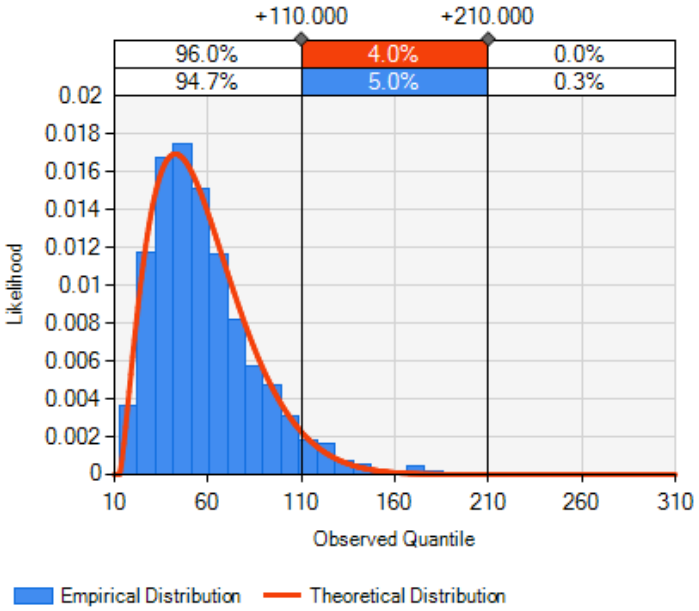

Figure 5. 6. Distribution of excavation time based on mechanistic model.

The type of distribution having been determined, the next step is to define the uncertainties of the parameters in "Beta distribution", namely, Alfa, Beta, Low, and High. To find the distributions for each of the "Beta distribution" parameters, the simulation model shown in Figure 5.5 is experimented several times (each experiment has 1,000 simulation runs). Records of beta distribution parameters for each run are collected, and distributions for the parameters of "Beta distribution of excavation time" are determined accordingly (Figure 5.7).

Beta ditribtion-1000 runs				
Experiment number	Alfa	beta	Low	High
1	3.00	24.86	7.95	490.21
2	3.22	23.27	8.82	382.61
3	2.33	13.41	12.76	296.41
4	2.49	10.99	11.52	250.82
5	2.75	10.87	9.25	236.49
6	2.95	16.55	8.21	315.48
7	2.39	11.86	12.76	262.85
8	2.51	16.01	11.52	346.75
9	3.26	9.92	4.70	205.85
10	2.41	13.17	12.79	301.16
11	2.83	10.12	7.58	226.63
12	2.93	14.07	9.41	268.61
13	2.73	13.58	9.53	279.98
14	2.69	10.96	9.51	240.97
15	2.64	14.12	11.18	293.78
16	2.68	16.30	11.51	321.03
17	2.34	8.59	12.86	213.55
18	2.99	12.45	8.43	244.86
19	2.86	12.03	8.07	254.90
20	2.21	8.87	13.72	224.83
....				
Distribution	Triangular	Beta	Uniform	Triangular
	1.889	1.343	6.399	182.656
	3.369	3.679	13.644	402.500
	2.766	8.586		229.704
		24.861		182.656

Figure 5. 7. Example of experiment records for determining distributions for the parameters of "Beta distribution of excavation time".

5.3.2.2.2. Obtaining PR / excavation time observations

During microtunneling excavation, observations of PR or excavation time for each pipe section can be made. These observations can be used to "update" the prior understanding concerning the distribution of MTBM excavation time as obtained from the mechanistic model.

5.3.2.2.3. Obtaining posterior predictive distributions of PR / excavation time

Once observations of excavation times become available, the posterior predictive distribution based on Bayes' rule can be determined. Figure 5.8 shows the posterior predictive distribution (green line), prior predictive distribution (red line), and histogram of excavation time observations (blue histogram).

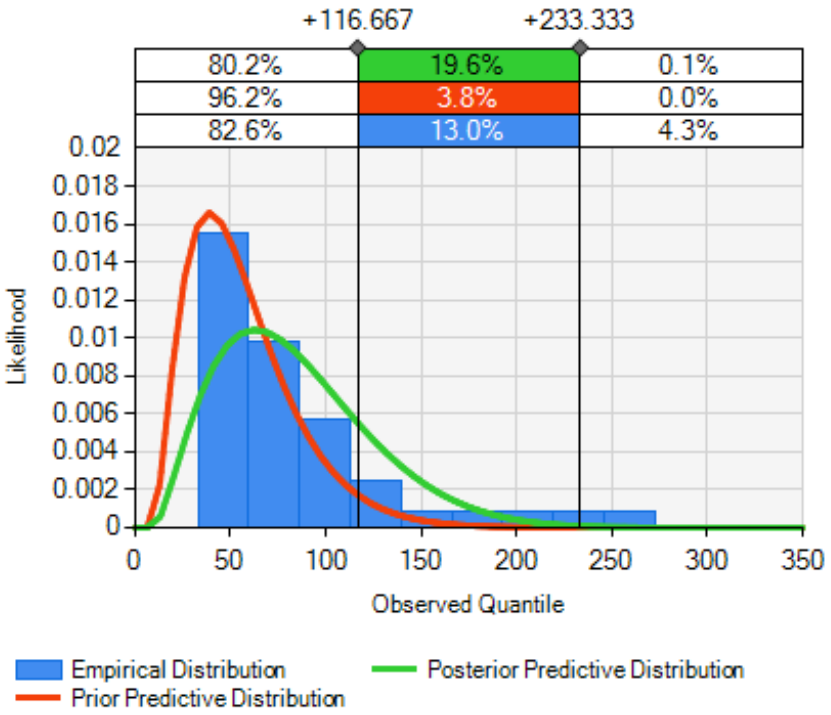

Figure 5. 8. Example of updating the prior predictive distribution using observations and obtaining posterior predictive distribution of excavation time.

The figure above demonstrates the successful deployment of Bayes' theorem to integrate the mechanistic model for MTBM PR with simulation. Using this approach, not only can practitioners benefit from the predictions made by the mechanistic model for MTBM PR, but they can also enhance the performance of the mechanistic model by updating it using the Bayesian updating technique.

5.4. Integrating Machine-learning model for MTBM PR with Simulation

To integrate the machine-learning model for MTBM PR with the simulation model for microtunneling construction, a database is created in the simulation model (Figure 5.10) that calls the results of the machine-learning model for MTBM PR. This database includes both the predicted PR and the location along the tunnel length where the PR prediction is made. Figure 5.9 shows an example MTBM PR prediction between boreholes in the "St. Albert project" (referenced in the case study section below).

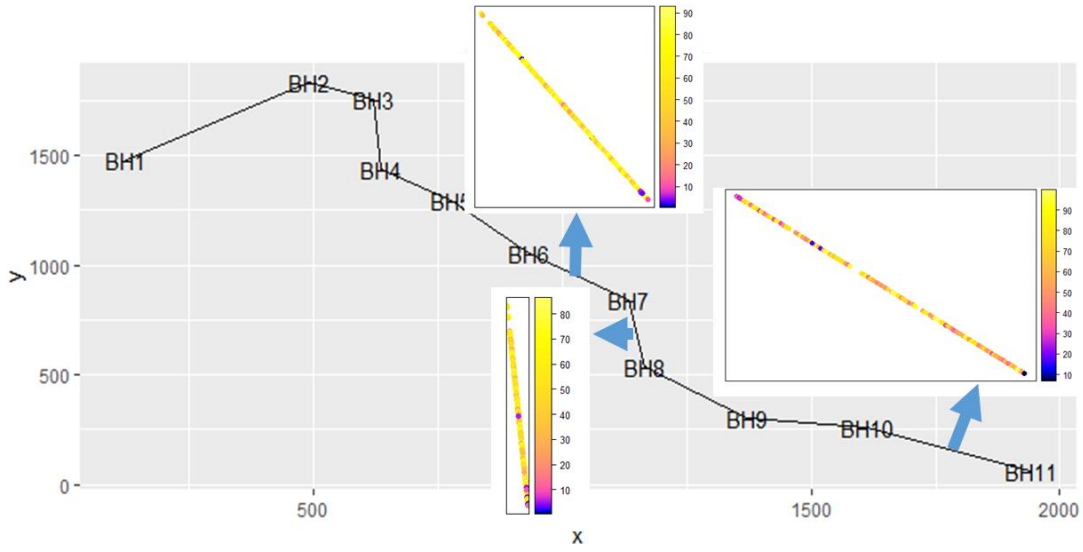

Figure 5. 9. Example of MTBM PR predicted spectrum between boreholes in St. Albert microtunneling project.

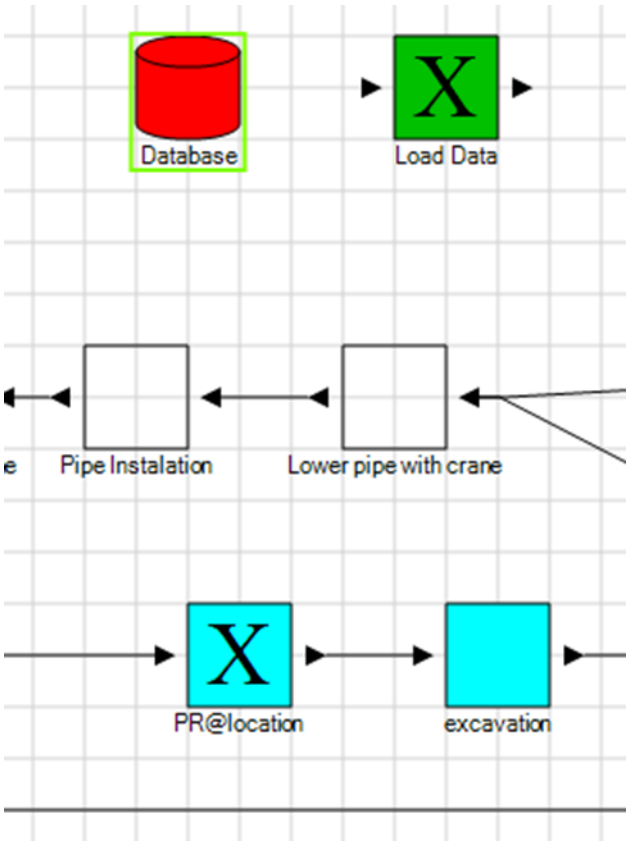

Figure 5. 10. Simulation environment that includes “Database” element for calling the predicted PR using machine-learning approach and “Load Data” element to load the data into simulation model.

The predictions of PR along the tunnel length having been inputted to the simulation model, these data will be read. Based on the predicted PR, the excavation time for pipe sections can be calculated and used to model the MTBM excavation time in the simulation environment.

5.5. Case study analysis

Two actual microtunneling construction projects in the Alberta, Canada are used to test the proposed approaches of integrating MTBM PR prediction models with simulation. With respect to each of the microtunnelling projects, the aim is to update the project productivity and expected project duration during project execution. To examine the effect of continuous updating of the

project plan during construction, each project plan is updated at various percentages of project completion. In the following subsections, these projects are described in greater detail.

5.5.1. Case study 1

To validate the application of the "integrated simulation + Bayesian updating mechanistic model for MTBM PR prediction" and the "integrated simulation + machine-learning model for MTBM PR prediction", the predicted project durations are compared to the actual values obtained from microtunnelling construction of a sanitary trunk in Alberta, Canada. (A detailed description of this case study is provided in Section 2.5.2.) The tunnel length is divided into four sections, as shown in Figure 5.11. The first tunnel section is used to obtain (1) the initial estimate of mechanistic model parameters, and (2) the MTBM data required for training the first artificial neuron network (ANN) model. Based on the respective predictions of PR for the remaining tunnel length at 37% and 60% project completion, the project plan is updated and the predicted project durations are compared with the actual project duration. As shown in Figure 5.12A, when the project duration is updated using the "integrated simulation + Bayesian updating mechanistic model for MTBM PR prediction" at 37% project completion, the actual project duration at 60%, 73%, and 100% project completion is found to fall between the predicted upper and lower ranges of project duration. As the project progresses and more information about the MTBM–ground interaction becomes available, the predicted range for project duration becomes narrower and closer to the actual project duration. This is shown in Figure 5.12B, where the project duration is predicted at 60% project completion. To examine the "integrated simulation + machine-learning model for MTBM PR prediction", the project duration is updated at 37% and 60% project completion (Figure 5.13). The approach integrating the simulation model with machine-learning model for MTBM PR, like the approach integrating simulation with the mechanistic model, yields promising results,

with the actual project durations obtained by updating it at 37% and 60% project completion being found to fall within the predicted ranges of project duration. Moreover, a comparison of these results with the predictions obtained based on expert opinion and the CPM method reveals that the proposed integrated simulation-based models improves the accuracy of the predictions of project duration while updating it at various percentages of project completion

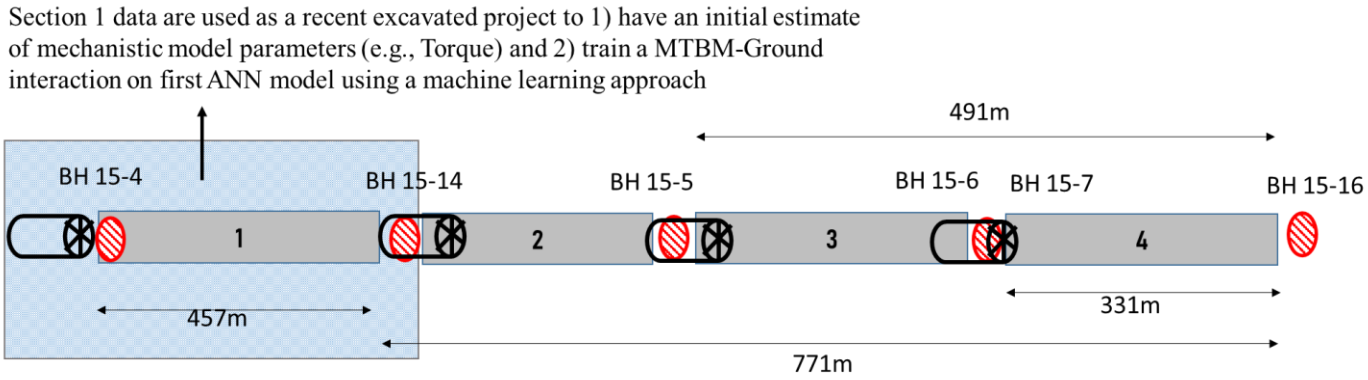

Figure 5. 11. Obtaining the initial information required for both the mechanistic model and the machine-learning model for MTBM PR.

A.

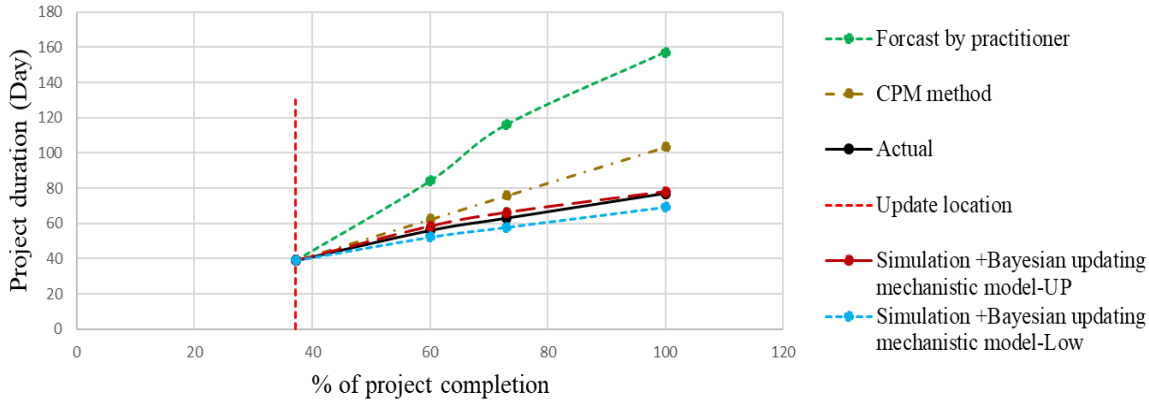

B.

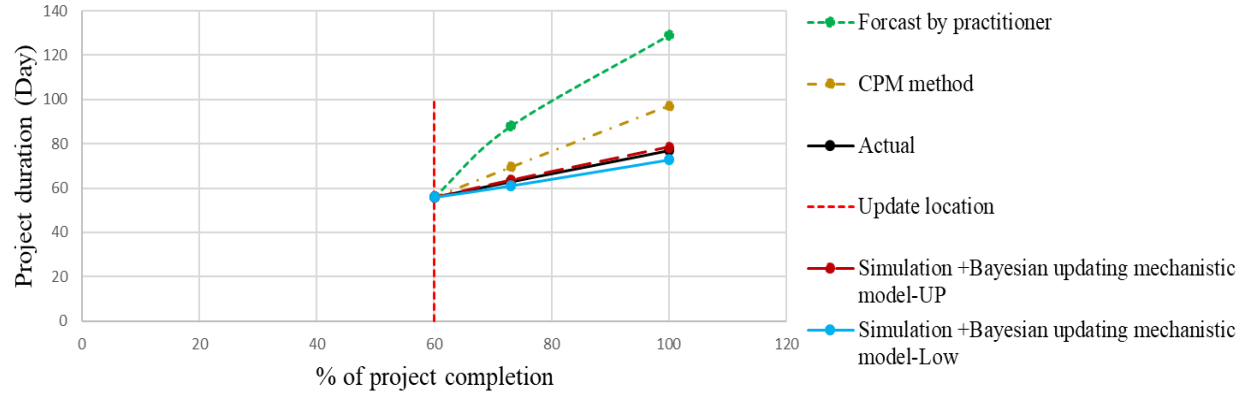

Figure 5. 12. Results of updating the project duration at (A) 37% project completion and (B) 60% project completion using the "integrated simulation and Bayesian updating mechanistic model for MTBM PR prediction" and comparison with predictions generated by practitioners and by the CPM method.

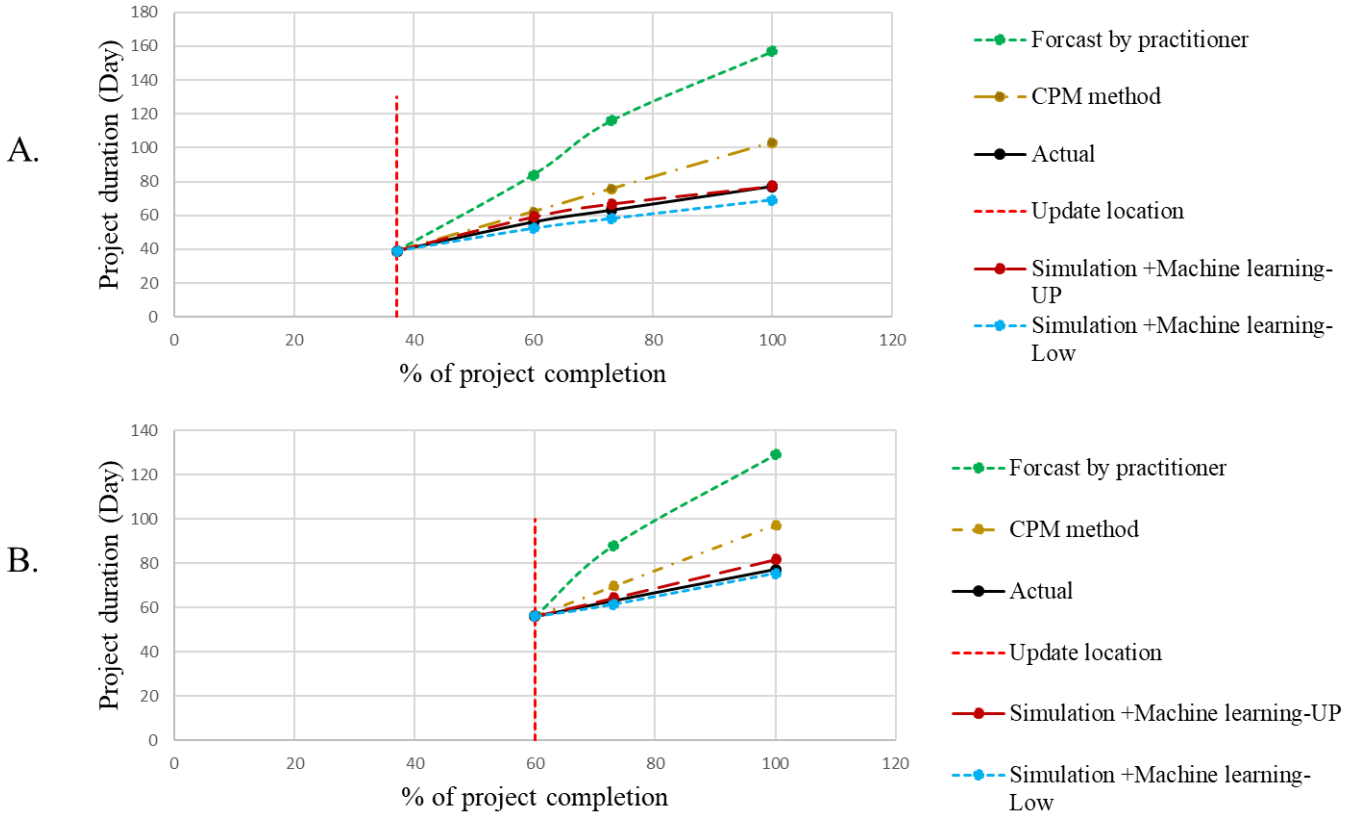

Figure 5. 13. Results of updating the project duration at (A) 37% project completion and (B) 60% project completion using an " integrated simulation and machine-learning model for MTBM PR prediction" and comparison with predictions generated by practitioners and by the CPM method.

5.5.2. Case study 2

The second case study is a microtunnelling construction project in Alberta, Canada. This project consists of two microtunneling sections, one between borehole 18 (BH18) and BH15 (i.e., Section A) and another between BH4 and BH10 (i.e., Section B). (The project is described in greater detail in Chapter 2, Section 2.5.3.) To examine the performance of the integrated MTBM PR prediction models, the project duration is updated after 22% excavation of Section B and using the excavation time observations, and the predicted project durations are compared with the actual project duration.

Analysis of the results for the two developed approaches shows that the actual project durations for completing excavation to 52% and 100% of the project fall within the predicted ranges for both

approaches (Figure 5.14A, and 5.14B). Moreover, a comparison of the simulation-based prediction models with forecast by practitioners shows that the proposed integrated simulation-based productivity models significantly improve the accuracy of the predictions. This improvement in predicting the project duration is illustrated in Figure 5.14A, where the difference between the predicted project duration by practitioner (at 100% completion) and actual project duration is much higher (100 days − 60 days = 40 days) compared with the predicted range generated using the "integrated simulation + Bayesian updating mechanistic model for MTBM PR prediction", i.e., a maximum duration of 64 days and a minimum duration of 55 days. Further analysis of the results of both approaches, i.e., both the "integrated simulation + Bayesian updating mechanistic model for MTBM PR prediction" and the "integrated simulation + machine-learning model for MTBM PR prediction", shows that, as the distance between the updating location and the target location decreases, the predicted window of project duration becomes smaller, meaning that the degree of uncertainty concerning the project duration is decreasing.

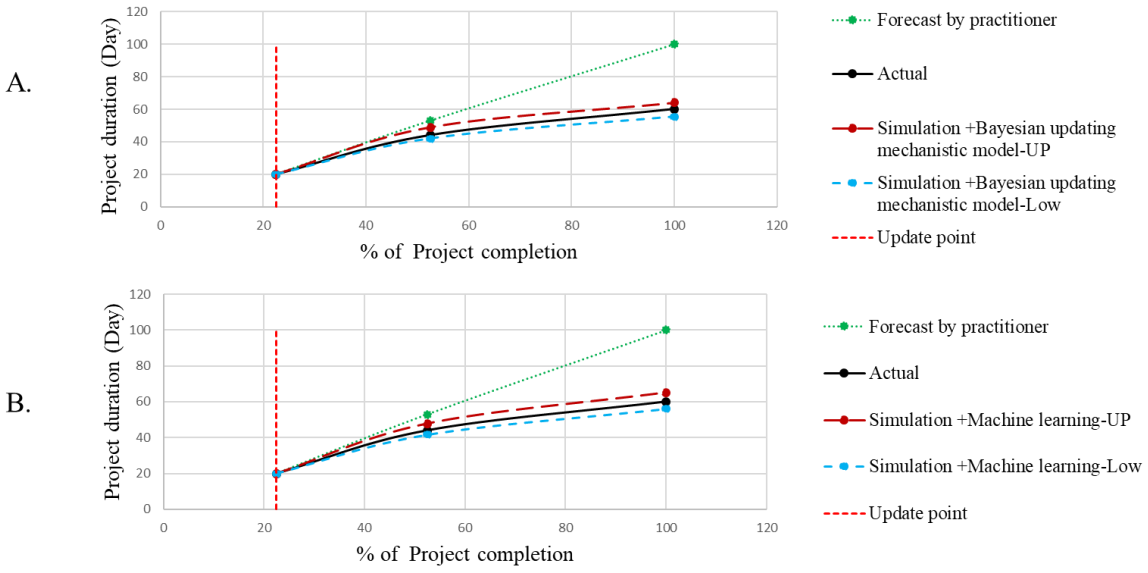

Figure 5. 14. Results of updating the project duration at 22% project completion using (A) Simulation + Bayesian updating mechanistic model for MTBM PR and (B) Simulation + Machine-learning model for MTBM PR.

5.6. Validation of integrated simulation and MTBM PR prediction models using Monte Carlo project generation approach

5.6.1. Introduction

When examining a complex system with multiple interacting components, a large number of data points (or projects) is needed to serve as inputs for evaluating the system. In this regard, the idea of generating synthetic data to simulate the real system has been used for evaluating model performance in various fields, including electrical engineering (Schweitzer et al., 2017), transport planning (Frick and Axhausen, 2003), robotics (Buch and Kraft, 2017), health care (Walonoski et al., 2018), and construction management (Ead, 2020). For example, Frick and Axhausen (2003) generated synthetic populations in order to acquire useful data for large-scale multi-agent-based microsimulations in the field of transport planning. Since the Public Use Sample (PUS) often used in transportation studies represents only a small percentage of the complete census records for each individual, Frick and Axhausen (2003) generated, in a synthetic manner, a large number of individuals with appropriate characteristic values representative of demographic variables. Walonoski et al. (2018) to address the lack of freely distributable health records that is a hindering factor for innovations in health care system, created a source of synthetic electronic health records and generated synthetic patients. In simulating construction operation, the uniqueness of each project typically results in an inadequate dataset of actual projects that can be used for validation and comparison of simulation-based prediction models (Ead, 2020). To overcome this issue, Ead (2020) employed a random project generation approach Monte Carlo approach in order to test the performance of various forecasting theories used for project control purposes.

Due to the relatively limited number of actual microtunnelling project case studies available based upon which to test the integrated models for MTBM PR prediction (to forecast the project duration during construction), synthetic pseudo-random microtunneling projects are generated in the

present research for validation of the "integrated simulation + Bayesian updating mechanistic model for MTBM PR prediction" and the "integrated simulation + machine-learning model for MTBM PR prediction".

5.6.2. Methodology

To generate microtunneling projects using the Monte Carlo approach, the following considerations need to be taken into account:

1) MTBM behaviours such as PR and operational excavation loads strongly depend on the soil properties (stiffness, moisture content, etc.)

2) Selection of MTBM and its characteristics, such as opening ratio, also depends on the soil properties and tunnel conditions.

3) Soil properties are inter-dependent.

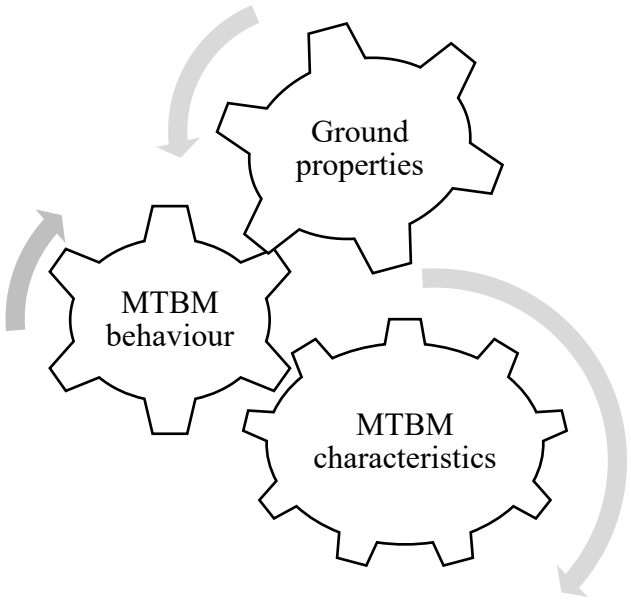

Figure 5. 15. Schematic representation of inter-dependencies among primary components of MTBM excavation.

As such, when generating microtunneling projects, it is important to model these inter-dependencies (Figure 5.15) and incorporate them into the algorithm used for project generation.

5.6.2.1. Main algorithm for microtunneling project generation

The main algorithm for the generation of microtunneling projects is shown in Figure 5.16. The first step in generating microtunneling projects is to generate the microtunneling project specifications (detailed in Algorithm A). The soil parameters at each borehole along the tunnel length are then generated in order to simulate the initial geotechnical data available at each microtunneling project (Algorithm B). The soil properties at each borehole along tunnel length having been specified, they are then interpolated in the third step. In the fourth step, which is the most complex step, the MTBM data corresponding to the soil properties and tunnel conditions is generated, and independent MTBM parameters are also generated (as is addressed in greater detail in the description of Algorithm C). Once all the soil properties have been interpolated and the MTBM data generated, the next step is to determine the locations at which the project duration is to be updated and examine the dynamic performance of integrated simulation and MTBM PR prediction models. In this regard, the tunnel is broken down into four sections divided at 10%, 20%, and 30% of project completion in order to update the project duration. As the last step in the main algorithm of project generation, a PR observation must be collected for the same locations at which the project duration is to be updated. (This last step is required due to the fact that the Bayesian updating technique in the PR prediction model uses observations.)

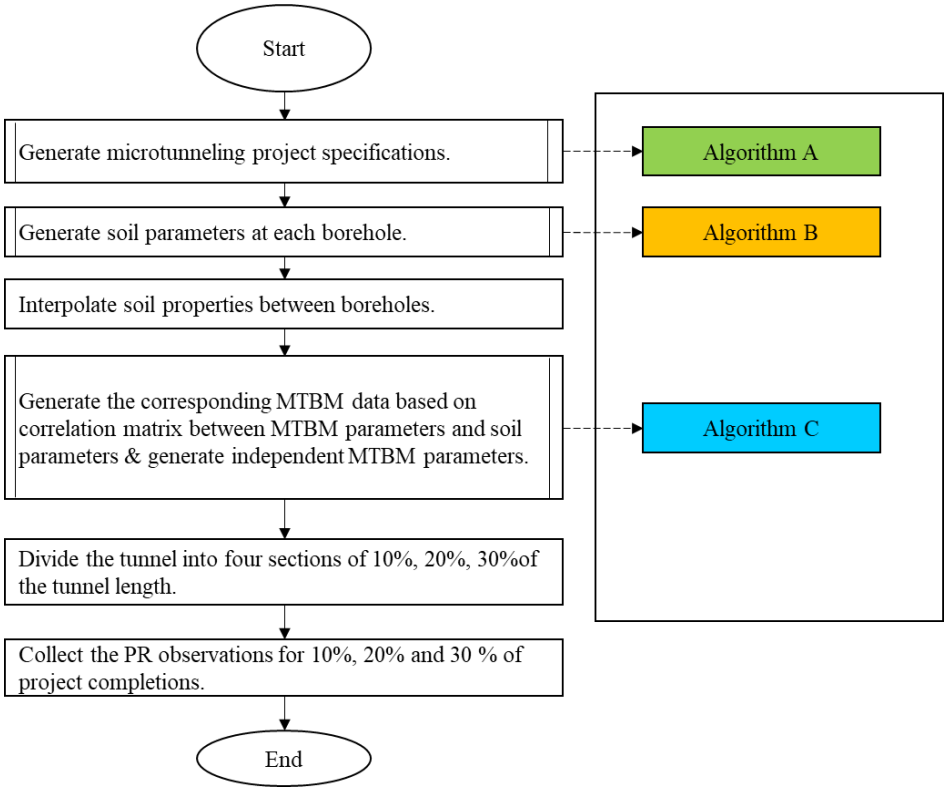

Figure 5. 16. Main algorithm for the generation of microtunneling projects.

5.6.2.2. Generation of microtunneling project specifications (Algorithm A)

The process of generating microtunneling project specifications is initiated by generating a random tunnel length (Figure 5.17). The MTBM type and specifications are then determined. In this regard, based on information obtained from various MTBM manufacturers' websites, a database of 27 actual MTBM types with their specifications is created (Figure 5.18) and, for each project, a random MTBM type and specifications are selected. The MTBM specifications include MTBM type (brand), maximum torque capacity (kN.m), diameter (m), and maximum RPM. The various cutterhead characteristics, including the opening ratio, are then generated. Regarding tunnel condition, a random cover depth, fixed distance between boreholes, and number of tunnel sections are generated. A borehole table that includes borehole ID (BHID) and borehole locations (BH locations) can then be generated accordingly. Ultimately, taking into account the MTBM

specifications for each project, the distributions for the MTBM parameters (e.g., torque) and soil parameters (e.g., SPT) are generated for use in random sampling.

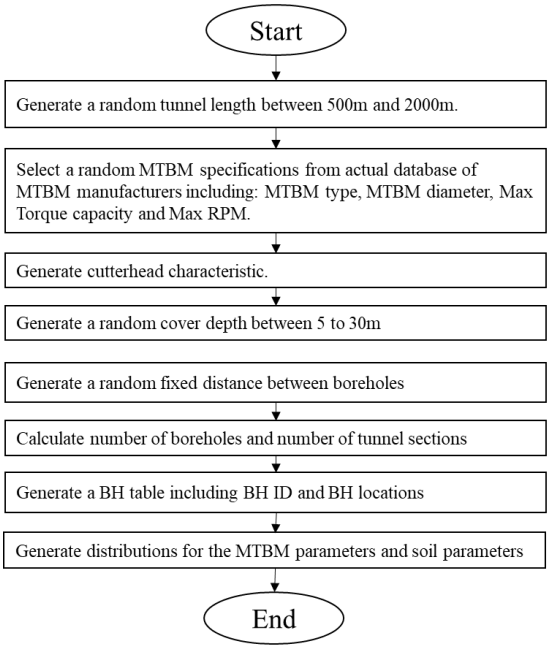

Figure 5. 17. Algorithm for generation of microtunneling project specifications (Algorithm A).

	MTBMtype	MaxTorque(kN.m)	Diameter(m)	MaxRPM
1	Akkerman SL36	85.4	1.00	8.0
2	Akkerman SL44	85.4	1.37	8.0
3	Akkerman SL30	53.2	0.81	13.0
4	Akkerman SL51	120.4	1.30	9.5
5	Akkerman SL60	298.0	1.52	7.7
6	Akkerman SL74	298.0	1.88	7.7
7	Akkerman SL82	490.0	1.98	9.0
8	Herrenknecht AVN 1200	195.0	1.52	3.5
9	Herrenknecht AVN 1500	310.0	1.50	3.2
10	Herrenknecht AVN 1600	310.0	1.65	3.2
11	Herrenknecht AVN 1800	445.0	1.73	3.3
12	Herrenknecht AVN 600	33.5	0.76	13.0
13	Herrenknecht AVN 900	298.0	0.90	5.0
14	Herrenknecht AVN 1000	150.0	1.32	5.4
15	Herrenknecht AVN 1200TB	258.0	1.52	6.7
16	Herrenknecht AVN 1200TC	258.0	1.52	5.0
17	Herrenknecht AVN1800TB	554.0	2.44	11.9
18	Herrenknecht AVN 800	55.0	1.30	7.4
19	Herrenknecht AVN-800A	90.0	1.35	7.1
20	Iseki TCC1000	121.5	1.22	2.0
21	Iseki TCC1350	298.0	1.68	1.5
22	Iseki TCC500	120.0	0.61	3.7
23	Iseki TCC600	270.0	0.76	2.2
24	Iseki TCC900	96.0	1.07	1.8
25	Iseki TCS900	120.0	1.07	2.6
26	RASA DH 1900	411.0	2.44	2.1
27	RASA DT 1500	91.0	1.78	3.2

Figure 5. 18. Database of 27 microtunneling types and their specifications.

5.6.2.3. Generation of soil parameters at each borehole (Algorithm B)

To generate the soil parameters at each borehole, the algorithm shown in Figure 5.19 is used. First, two main soil categories (cohesive and cohesion-less) are created. Then, a Markov chain representing the transition between cohesive and cohesion-less soil zones is created (Figure 5.20). Based on the initial-state soil category (i.e., either cohesive or cohesion-less) and the project number generated, a probability of choosing a given soil category is generated. Then, based on the soil category probability for each borehole location, a soil category is randomly sampled. Once a

soil category for each borehole in the given project has been specified, the SPT-N value (i.e., one of the soil properties) can be determined in accordance with Algorithm B-6. The SPT-N value for each borehole having been specified, the other geotechnical parameters corresponding to the generated SPT-N values can be generated using the soil correlation matrix detailed in Algorithm B-7.

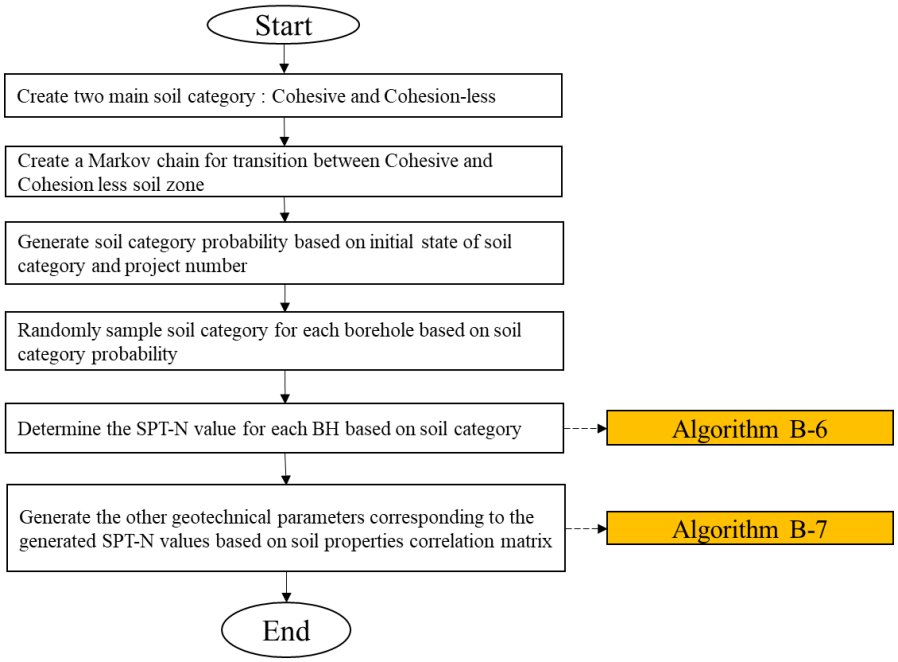

Figure 5. 19. Algorithm for generation of soil parameters at each borehole (Algorithm B).

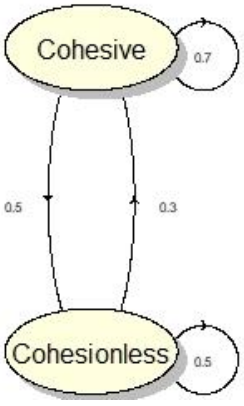

Figure 5. 20. Schematic representation of Markov chain for transition between cohesive and cohesion-less soil zones.

5.6.2.3.1. Determining the SPT-N value for each borehole based on soil type category (Algorithm B-6)

For the purpose of determining the SPT-N value for each borehole, the algorithm shown in Figure 5.21 is developed. First, for each category of soil (cohesive and cohesion-less), different states of relative density are created, and the probability of choosing a given state within a given soil category is determined. In this regard, two well-known tables that classify the various states of soil for each soil category and also determine the ranges of SPT-N value for each status are adopted and redefined based on Peck et al. (1974). For cohesive soils, the "consistency table" (Table 5.1) and for granular soil (cohesion-less) the "relative density table" (Table 5.2) are created. In looking at each borehole soil category, if the borehole is cohesive, then a soil status from the consistency table is sampled randomly (considering the probability of each status selection), whereas, if the borehole is cohesion-less, then a soil status from the relative density table is sampled randomly. Then, depending on the status of the sampled soil, the corresponding SPT-N value from the specified ranges (available in both the consistency table and the relative density table) is randomly selected.

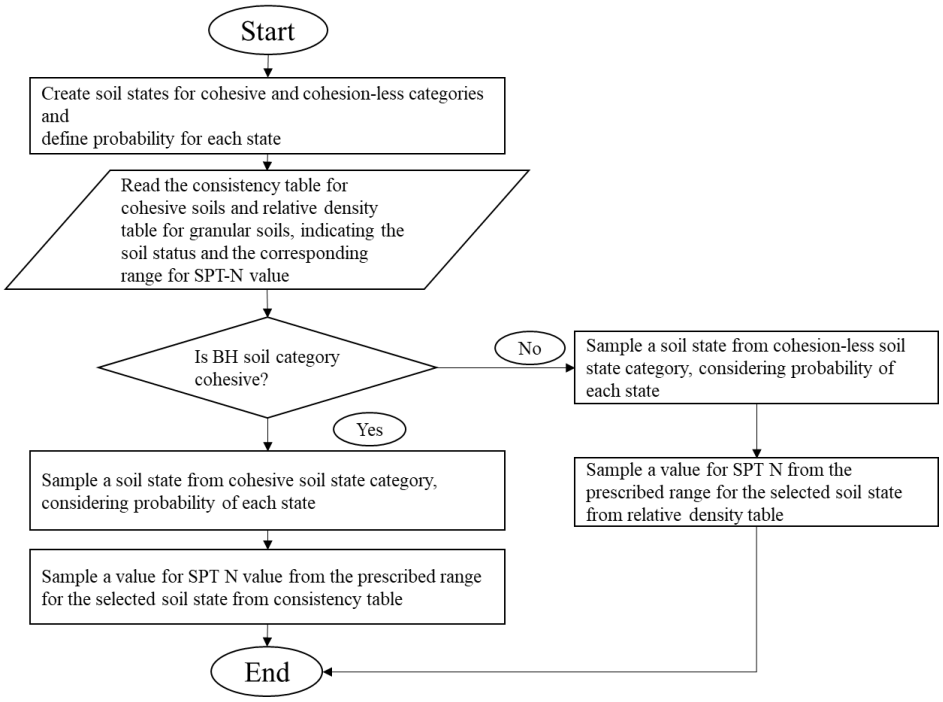

Figure 5. 21. Algorithm for determining the SPT-N value for each borehole based on soil category.

Table 5. 1. Consistency table defining SPT-N value for cohesive soils states.

	minN	maxN
soft	2	4
medium	5	8
Stiff	9	15
VeryStiff	16	30
Hard	31	50

Table 5. 2. Relative density table defining SPT-N value for cohesion-less soils states.

	minN	maxN
VeryLoose	2	4
Loose	5	10
Medium	11	30
Dense	31	50
VeryDense	51	70

5.6.2.3.2. Generation of the other geotechnical parameters corresponding to the generated SPT-N values based on soil properties correlation matrix (Algorithm B-7)

In this step, the aim is to generate the other geotechnical parameters based on consideration of their inter-correlations among one another and with SPT (Figure 5.22). The soil environment, it should be noted, is highly complex in terms of the inter-correlations among various properties. To capture these inter-correlations in generating the soil environment, the correlation matrix linking the various soil properties is defined based on analysis of geotechnical data from available projects. To capture uncertainty in the generated soil correlation matrix, meanwhile, two soil correlation matrices are defined. For each generated project, one of the soil correlation matrices is randomly sampled.

Before discussing the manner in which the other geotechnical parameters are generated, an explanation of the procedure for generating samples from joint multivariate correlated distributions is warranted. In this procedure, based on correlation matrices between various attributes, samples from joint correlated distributions can be obtained. The procedure is as follows:

Step 1: Compute a correlation matrix, P, comprising all variables.

Step 2: Compute the Cholesky decomposition, C, of P such that $\mathrm{P} = \mathrm{C}^{\mathrm{T}}\mathrm{C}$.

Step 3: Generate the vector of independent random variables from standard normal distribution $Z = (Z1, \dots, Zn)$ for each parameter.

Step 4: Generate samples from joint multivariate normal distribution (U) using the calculation $U = C \times Z$.

Step 5: Transform the samples from the joint correlated distribution to attributes' values using the inverse transform method.

Applying this procedure, the following specific steps are taken to obtain the other geotechnical factors (i.e., those corresponding to the generated SPT-N values at each borehole). Based on the selected correlation matrix, the Cholesky decomposition of soil correlation matrix is determined. The marginal distributions for the soil properties (e.g., water content) and MTBM data (e.g., torque) are then defined. Then, the U matrix, which is in fact the samples from the joint correlated normal distributions, can be obtained by transforming the SPT-N values to a sample from a standard normal distribution using the inverse transform method. The U matrix is then multiplied by the inverse of the Cholesky decomposition to obtain the Z matrix. By sampling the missing entries of Z from the standard normal distribution and multiplying the samples by the Cholesky decomposition, a matrix containing a sample from the joint correlated distribution can be obtained. By transforming the joint correlated sample to the specified ranges for each of the soil properties (using the inverse transform method), the values of the other soil properties corresponding to the SPT-N values are obtained. The last step in this algorithm (i.e. Algortihm B-7) is to generate a database of soil parameters for each borehole ID and borehole location.

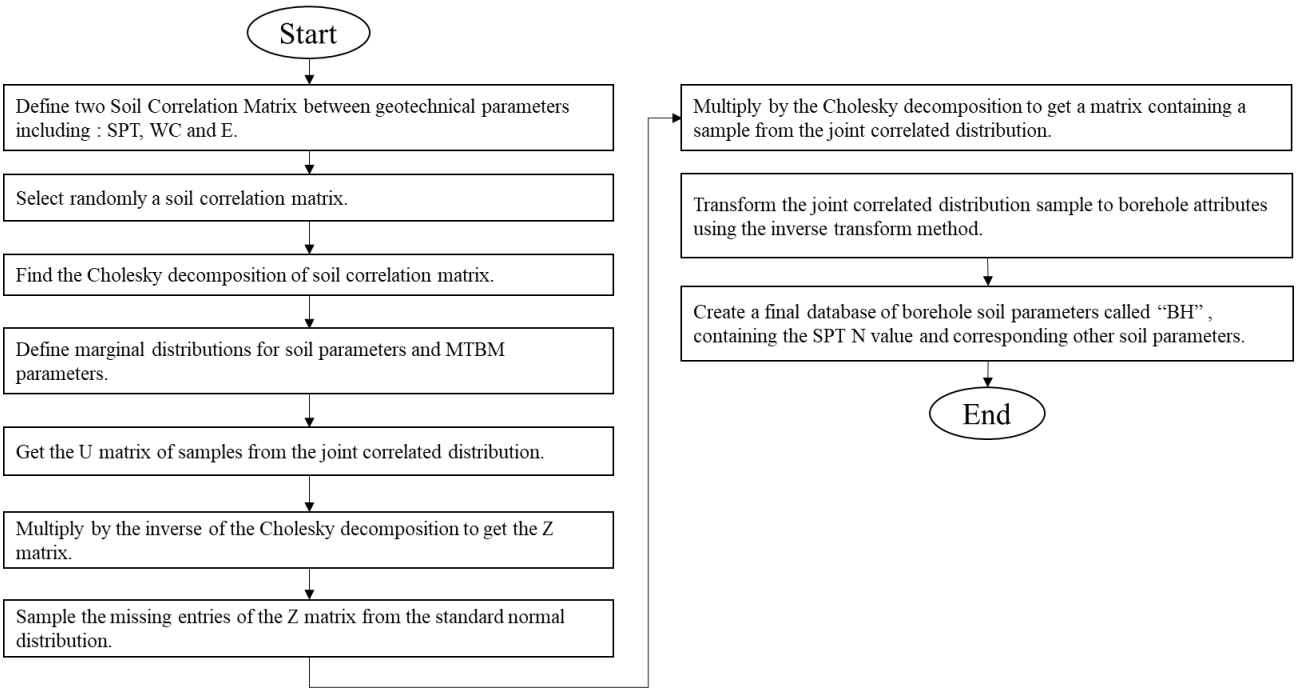

Figure 5. 22. Algorithm for generation of the other geotechnical parameters corresponding to the generated SPT-N values based on soil properties correlation matrix.

The next step in the main algorithm (Figure 5.16) is interpolation of the soil properties between boreholes.

5.6.2.4. Interpolation of soil properties between boreholes

To interpolate soil properties between boreholes, the inverse weighted distance (IWD) approach is used. (The detail explanation of the IWD method can be found in Section 4.3.3 above.) Once the interpolation of soil properties between boreholes along the tunnel path is completed, the next step is to generate the corresponding MTBM data along the tunnel path (at specified interpolated locations) based on the correlation matrix between MTBM parameters and soil properties, and also to generate the independent MTBM parameters.

5.6.2.5. Generate the MTBM data based on correlation matrix between MTBM parameters and soil properties and generate independent MTBM parameters (Algorithm C)

In this step, the MTBM data are generated using the algorithm shown in Figure 5.23. To generate MTBM data based on analysis of two actual case studies, four correlation matrices between MTBM parameters and soil properties are constructed. Then, for each project generated, one of the correlation matrices is randomly selected. This selection is done in consideration of the selected soil correlation matrix described in Section 5.6.3.2. Using the method explained for generating samples from joint multivariate correlated distributions (Section 5.6.2.3.2), the MTBM data that are correlated with soil properties are generated as follows. The Cholesky decomposition of the correlation matrix between MTBM parameters and soil properties is calculated (C). The marginal distributions for soil properties and MTBM parameters are then defined accordingly. Next, using the inverse transform method, the values of soil properties are transformed to samples from a standard normal distribution, and the U matrix is obtained. By multiplying the inverse of the Cholesky decomposition (C) by the U matrix, the Z matrix is also calculated. The missing entries of the Z matrix are then obtained by sampling from the standard normal distribution. Finally, the Z matrix is multiplied by the Cholesky decomposition matrix (C) to obtain a matrix containing a sample from the joint correlated distribution. Since the values of the joint correlated distribution are normal, they need to be transformed to the MTBM data based on their distribution using the inverse transform method. The MTBM parameters correlated with soil properties having been generated, the independent MTBM parameters are randomly generated from their distribution, culminating in the final database containing the interpolated soil properties and MTBM parameters.

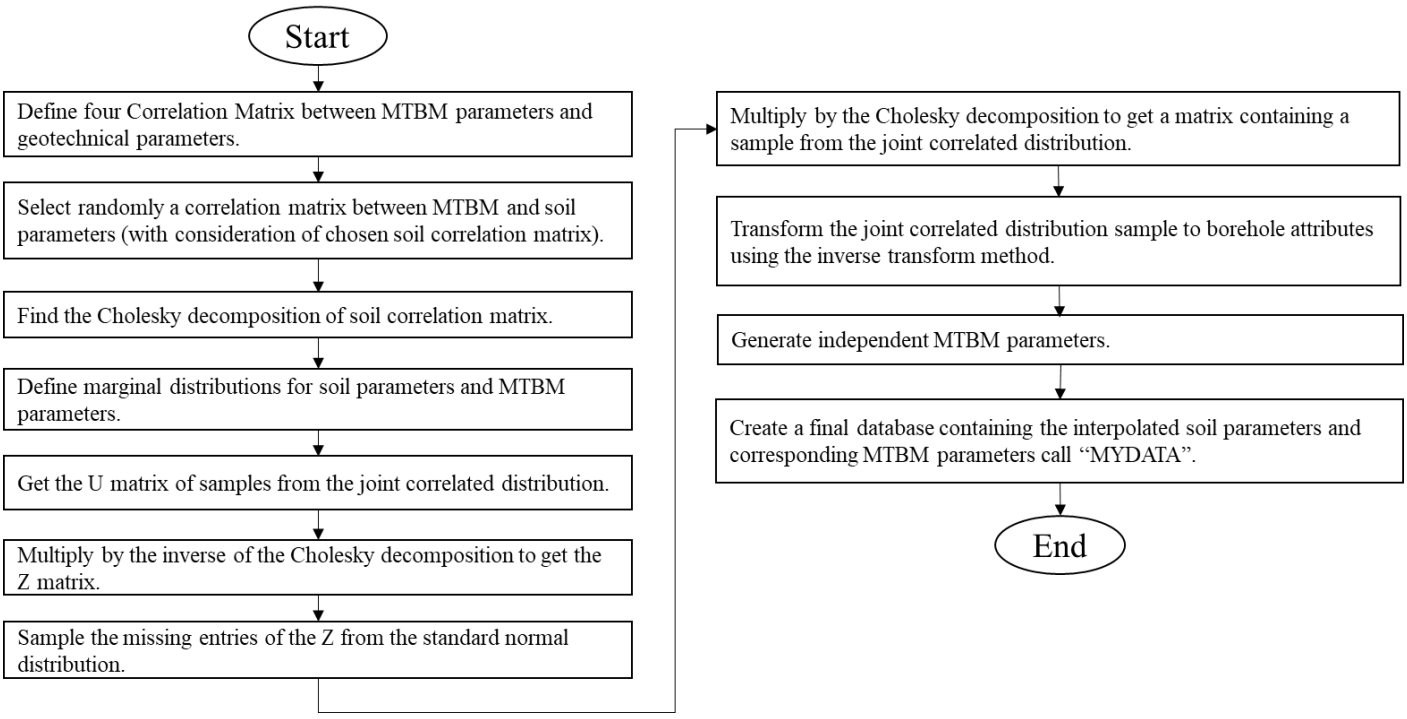

Figure 5. 23. Algorithm for generating MTBM data based on correlation matrix between MTBM parameters and soil properties (Algorithm C).

Once the final database including all interpolated soil properties along the tunnel length and corresponding MTBM parameters has been generated, the next step is to determine the locations along the tunnel for updating the project duration. In this regard, the next step in the main algorithm (Figure 5.16) is to break the tunnel down into four sections divided at 10%, 20%, and 30% of the tunnel length (Figure 5.24).

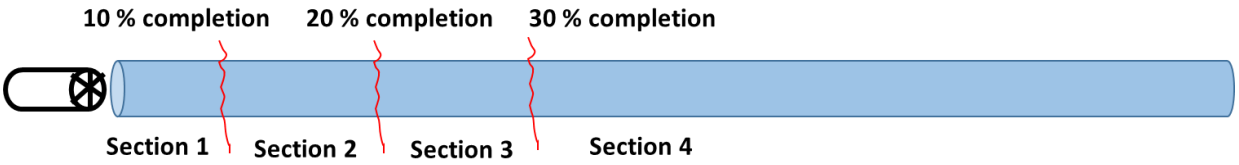

Figure 5. 24. Schematic representation of four tunnel sections divided at 10, 20, and 30% project completion.

Once the tunnel has been divided into four sections, the last step in the main algorithm is to collect the PR observations from the PR readings generated as described in Section 5.6.2.3.2.

5.6.2.6. Considerations of external factors affecting the performance of MTBM excavation

To make sure that the developed models work well under actual working conditions, consideration of external factors is incorporated into the generated projects. It should be noted that, although the external factors are not a part of the PR prediction models, they do affect the microtunneling construction practice. In this regard, an algorithm is developed to generate the external factors (e.g., presence of boulders, mix face conditions, utility lines, high water level), as shown in Figure 5.25.

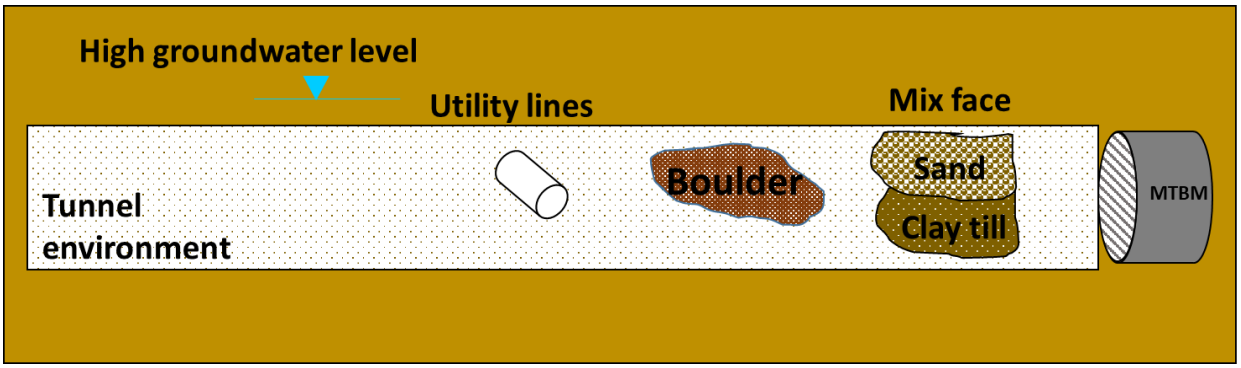

Figure 5. 25. Schematic representation of external factors considered in the generated projects.

The first step to generate the external factors (Figure 5.26) is to randomly determine for each project whether or not it is to be assigned external factors. If it is determined that a given project is not to be assigned any external factors, the algorithm procedure ends; if, on the other hand, the given project has external factors, then the number of each of the external factors to be generated along the project are determined. Then, the locations of the external factors along the tunnel length are randomly determined. The next step is to determine the influence of each external factor in terms of its effect in delaying the MTBM excavation. In this regard, for each external factor, an influence value is considered. The influence value is defined as a multiplication factor that reduces the excavation speed. For example, an influence value of 0.1 for high water level means that the

excavation speed will be one tenth of its original speed due to the influence of this factor. The last step is to generate observations of PR along the tunnel length for tunnel sections specified at 10%, 20%, and 30% of project completion.

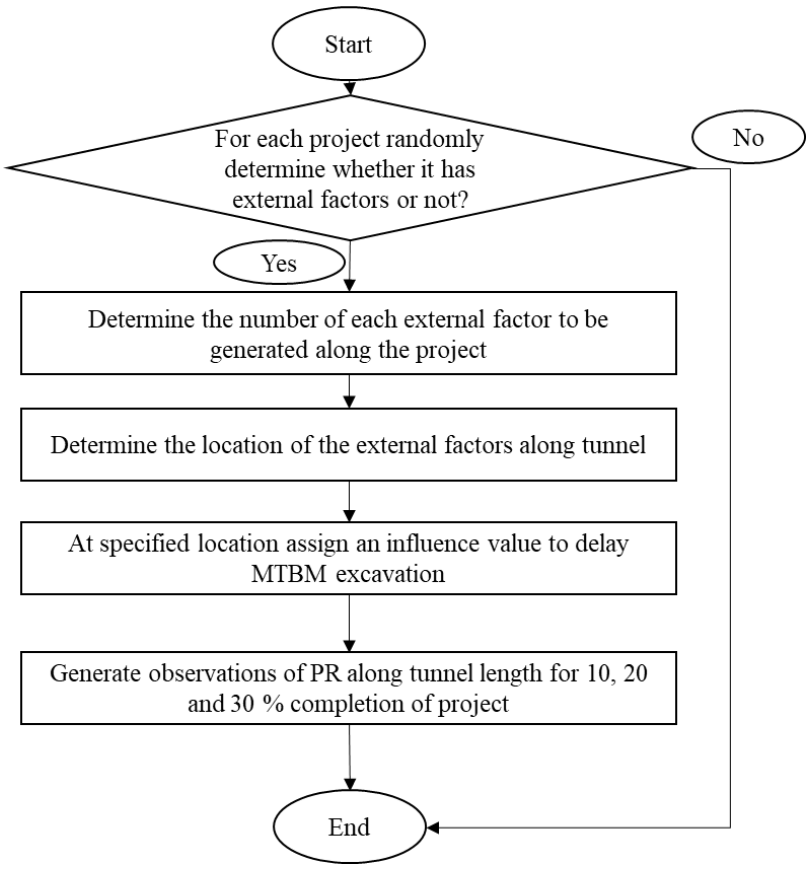

Figure 5. 26. Algorithm for considering the influence of external factors on generated projects.

5.6.3. Results of project generation

Using the developed algorithm (i.e. main algorithm for microtunneling project generation), fifty microtunneling projects are generated (Figure 5.27). Each generated project has a separate database that includes both MTBM data and soil properties data interpolated along the tunnel length.

ProjectNumber	TunnelLength	MTBMtype	MaxTorque(kN.m)	Diameter(m)	MaxRPM	Coverdepth	BHDistance	NBH	SectionNumber
1	999	Herrenknecht AVN 900	298	0.9	5	12	353	3	2
2	890	Iseki TCC600	270	0.76	2.2	28	381	3	2
3	753	Herrenknecht AVN-800A	90	1.35	7.1	22	483	2	1
4	585	Akkerman SL30	53.2	0.81	13	20	341	2	1
5	849	Herrenknecht AVN 1600	310	1.65	3.2	14	320	3	2
6	733	Herrenknecht AVN-800A	90	1.35	7.1	7	450	2	1
7	780	Herrenknecht AVN 1500	310	1.5	3.2	17	329	3	2
8	1959	Herrenknecht AVN 1200TC	258	1.52	5	25	330	6	5
9	609	Iseki TCC600	270	0.76	2.2	11	303	3	2
10	896	Akkerman SL82	490	1.98	9	25	482	2	1
11	1935	Herrenknecht AVN 1600	310	1.65	3.2	12	374	6	5
12	1269	RASA DT 1500	91	1.78	3.2	14	303	5	4
13	1153	Herrenknecht AVN 1200TB	258	1.52	6.7	25	443	3	2
14	602	Iseki TCS900	120	1.07	2.6	13	452	2	1
15	1309	Akkerman SL74	298	1.88	7.7	13	372	4	3
16	1139	Iseki TCC900	96	1.07	1.8	9	314	4	3
17	1132	Akkerman SL74	298	1.88	7.7	20	482	3	2
18	1422	Herrenknecht AVN 1800	445	1.73	3.3	5	373	4	3
19	1168	Akkerman SL60	298	1.52	7.7	8	342	4	3
20	622	Herrenknecht AVN 1200	195	1.52	3.5	13	494	2	1
21	753	Iseki TCS900	120	1.07	2.6	15	303	3	2
22	1365	RASA DH 1900	411	2.44	2.1	21	351	4	3
23	1318	Herrenknecht AVN 800	55	1.3	7.4	6	469	3	2
24	1228	Herrenknecht AVN 600	33.5	0.76	13	24	330	4	3
25	993	Akkerman SL44	85.4	1.37	8	21	316	4	3
26	966	Herrenknecht AVN1800TB	554	2.44	11.9	7	305	4	3
27	1558	Herrenknecht AVN 1200	195	1.52	3.5	29	363	5	4
28	1546	Iseki TCC1350	298	1.68	1.5	7	480	4	3
29	830	RASA DT 1500	91	1.78	3.2	20	406	3	2
30	1357	Herrenknecht AVN 1000	150	1.32	5.4	7	307	5	4
31	975	RASA DH 1900	411	2.44	2.1	26	388	3	2
32	1598	Akkerman SL30	53.2	0.81	13	26	318	6	5
33	785	Herrenknecht AVN 1200TB	258	1.52	6.7	29	320	3	2
34	1149	RASA DH 1900	411	2.44	2.1	7	305	4	3
35	1660	Herrenknecht AVN 1200TB	258	1.52	6.7	20	317	6	5
36	1488	Akkerman SL36	85.4	1	8	6	473	4	3
37	551	Herrenknecht AVN 1500	310	1.5	3.2	20	331	2	1
38	1323	Herrenknecht AVN1800TB	554	2.44	11.9	14	422	4	3
39	824	Herrenknecht AVN1800TB	554	2.44	11.9	27	442	2	1
40	1567	Herrenknecht AVN 1200TC	258	1.52	5	6	382	5	4
41	1341	Herrenknecht AVN-800A	90	1.35	7.1	27	350	4	3
42	865	Iseki TCC1000	121.5	1.22	2	7	340	3	2
43	1074	Iseki TCC1350	298	1.68	1.5	9	455	3	2
44	1096	Herrenknecht AVN 600	33.5	0.76	13	22	334	4	3
45	1257	Akkerman SL60	298	1.52	7.7	7	410	4	3
46	1241	Herrenknecht AVN 1800	445	1.73	3.3	24	439	3	2
47	886	Iseki TCC600	270	0.76	2.2	12	324	3	2
48	1703	Herrenknecht AVN1800TB	554	2.44	11.9	28	380	5	4
49	791	Akkerman SL60	298	1.52	7.7	16	315	3	2
50	524	Akkerman SL30	53.2	0.81	13	26	337	2	1

Figure 5. 27. Results of generated projects.

The distribution of project characteristics (e.g., tunnel length, diameter, cover depth) over the generated projects are shown in Figure 5.28.

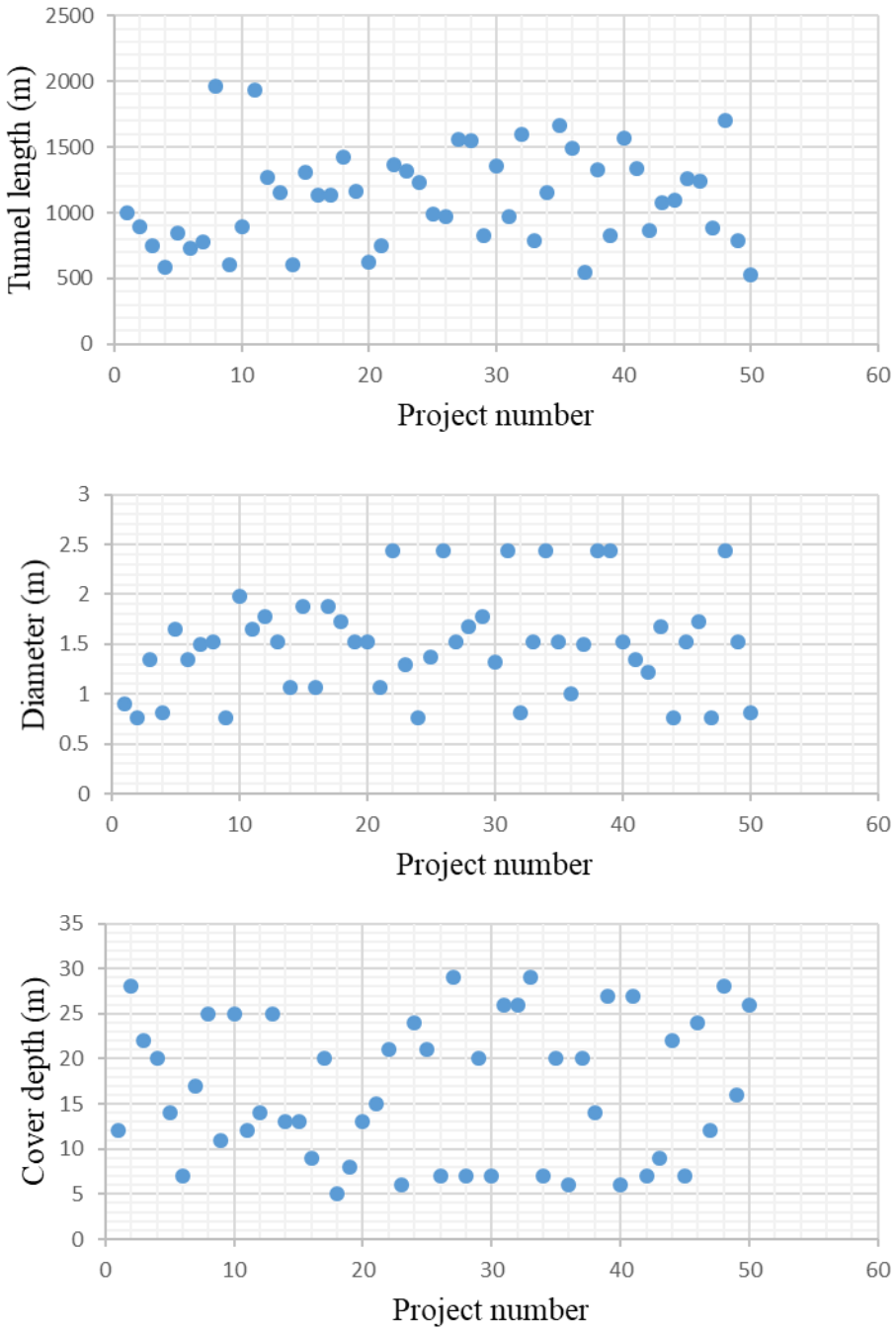

Figure 5. 28. Distribution of project characteristics over the generated projects.

5.6.4. Randomness test on generated projects

To test whether or not the projects have been generated in a pseudo-random manner, the Wald-Wolfowitz runs test (often referred to simply as the "runs test") is performed on all the project characteristics. The runs test, it should be noted, is a type of non-parametric statistical test that determines whether or not a sequence of data has been derived through a random process. A common application of the runs test is a test for randomness of observations as evidence that there was no bias in a selection process.

In this approach, data is transformed into a dichotomous vector by determining that each value is above (U) or below (L) a given threshold. The threshold used is usually a median, where values in the sample data that are equal to the median are removed. Once the data has been transformed, the number of runs is calculated. A "run" is defined as a series of consecutive observations. A sample with too many or too few runs suggests that it may not be random (Bujang and Sapri, 2018). Two hypotheses are used: the null hypothesis, $H_{0\,(null)}$, is that the data was produced in a random manner, and the alternative hypothesis, H_1, is that the data was not produced in a random manner. The runs test determines whether the null hypothesis, $H_{0\,(null)}$, is correct (i.e., whether the data has been produced in a pseudo-random manner) or there is enough evidence to reject the null hypothesis. After defining the hypothesis, the next step is to calculate the test statistics, which show whether or not the null hypothesis should be rejected. The method of calculating test statistics and critical values differs depending on the size of the sample. Generally, for small samples (fewer than 20 data points), the test statistics are calculated based on the number of runs, whereas, for large samples, approximation is used. The critical value (i.e., the value against which the number of runs is compared), meanwhile, is obtained from a runs test on a randomness table in the case of a small

sample, whereas in the case of a large sample the critical value is determined based on a formula stated in the following (Bujang and Sapri, 2018).

The test statistics for a large sample can be calculated using the following equation (Bradley, 1968):

$$z = \frac{r-\mu_r}{\sigma_r} \tag{5.6}$$

where r is the number of runs, μ_r is the expected number of runs, and σ_r is the standard deviation of the number of runs. The values for μ_r and σ_r, in turn, can be computed using the following equations based on the number of samples below the median (n_1) and above the median (n_2).

$$\mu_r = \frac{2n_1n_2}{n_1+n_2} + 1 \tag{5.7}$$

$$\sigma_r = \sum \sqrt{\frac{(2n_1n_2)(2n_1n_2-n_1-n_2)}{(n_1+n_2)^2(n_1+n_2-1)}} \tag{5.8}$$

Once the test statistic (z) has been calculated, it needs to be compared with the critical value. For a large sample and considering two tail of distribution, the $z_{1-\alpha/2}$ score from the standard normal distribution is the critical value, whereas, for a one-sided tailed runs test, the critical value is $z_{1-\alpha}$, where α is the significance level (Bujang and Sapri, 2018).

5.6.5. Randomness test results

The runs randomness test is performed on project characteristics and also on the data produced in sample project #11, including both MTBM and soil data (Figure 5.29). All of the p-values are found to exceed the significance level $\alpha = 0.05$, which means that the null hypothesis is confirmed, i.e., there is sufficient evidence to conclude that the generated projects have been produced in a pseudo-random manner.

```
        Runs Test

data:  AllProjects$TunnelLength
statistic = -0.28577, runs = 25, n1 = 25, n2 = 25, n = 50, p-value = 0.7751
alternative hypothesis: nonrandomness


        Runs Test

data:  AllProjects$Diameter
statistic = 1.3595, runs = 25, n1 = 18, n2 = 22, n = 40, p-value = 0.174
alternative hypothesis: nonrandomness


        Runs Test

data:  AllProjects$NBH
statistic = -0.49051, runs = 13, n1 = 24, n2 = 9, n = 33, p-value = 0.6238
alternative hypothesis: nonrandomness


        Runs Test

data:  AllProjects$BHDistance
statistic = 0.57155, runs = 28, n1 = 25, n2 = 25, n = 50, p-value = 0.5676
alternative hypothesis: nonrandomness


        Runs Test

data:  MYDATA$Torque
statistic = 0.42967, runs = 102, n1 = 98, n2 = 98, n = 196, p-value = 0.6674
alternative hypothesis: nonrandomness


        Runs Test

data:  MYDATA$PR
statistic = 0.5729, runs = 103, n1 = 98, n2 = 98, n = 196, p-value = 0.5667
alternative hypothesis: nonrandomness


        Runs Test

data:  MYDATA$SPT
statistic = 0.5729, runs = 103, n1 = 98, n2 = 98, n = 196, p-value = 0.5667
alternative hypothesis: nonrandomness
```

Figure 5. 29. Runs randomness test results for project characteristics and for a data point produced in sample project #11.

5.6.6. Analysis of integrated Simulation + MTBM PR prediction models using generated projects

To analyze the performance of the "integrated simulation + Bayesian updating mechanistic model for MTBM PR prediction" and "integrated simulation + machine-learning model for MTBM PR

prediction", the predicted project durations are updated at 10%, 20%, and 30% project completion, while the actual durations (obtained from inputting the generated PRs into the simulation model) are compared with the predicted ranges obtained from both models. The results generated by both models for sample project #43 are shown in Figure 5.30. For both models, in updating the project durations at 10%, 20%, and 30% project completion, the actual project durations are found to fall within the predicted range of project durations.

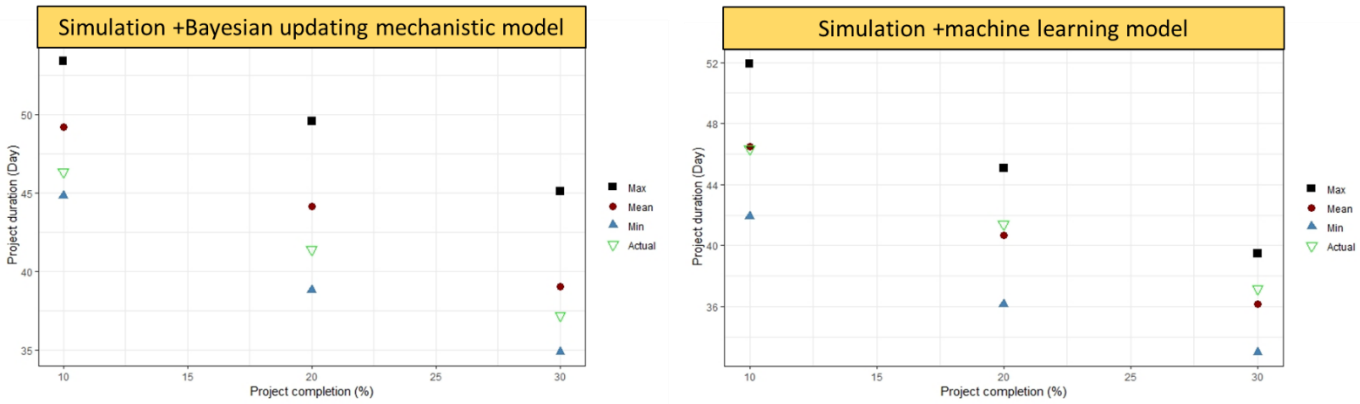

Figure 5. 30. Results of integrated Simulation + Bayesian updating mechanistic model and Simulation + Machine-learning model for updating the project #43 duration at 10%, 20%, and 30% of project completion.

All of the generated projects are analyzed in order to evaluate the performance of the developed models in dynamically predicting the project durations at 10%, 20%, and 30% of project completion (Figure 5.31). At each project completion location, the percentage of the fifty generated projects to have been correctly predicted is calculated. Analysis of the "integrated simulation + MTBM PR prediction models" reveals that both models perform well even at the early stages of a given project, and that their performance improves as the project progresses, this being due to continuous learning and updating on the part of the models based on observations made during excavation.

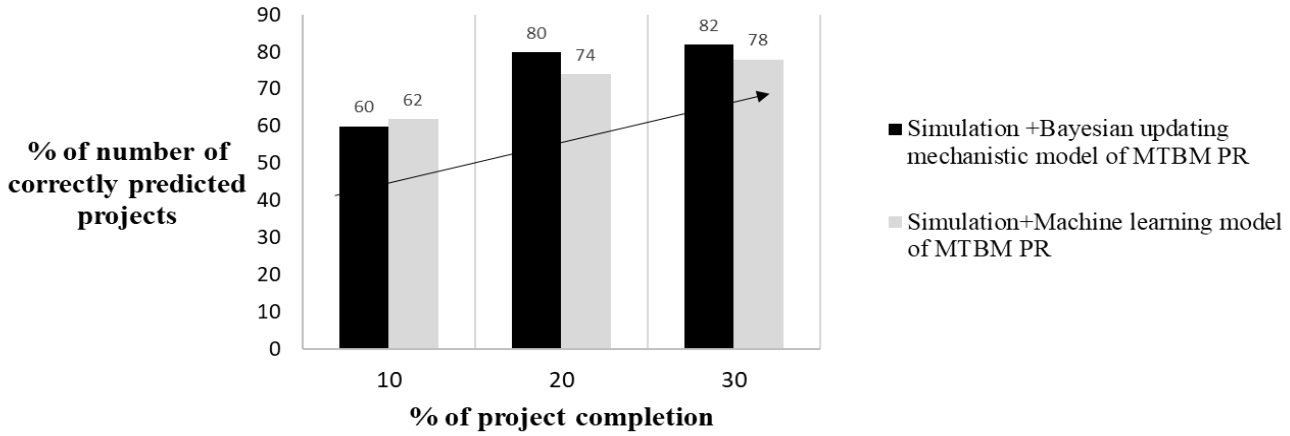

Figure 5. 31. Percentage of correctly predicted projects at 10%, 20%, and 30% project completion (by consideration of external factors).

The further analysis of the integrated models for MTBM PR prediction is depicted in Figure 5.32. This figure shows that, when including the external factors, the performance of models decreased (compared to when the external factors are excluded). This decrease in on proportion of correctly predicted projects is due to the fact that the external factors were not originally part of the prediction models, but that they nevertheless have a strong influence on project duration. However, the reduction is found to be less pronounced in the case of the "integrated simulation + machine-learning model for MTBM PR prediction" than in the case of the "integrated simulation + Bayesian updating mechanistic model". This shows that the "integrated simulation + machine-learning model for MTBM PR prediction" is more flexible in learning and taking into account the influence of various important external factors on MTBM excavation during microtunneling construction. Although the "integrated simulation + Bayesian updating model for MTBM PR prediction" uses the observations and updates the excavation durations (predicted based on mechanistic model), the percentage of correctly predicted projects decreases more, (i.e., the model did not perform as well as the "integrated simulation + machine-learning model for MTBM PR prediction".

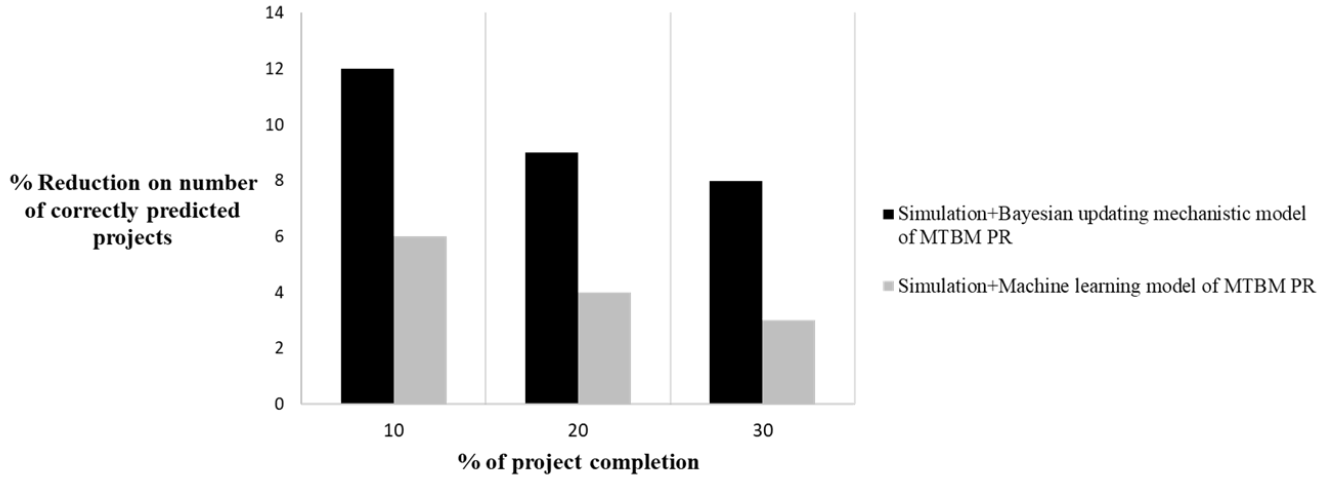

Figure 5. 32. Percentage reduction on number of correctly predicted projects at 10%, 20%, and 30% project completions by including external factors for both the "integrated simulation + Bayesian updating mechanistic model for MTBM PR prediction" and the "integrated simulation + machine-learning model for MTBM PR prediction".

5.7. Summary and Conclusion

A review of simulation-based productivity models for tunneling/microtunneling projects reveals a deficiency with respect to modelling the activity durations in simulation. One of the key activities in microtunnelling is the process of excavation by MTBM and penetration of the MTBM into the ground. In this regard, and to enhance the simulation-based productivity models for dynamically predicting the project duration, two developed MTBM PR prediction models (a mechanistic model and a dynamic machine-learning model) are integrated with an operation simulation model. To integrate the mechanistic model with simulation, it is important to consider and model the inter-correlations among the various attributes of the mechanistic model parameters, including soil properties, operational loads, and cutterhead characteristics. These inter-correlations are incorporated into the simulation model by defining the joint correlated distribution among all variables, such that the samples from the distribution of each mechanistic parameters can be obtained from the joint correlated distribution. To integrate the mechanistic model with simulation, two approaches are developed. The first approach is to incorporate the exact mathematical formula

underlying the mechanistic model into the simulation, while the second approach is to leverage the Bayesian updating technique to update the predictions being generated by the mechanistic model based on observations made during excavation. This approach, referred to herein as the Bayesian updating mechanistic model, is found to improve the predictive performance of the mechanistic model by taking into account the actual excavation time observations. To validate the proposed integrated models for MTBM PR prediction, they are applied to two actual case studies of microtunnelling projects in Alberta, Canada, and the performance of these models for dynamically updating the project duration at various percentages of project completion is evaluated. To further test the models, they are applied on fifty microtunneling projects synthetically generated. For this purpose, an algorithm for generating microtunnelling projects is developed and elaborated. To model the actual work conditions, external factors (e.g., presence of boulders, high water level, utility line, mix face conditions) are taken into consideration in the generated projects. The randomness test is also performed to confirm that the generated projects have been produced in a pseudo-random manner. In evaluating them on generated projects, both models are found to perform well even at the early stages of a given project; moreover, both the "integrated simulation + Bayesian updating mechanistic model for MTBM PR prediction" and the "integrated simulation + machine-learning model for MTBM PR prediction" see improved performance as the excavation continues, as they learn/update based on observations made during the project progress. The analysis of the influence of external factors, meanwhile, reveals that, although both models see a decrease in the number of correctly predicted project durations (at 10%, 20%, and 30% project completion) when external factors are included compared to when they are excluded, the "integrated simulation + machine-learning model for MTBM PR prediction" is found to be less sensitive to the influence of external factors, and the decrease in correct

predictions is less pronounced than in the other model due to its relative flexibility in learning new information (presence of external factors) as the project proceeds. The evaluation of the performance of the integrated models for MTBM PR prediction reveals that the integration of simulation with models that utilize ongoing project information to update their predictions (whether using machine-learning model to learn the behaviour of the system or using mechanistic model combined with Bayesian updating technique to update the prior mechanistic prediction based on observations) can improve the accuracy of dynamic productivity prediction. This robust and accurate method of dynamic productivity prediction, in turn, can aid practitioners in adjusting the construction plan to prevent delays and cost overruns and can provide more accurate insights with respect to forecast project timelines.

Chapter 6: Conclusions, Limitations, and Future Directions

6.1. Research Conclusions

This thesis outlines the development of mechanistic and machine-learning models to enhance micro tunnel boring machine (MTBM) penetration rate (PR) prediction and productivity estimation in microtunneling construction.

Chapter 2 investigates the mechanistic analysis of MTBM–ground interaction and proposed a novel approach for modelling MTBM penetration into soft ground. By employing contact mechanics theory for mechanistic analysis of MTBM penetration, and solving the contact mechanic problem defined between MTBM and ground, the interaction between MTBM and ground is modelled and the mathematical formula revealing the relationship between PR and the fundamental factors including soil properties, operational loads and cutterhead characteristics is developed. The key contribution of the developed mechanistic model is that, the fundamental law governing the behaviour of the MTBM having been defined, engineers can use the model as an experimental platform to assess the influence on the output (i.e., PR) of the mechanistic parameters involved both as individual factors (e.g., opening ratio) and as groups of factors (e.g., cutterhead characteristics). Moreover, it provides the opportunity to forecast PR based on the existing MTBM operational load capacity as well as expected ground conditions during tunneling. The functionality and validity of the mechanistic model are demonstrated using two actual microtunneling projects. The analysis of the mechanistic model using these two projects shows that not only does it provide accurate predictions of MTBM PR, but the predictions also follow

the actual trend of PR along the tunneling length. This confirms that the behaviour of the MTBM along the tunnel length while excavating different ground conditions is modelled correctly.

Chapter 3 further explored the mechanistic behaviour of MTBMs in order to enhance the mechanistic model developed in Chapter 2. In this regard, the engagement phenomenon occurring at the interface between cutting blade and ground is analyzed. To model this phenomenon, the contact mechanics theory proposed in the previous chapter is used, and the engagement area between cutterhead and soil at the tunnel face is simulated. Based on the simulated engagement area and solving the contact mechanic problem, a mechanistic model for MTBM PR prediction that considers engagement behaviour is modelled. In the developed model, the influence of the engagement phenomenon is formulized as the "engagement factor", which quantifies the influence of this particular interaction on the MTBM PR. Based on the consideration of the two extreme cases of high and low engagement areas at the tunnel face, upper and lower boundaries, respectively, of MTBM PR along the tunnel length are developed. These boundary models are examined on two microtunneling projects, with the results showing that the actual PR falls within the boundaries and is closer to the upper boundary. In other words, the MTBM engagement areas on these projects are found to be high, in turn resulting in a relatively high PR along the tunnel path. This analysis of MTBM engagement can assist (1) practitioners in evaluating how well the particular MTBM is excavating and (2) designers and engineers in enhancing the MTBM performance by designing MTBMs that achieve a high engagement area at the tunnel face. Moreover, the upper and lower boundary models can be used to estimate the fluctuation range of MTBM PR for the particular project more precisely and plan the project accordingly.

Chapter 4 describes how to use the MTBM data generated during the project to enhance prediction of MTBM PR dynamically as a project progresses. In this regard, a procedure is established that

explains the steps required to utilize the generated MTBM data, along with available geotechnical data, to predict the PR for the unexcavated tunnel lengths. In this procedure, using an artificial neural network (ANN) model, the MTBM PR is predicted by inputting the geotechnical parameters to the model. The dynamic aspect of the procedure is that it manages the continuously generated MTBM data during excavation. Through the continuous updating of the database with MTBM data and soil properties data, a new ANN model is created by which to predict the next tunnel section. Applying this approach to two cases of microtunneling projects shows that, as the project progresses, the prediction accuracy improves due to the continuous learning of the MTBM–ground interaction. This demonstrates the benefits of using the data generated during construction to improve the prediction of the MTBM PR and productivity for the overall microtunneling construction.

Chapter 5 demonstrates the integration of the machine-learning and mechanistic models for MTBM PR prediction with operation simulation model to enhance productivity prediction in microtunneling projects. In this regard, to leverage the observations made during excavation, a Bayesian updating technique is applied on the mechanistic model to update its predictions. This Bayesian updating mechanistic model for MTBM PR prediction is integrated with simulation to forecast the productivity of the overall project. Evaluation of "integrated simulation + Bayesian updating mechanistic model for MTBM PR prediction" and the "integrated simulation + machine-learning model for MTBM PR prediction" is performed by applying each of the two integrated models on two actual microtunneling projects. Then, to further evaluate their performance for wider ranges of project specifications and tunnel conditions, they are applied to several synthetic projects generated using the Monte Carlo approach. The procedure for generating microtunneling projects is addressed in this chapter, and, to ensure that the generated projects accurately simulate

the actual site conditions, the influence of external factors such as presence of boulders and utility lines along the tunnel path is also considered. Analysis of the results of applying the two integrated simulation-based models to fifty projects reveals that they both perform well in predicting the project duration at 10% project completion and that, as the project progresses and the productivity is updated at 20% and 30% project completion, the prediction accuracy improves. This demonstrates the benefits of updating the initial PR predictions to enhance the productivity prediction and update the ongoing construction plan more accurately. The dynamic updating of project duration, meanwhile, can aid practitioners in avoiding delays by redirecting the project progress to its original plan and/or can assist decision makers in planning the future construction taking into account the forecasted project durations at various percentages of project completions.

6.2. Academic Contributions

This research makes several academic contributions, including:

- Demonstrating the benefits of dynamic utilization of MTBM-generated data for enhancing the prediction of MTBM PR;
- Improving the accuracy of PR prediction for remaining (unexcavated) tunnel length by dynamically learning the MTBM interaction with the ground;
- Introducing a novel approach for mechanistically analyzing and modelling the MTBM–ground interaction;
- Establishing a mechanistic formula by which to characterize and quantify the relationship between PR and the combined influence of soil properties, cutterhead characteristics, and operational loads;

- Developing a mechanistic model of MTBM engagement with the ground that quantifies the influence of this phenomenon on PR, and developing upper and lower boundaries of MTBM PR based on consideration of high and low engagement areas at the tunnel face;
- Enhancing productivity estimation during construction by improving MTBM PR prediction and integrating simulation with the PR prediction models in order to dynamically update the project duration; and
- Establishing a procedure for generating synthetic microtunneling projects using the Monte Carlo approach for evaluating different microtunneling productivity prediction models.

6.3. Industrial Contributions

This research makes several contributions to industry practice, including:

- Bridging the gap between geotechnical engineering and management aspects of microtunneling construction by providing a tool (i.e., "integrated simulation + Bayesian updating mechanistic model for MTBM PR prediction") that allows practitioners to evaluate the influence of various mechanistic engineering factors (such as cutterhead characteristics) on microtunneling construction productivity;
- Developing a procedure for the use of MTBM-generated data obtained during construction to forecast PR for the unexcavated tunnel length and update the microtunneling construction plan as the project progresses;
- Providing practitioners with a better understanding of the quantitative relationship between PR and the combined influence of soil properties, cutterhead characteristics, and operational loads, as well as a means of quantifying the influence of these factors on MTBM PR;

- Providing a novel tool by which to evaluate the degree of MTBM engagement with the ground and assess the performance of MTBM excavation under various ground conditions; and
- Improving the prediction of MTBM productivity by developing integrated simulation-based models that incorporate the enhanced models for prediction of MTBM PR.

6.4. Research Limitations

The limitations of this research are as follows:

- The mechanistic model presented in Chapter 2 and Chapter 3 is developed based on the assumption that the tunnel face is continuously stable during MTBM excavation. Moreover, the excavation medium is limited to soft ground conditions (i.e., soil), whereas hard rock excavation is not considered in the model due to the inherent differences between the respective mechanisms underlying soil excavation and rock excavation.
- The analysis of the engagement phenomenon in Chapter 3 is limited in that it is assumed that clogging between the cutting blade and soil at the tunnel face will not occur. The value of the engagement factor for a specific MTBM needs to be assessed based on experimental analysis.
- The application of the machine-learning model for dynamic prediction of MTBM PR presented in Chapter 4 is limited in that it is reliant on the ready availability of (1) MTBM data generated during construction, and (2) geotechnical baseline reports (for extraction of information on soil properties at different borehole sites). Moreover, it is

assumed in the present work that the same type of MTBM is being used for the entire microtunneling construction.

- The microtunneling project generation procedure explained in Chapter 5 may need to be adjusted depending on the MTBM type and geological and geotechnical conditions of interest. To generate the excavation environment and corresponding MTBM behavioural data, the correlation matrix between various soil properties and also between soil properties and MTBM parameters may need to be revised based on further investigations.
- The accuracy and reliability of the developed integrated simulation-based models in presented Chapter 5 is largely dependent on the quality of the inputs, including the mechanistic parameters (for modelling excavation activity) and information pertaining to other activities involved in microtunneling construction. The inputs to the mechanistic model must be carefully chosen based on the MTBM's specifications, the soil properties, and the tunnel conditions for the given project.

6.5. Future Directions

The following avenues of future research are recommended:

- The development of an advanced integrated system that automates extraction of geotechnical parameters from geotechnical reports, updates them (if information is available) and interpolates them along the tunnel path to reduce the preparation time for developing the machine-learning model for MTBM PR prediction;
- The exploration and development of simple and rapid methods of automating the streaming of the raw MTBM-generated data to the engine that cleans, prepares, and updates the database for prediction of MTBM performance;

- Research and development of mechanistic models based on (1) further analysis of MTBM engagement phenomenon, leading to enhanced MTBM design, (2) analysis of the influence of cutterhead wear on the MTBM PR, and (3) analysis of MTBM excavation through unstable soil conditions and rock formations; and
- Investigation and incorporation of additional types of data sources, such as behavioural data (including MTBM operator competency) as a means of comprehensively enhancing the simulation-based decision support system for productivity evaluation of microtunneling construction.

References

Akhavian, R., & Behzadan, A. H. (2015). Construction equipment activity recognition for simulation input modeling using mobile sensors and machine learning classifiers. Advanced Engineering Informatics, 29(4), 867-877.

Akhavian, R., & Behzadan, A. H. (2014, December). Construction activity recognition for simulation input modeling using machine learning classifiers. In Proceedings of the Winter Simulation Conference 2014 (pp. 3296-3307). IEEE.

Al-Bataineh, M., AbouRizk, S., & Parkis, H. (2013). Using simulation to plan tunnel construction. Journal of construction engineering and management, 139(5), 564-571.

Alvarez Grima, M.P.A., Bruines, P.A., Verhoef, P.N.W., 2000. Modeling tunnel boring machine performance by neuro-fuzzy methods. Tunnell. Undergr. Space Technol. 15 (3), 259–269.

American Society of Civil Engineers (ASCE). 2015. ASCE/CI 36-15. Standard design and construction guidelines for microtunneling. Reston: ASCE. https://doi.org/10.1061/9780784413630.

Ang, A. H-S., and Tang, W. H. _1975_. Probability concepts in engineering planning and design, Vol. 1, Wiley, New York.

Bamford, W.F. 1984. “Rock test indices are being successfully correlated with tunnel boring machine performance.” In Proc., 5th Australian Tunneling Conf., Melbourne, 2, 9–22. http://worldcat.org/isbn/0858252023.

Bradley, J. V. (1968). Distribution-free statistical tests. Englewood Cliffs, New Jersey: Prentice-Hall.

Bruland, A. 1998. Hard Rock Tunnel Boring. Ph.D. Thesis, Norwegian University of Science and Technology, Trondheim. ISBN 82-471-0281-1.

Buch, A. G., & Kraft, D. (2017, September). Prediction of ICP pose uncertainties using Monte Carlo simulation with synthetic depth images. In 2017 IEEE/RSJ International Conference on Intelligent Robots and Systems (IROS) (pp. 4640-4647). IEEE.

Bujang, M. A., & Sapri, F. E. (2018). An application of the runs test to test for randomness of observations obtained from a clinical survey in an ordered population. The Malaysian Journal of Medical Sciences: MJMS, 25(4), 146.

Chung, T. H. (2007). Simulation-based productivity modeling for tunnel construction operations.

Chung, T. H., Abraham, D. M., & Gokhale, S. B. (2004). Decision support system for microtunneling applications. Journal of construction engineering and management, 130(6), 835-843.

Chung, T. H., Mohamed, Y., & AbouRizk, S. (2006). Bayesian updating application into simulation in the North Edmonton Sanitary Trunk tunnel project. Journal of Construction Engineering and Management, 132(8), 882-894.

De Myttenaere, A., Golden, B., Le Grand, B., and Rossi, F. 2016. “Mean absolute percentage error for regression models.” Neurocomputing, 192, 38–48. https://doi.org/10.1016/j.neucom.2015.12.114.

Ead, R. (2020). Using Monte Carlo Simulation to Evaluate Performance of Forecasting Models in Project Control.

Eftekhari, M., Baghbanan, A., Bayati, M., 2010. Predicting penetration rate of a tunnel boring machine using artificial neural network. In: ISRM International Symposium-6th Asian Rock Mechanics Symposium. International Society for Rock Mechanics, pp. 1–7.

Einstein, H. H. (2004). Decision aids for tunneling: Update. Transportation Research Record, 1892(1), 199-207.

Elwakil, E., & Hegab, M. (2018). Probabilistic Estimation for Microtunneling Projects' Penetration Time. In ICCREM 2018: Construction Enterprises and Project Management (pp. 27-33). Reston, VA: American Society of Civil Engineers. https://doi.org/10.1061/9780784481752.004.

Fang, Y., Z.Yao, W.Xu., Q. Tian., C. He., & S. Liu. 2021. “The performance of TBM disc cutter in soft strata: A numerical simulation using the three-dimensional RBD-DEM coupled method.” Eng. Fail. Anal., 119, 104996. https://doi.org/10.1016/j.engfailanal.2020.104996.

Farmer, I. W., and Glossop, N. H. 1980. “Mechanics of disc cutter penetration.” Tunnels Tunnell. Int. 12 (6), 22–25. https://doi.org/10.1016/0148-9062(80)90769-x.

Farrokh, E., Rostami, J., and Laughton, C. 2012. “Study of various models for estimation of penetration rate of hard rock TBMs.” Tunn. Undergr. Space. Technol., 30 (2012), 110–123. https://doi.org/10.1016/j.tust.2012.02.012.

Frick, M., & Axhausen, K. W. (2003). Generating Synthetic Populations using Iterative Proportional Fitting (IPF) and Monte Carlo Techniques. In 3rd Swiss Transport Research Conference 2003 (STRC 2003). STRC.

Frough, O., Khetwal, A., & Rostami, J. (2019). Predicting TBM utilization factor using discrete event simulation models. Tunnelling and underground space technology, 87, 91-99.

Gholami, M., Shahriar, K., Sharifzadeh, M., Hamidi, J.K., 2012. A comparison of artificial neural network and multiple regression analysis in TBM performance prediction. In: ISRM Regional Symposium-7th Asian Rock Mechanics Symposium. International Society for Rock Mechanics.

Gholamnejad, J., Tayarani, N., 2010. Application of artificial neural networks to the prediction of tunnel boring machine penetration rate. Min. Sci. Technol. (China) 20 (5), 727–733.

Gong, Q.M. and Zhao, J. 2009. “Development of a rock mass characteristics model for TBM penetration rate prediction.” Int. J. Rock Mech. Min. Sci., 46 (1), 8–18. https://doi.org/10.1016/j.ijrmms.2008.03.003.

Gong, Q., Xu, H., Lu, J., Wu, F., Zhou, X., & Yin, L. (2022). Rock mass characteristics model for TBM penetration rate prediction–an updated version. International Journal of Rock Mechanics and Mining Sciences, 149, 104993. https:// DOI: 10.1016/j.ijrmms.2021.104993.

Graham, P.C. 1976. “Rock exploration for machine manufacturers.” In Bieniawski, Z.T. (Ed.), Exploration for Rock Engineering. Johannesburg, Balkema, 173–180.

Haas, C., & Einstein, H. H. (2002). Updating the decision aids for tunneling. Journal of construction engineering and management, 128(1), 40-48.

Hamidi, J.K., Shahriar, K., Rezai, B., and Rostami, J. 2010. “Performance prediction of hard rock TBM using rock mass rating (RMR) system.” Tunnell. Undergr. Space Technol., 25 (4), 333–345. https://doi.org/10.1016/j.tust.2010.01.008.

Hassanpour, J., Rostami, J., Khamehchiyan, M., Bruland, A., and Tavakoli, H.R. 2010. “TBM performance analysis in pyroclastic rocks: a case history of Karaj Water Conveyance Tunnel.” J. Rock Mech. Rock Eng., 43 (4), 427–445. https://doi.org/10.1007/s00603-009-0060-2.

Hassanpour, J., Rostami, J., Khamehchiyan, M., and Bruland, A. 2009b. “Developing new equations for TBM performance prediction in carbonate-argillaceous rocks: a case history of Nowsood water conveyance tunnel.” Geo Mech. Geoeng.: Int. J. 4 (4), 287–297. https://doi.org/10.1080/17486020903174303.

Hassanpour, J., Rostami, J., Khamehchiyan, M., Bruland, A., Tavakoli, H.R., 2009a. TBM Performance Analysis in Pyroclastic Rocks: A Case History of Karaj Water Conveyance Tunnel. Rock Mech. Rock Eng.

Hassanpour, J., Rostami, J., & Zhao, J. (2011). A new hard rock TBM performance prediction model for project planning. Tunnelling and Underground Space Technology, 26(5), 595-603.

Hegab, M. Y. (2005). “Prediction of Productivity for Microtunneling Projects in Bidding Phase.” In Construction Research Congress 2005: Broadening Perspectives, 1–10. https://doi.org/10.1061/40754(183)55.

Hegab, M., Smith, G. R., and Salem, O. M. (2006). “Soil penetration modeling in microtunneling projects.” J. Constr. Eng. Manag., 132 (6), 598–605. https://doi.org/10.1061/(ASCE)0733-9364(2006)132:6(598).

Hegab, M. Y., & Salem, O. M. (2010). Ranking of the factors affecting productivity of microtunneling projects. Journal of Pipeline Systems Engineering and Practice, 1(1), 42-52.

Heuer, R. E. (1974, August). Important ground parameters in soft ground tunneling. In Subsurface exploration for underground excavation and heavy construction (pp. 41-55). ASCE.

Innaurato, N., Mancini, R., Rondena, E., and Zaninetti, A. 1991. “Forecasting and effective TBM performances in a rapid excavation of a tunnel in Italy.” In Proc., 7th Int. Congress ISRM, Aachen, 1009–1014. https://doi.org/10.1016/0148-9062(93)92171-l.

Jamshidi, A. 2018. “Prediction of TBM penetration rate from brittleness indexes using multiple regression analysis.” Model. Earth Syst. Environ., 4 (1), 383–394. https://doi.org/10.1007/s40808-018-0432-2.

Ji, W., & AbouRizk, S. M. (2017). Credible interval estimation for fraction nonconforming: Analytical and numerical solutions. Automation in Construction, 83, 56-67.

Ji, X., Zhao, W., Ni, P., Barla, M., Han, J., Jia, P., ... & Zhang, C. (2019). A method to estimate the jacking force for pipe jacking in sandy soils. Tunnelling and Underground Space Technology, 90, 119-130.

Jin, D., Z. Zhang., and D. Yuan. 2021. "Effect of dynamic cutterhead on face stability in EPB shield tunneling." Tunnell. Undergr. Space Technol., 110, 103827. https://doi.org/10.1016/j.tust.2021.103827.

Johnson, K. L. 1985. Contact Mechanics. Cambridge University Press, Cambridge. https://doi.org/10.1002/zamm.19890690713.

Khazaei, S., Shimada, H., & Matsui, K. (2004). Analysis and prediction of thrust in using slurry pipe jacking method. Tunnelling and Underground Space Technology, 19(4/5), 356.

Lin, S. S., Shen, S. L., & Zhou, A. (2022). Real-time analysis and prediction of shield cutterhead torque using optimized gated recurrent unit neural network. Journal of Rock Mechanics and Geotechnical Engineering, 14(4), 1232-1240.

Ling, X., X. Kong., L. Tang., S. Cong., & W. Tang. 2022. "Preliminary identification of potential failure modes of a disc cutter in soil-rock compound strata: Interaction analysis and case verification." Eng. Fail. Anal.,131, 105907. https://doi.org/10.1016/j.engfailanal.2021.105907.

Lislerud, A. 1988. "Hard rock tunnel boring: prognosis and costs." Tunn. Undergr. Space. Technol., 3 (1), 9–17. https://doi.org/10.1016/0886-7798(88)90029-6.

Lu, G. Y., & Wong, D. W. (2008). An adaptive inverse-distance weighting spatial interpolation technique. Computers & geosciences, 34(9), 1044-1055.

Luo, Y. (2005). Productivity analysis of microtunneling pipe installation using simulation. Michigan State University.

Luo, R. Y., and Najafi, M. 2007. "Productivity study of microtunneling pipe installation using simulation". J. Infrastruct. Syst, 13(3). https:// doi.org /10.1061/(ASCE)1076-0342(2007)13:3(247).

Mahmoodzadeh, A., Mohammadi, M., Abdulhamid, S. N., Ibrahim, H. H., Ali, H. F. H., & Salim, S. G. (2021). Dynamic reduction of time and cost uncertainties in tunneling projects. Tunnelling and Underground Space Technology, 109, 103774.

McCabe, B., Reilly, C. C., & Orr, T. L. (2012). Analysis of microtunnel jacking forces in alluvium and glacial till in Mullingar, Ireland. In World Tunnelling Conference.

Moharrami, S., A.Bayat., S. AbouRizk. (2022). "Modeling micro-tunnel boring machine penetration rate using a mechanistic approach" Journal of Construction Engineering and Management, 148(11), 04022128. https://doi.org/10.1061/(ASCE)CO.1943-7862.0002402

Oreste, P., & Spagnoli, G. (2022). Probabilistic estimation of the advancement rate of the Tunnel Boring Machines on the basis of rock mass characteristics. Geomechanics and Geophysics for Geo-Energy and Geo-Resources, 8(2), 1-20. https://doi.org/10.1007/s40948-022-00384-4.

Ozdemir L, Miller R, and Wang F. D. 1978. Mechanical tunnel boring, prediction and machine design. Annual report, CSM APR 73- 07776-A03. https://doi.org/10.1016/0148-9062(78)91060-4.

Peck, R. B., Hanson, W. E., & Thornburn, T. H. (1974). Foundation Engineering. New York, NY: Wiley and Sons Inc.

R Core Team (2013). R: A language and environment for statistical computing. R Foundation for Statistical Computing, Vienna, Austria. URL http://www.R-project.org/.

Ribacchi, R., and Fazio, A. L. 2005. "Influence of rock mass parameters on the performance of a TBM in a gneissic formation (Varzo Tunnel)." Rock Mech. Rock Eng., 38 (2), 105–127. https://doi.org/10.1007/S00603-004-0032-5.

Rostami, J., and L. Ozdemir. 1993. "A new model for performance prediction of hard rock TBMs." In Proc.,Rapid Excavation and Tunneling Conf., 793–809. Boston. ISBN 0873351274.

Roxborough, F.F., and Phillips, H.R. 1975. "Rock excavation by disc cutter." Int. J. Rock Mech. Mining Sci. Geomech., 12, 361–366. https://doi.org/10.1016/0148-9062(75)90547-1.

Salimi, A., & Esmaeili, M. (2013). Utilising of linear and non-linear prediction tools for evaluation of penetration rate of tunnel boring machine in hard rock condition. International Journal of Mining and Mineral Engineering, 4(3), 249-264.

Sapigni, M., Berti, M., Bethaz, E., Busillo, A., and Cardone, G. 2002. "TBM performance estimation using rock mass classifications." Int. J. Rock Mech. Min. Sci., 39 (6), 771–788. https://doi.org/10.1016/S1365-1609(02)00069-2.

Sargent, R. G. (2013). "Verification and validation of simulation models." J. of Simulation, 7 (1), 12–24. https://doi.org/10.1057/jos.2012.20.

Schweitzer, E., Scaglione, A., Monti, A., & Pagani, G. A. (2017). Automated generation algorithm for synthetic medium voltage radial distribution systems. IEEE Journal on Emerging and Selected Topics in Circuits and Systems, 7(2), 271-284.

Shi, H., Yang, H., Gong, G., & Wang, L. (2011). Determination of the cutterhead torque for EPB shield tunneling machine. Automation in Construction, 20(8), 1087-1095. https://doi.org/10.1016/j.autcon.2011.04.010.

Shahin, A., AbouRizk, S. M., Mohamed, Y., & Fernando, S. (2014). Simulation modeling of weather-sensitive tunnelling construction activities subject to cold weather. Canadian journal of civil engineering, 41(1), 48-55.

Snowdon, R.A., Ryley, M.D., and Temporal, J. 1982. "A study of disc cutting in selected British rocks." Int. J. Rock Mech. Min. Sci. Geomech. Abstr. 19 (3), 107–121. https://doi.org/10.1016/0148-9062(82)91151-2.

Špačková, O., Šejnoha, J., & Straub, D. (2013). Probabilistic assessment of tunnel construction performance based on data. Tunnelling and Underground Space Technology, 37, 62-78.

Sousa, R.L., Einstein, H.H., (2012). Risk analysis during tunnel construction using Bayesian Networks: Porto Metro case study. Tunnelling and Underground Space Technology 27, 86–100.

Tarkoy, P. J. 1975. Rock hardness index properties and geotechnical parameters for predicting tunnel boring machine performance. Ph.D. Thesis, University of Illinois at Urbana-Champaign, IL. https://doi.org/10.1016/0148-9062(77)90787-2.

Terzaghi, K. (1950). Geologic aspects of soft-ground tunneling.

Torabi, S.R., Shirazi, H., Hajali, H., Monjezi, M., 2013. Study of the influence of geotechnical parameters on the TBM performance in Tehran-Shomal highway project using ANN and SPSS. Arab. J. Geosci. 6 (4), 1215–1227.

Trung, T. D. (2013). Analysis of microtunnelling construction operations using process simulation.

Ueki, M., Haas, C. T., & Seo, J. (1999). Decision tool for microtunneling method selection. Journal of construction engineering and management, 125(2), 123-131.https://doi.org/10.1061/(ASCE)0733-9364(1999)125:2(123).

Walonoski, J., Kramer, M., Nichols, J., Quina, A., Moesel, C., Hall, D., ... & McLachlan, S. (2018). Synthea: An approach, method, and software mechanism for generating synthetic patients and the synthetic electronic health care record. Journal of the American Medical Informatics Association, 25(3), 230-238.

Wang, R., Guo, X., Li, J., Wang, J., Jing, L., Liu, Z., and Xu, X. 2020. "A mechanical method for predicting TBM penetration rates." Arab. J. Geosci, 13 (9), 1-15. https://doi.org/10.1007/s12517-020-05305-x.

Werner, M., & AbouRizk, S. (2015, December). Simulation case study: Modelling distinct breakdown events for a tunnel boring machine excavation. In 2015 *Winter Simulation Conference* (WSC) (pp. 3234-3245). IEEE.

Werner, M., Ji, W., & AbouRizk, S. (2018, December). Improving tunneling simulation using Bayesian updating and hidden Markov chains. In 2018 *Winter Simulation Conference* (WSC) (pp. 3930-3940). IEEE.

Wu, L., T. Guan., and L. Lei. 2013. “Discrete element model for performance analysis of cutterhead excavation system of EPB machine.” Tunnel. Undergr. Space Technol., 37, 37-44. https://doi.org/10.1016/j.tust.2013.03.003.

Yagiz, S. 2008. “Utilizing rock mass properties for predicting TBM performance in hard rock condition.” Tunn. Undergr. Space. Technol., 23 (3), 326339. https://doi.org/10.1016/j.tust.2007.04.011.

Yagiz, S., Gokceoglu, C., Sezer, E., Iplikci, S., 2009. Application of two non-linear prediction tools to the estimation of tunnel boring machine performance. Eng. Appl. Artif. Intell. 22 (4), 808–814.

Yagiz, S., & Karahan, H. (2011). Prediction of hard rock TBM penetration rate using particle swarm optimization. International Journal of Rock Mechanics and Mining Sciences, 48(3), 427-433. https://doi.org/10.1016/j.ijrmms.2011.02.013.

Yavari, M., Mahdavi, S., 2005. Prediction of penetration rate of TBM using ANN. In: National Mining Conference, 1–3 Feb 2005, Iran, pp. 1–10.

Zhang, L., Wu, X., Ji, W., & AbouRizk, S. M. (2017). Intelligent approach to estimation of tunnel-induced ground settlement using wavelet packet and support vector machines. Journal of Computing in Civil Engineering, 31(2), 04016053.

Zouaoui, F., & Wilson, J. R. (2003). Accounting for parameter uncertainty in simulation input modeling. Iie Transactions, 35(9), 781-792.